

**DESIGN AND ANALYSIS OF A BRAIN-COMPUTER
INTERFACE-BASED ROBOTIC REHABILITATION SYSTEM**

by
Ela Koyaş

Submitted to the Graduate School of Engineering and Natural Sciences
in partial fulfilment of
the requirements for the degree of
Master of Science

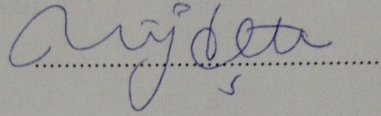
Sabancı University

October 2013

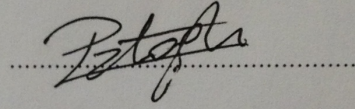
DESIGN AND ANALYSIS OF A BRAIN-COMPUTER INTERFACE-BASED
ROBOTIC REHABILITATION SYSTEM

APPROVED BY

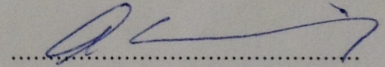
Assoc. Prof. Dr. Müjdat ÇETİN
(Thesis Supervisor)



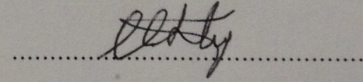
Assoc. Prof. Dr. Volkan PATOĞLU
(Thesis Co-supervisor)



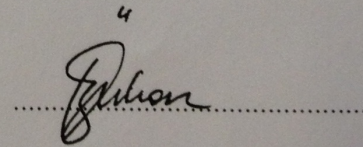
Prof. Dr. Aytül ERÇİL



Assoc. Prof. Dr. İlker HAMZAOĞLU



Assist. Prof. Dr. Naime Özben ÖNHON



DATE OF APPROVAL: 25/10/2013

© Ela Koyas 2013
All Rights Reserved

Acknowledgments

My sincere gratitude is to my supervisor Müjdat Çetin and to my co-supervisor Volkan Patoglu for their excellent guidance, patience, motivation, enthusiasm, and immense knowledge.

I am grateful to my committee members, Aytül Erçil, İlker Hamzaoglu and Naime Özben Önhon for taking the time to read and comment on my thesis.

I also would like to thank Sabancı University and TÜBİTAK for providing the necessary financial support for my graduate education¹.

I am also indebted to my colleagues and friends Mine Saraç, Elif Hocaoglu, Jaime Delgado Saa, Ahmetcan Erdoğan and Mehmet Umut Şen and my other fellow labmates from Computer Vision and Pattern Analysis Laboratory for their assistance and suggestions.

Most importantly, none of this would have been possible without the love and patience of my family. I would like to express my heart-felt gratitude to my family who are always supporting me and encouraging me with their best wishes.

¹This work was partially supported by Sabancı University under Grant IACF-11-00889, and by the Scientific and Technological Research Council of Turkey under Grants 11E056 and 111M186.

DESIGN AND ANALYSIS OF A BRAIN-COMPUTER INTERFACE-BASED ROBOTIC REHABILITATION SYSTEM

Ela Koyaş

EE, M.Sc. Thesis, 2013

Thesis Supervisor: Müjdat ÇETİN

Thesis Co-supervisor: Volkan PATOĞLU

Keywords: electroencephalogram, brain-computer interfaces, event-related synchronization and desynchronization, motor imagery movements, robotic rehabilitation systems

Abstract

In this thesis, we have investigated the effect of brain-computer interfaces (BCI) which enable direct communication between a brain and a computer, to increase the patient's active involvement to his/her task in the robotic rehabilitation therapy. We have designed several experimental paradigms using electroencephalography (EEG) based BCIs which can be used to extract information about arm movement imagery in the context of robotic rehabilitation experiments. In particular, we propose a protocol that extracts and uses information about the level of intention of the subject to control the robot continuously throughout a rehabilitation experiment. In this context we have developed and implemented EEG signal processing, learning and classification algorithms for offline and online decision-making.

We have used different types of controlling methods over the robotic system and examined the potential impact of BCI on rehabilitation, the effect of robotic haptic feedback on BCI, and information contained in EEG about the rehabilitation process. Our results verify that the use of haptic feedback through robotic movement improves BCI performance. We also observe that using BCI continuously in the experiment rather than only to trigger robotic movement may be preferable. Finally,

our results indicate stronger motor imagery activity in BCI-based experiments over conventional experiments in which movement is performed by the robot without the subject's involvement.

BEYİN-BİLGİSAYAR ARAYÜZÜ TABANLI ROBOTİK REHABİLİTASYON SİSTEMİ TASARIMI VE ANALİZİ

Ela Koyaş

EE, Yüksek Lisans Tezi, 2013

Tez danışmanı: Müjdat ÇETİN

Tez eş-danışmanı: Volkan PATOĞLU

Anahtar Kelimeler: elektroensefalografi, beyin-bilgisayar arayzleri, olgu ile ilgili senkronizasyon ve desenkronizasyon, hayali motor hareketleri, robotik rehabilitasyon sistemleri

Özet

Bu tezde, robotik rehabilitasyon terapilerinde hastanın görevine aktif katılımını arttırmak için, beyin ve bilgisayar arasında doğrudan iletişim sağlayan beyin-bilgisayar arayüzleri (BBA)nin etkisini araştırdık. Robotik rehabilitasyon deneyleri bağlamında, hayali kol hareketleri hakkında bilgi elde etmek için kullanılan elektroensefalografi (EEG) tabanlı BBA sistemleri ile çeşitli deneysel paradigmlar tasarladık. Özellikle, gönüllünün istek düzeyi bilgisini elde eden ve bu bilgiyi rehabilitasyon deneyi sırasında robotu sürekli olarak kontrol etmek için kullanan bir protokol öneriyoruz. Bu bağlamda, çevrimiçi ve çevrimdışı karar verebilmek için EEG sinyalini işleme, öğrenme ve sınıflandırma algoritmaları geliştirdik ve uygulamaya koyduk.

Robotik sistem üzerinde farklı kontrol yöntemleri kullandık ve rehabilitasyon süreci hakkında EEG'de yer alan bilgiyi, BBA'nın rehabilitasyona ve robotik dokunsal geribildirim de BBAYA olan etkisini inceledik. Sonuçlarımız robot hareket yoluyla yapılan dokunsal geribildirim kullanımının BBA performansını arttırdığını doğruluyor. Deneyde sürekli olarak BBA kullanımının, sadece robotik hareketi tetiklemek yerine tercih edilebilir olduğunu da görüyoruz. Son olarak, sonuçlarımız, BBA tabanlı deneylerde hareketin gönüllü katılımı olmadan robot tarafından yapıldığı ge-

leneksel deneylere göre daha güçlü hayali motor etkinliđi olduđunu göstermektedir.

Table of Contents

Acknowledgments	iv
Abstract	v
Özet	vii
1 Introduction	1
1.1 Scope	2
1.2 Motivation	3
1.3 Contributions	5
1.4 Outline	6
2 Background	8
2.1 Introduction	8
2.2 EEG Signals	9
2.2.1 Sensorimotor Rhythms	11
2.2.2 Classification Methods	12
2.3 EEG Based BCIs	14
2.4 Rehabilitation Systems	14
2.4.1 Conventional Robotic Rehabilitation Systems	15
2.4.2 BCI Based Rehabilitation Systems	16
3 Design and Evaluation of a Motor Imagery-based BCI System	21
3.1 Analysis of BCI Competition Data set	21
3.1.1 Feature Extraction	21
3.1.2 Classification	22
3.2 Analysis of Data Sets Recorded in Our Laboratory	23
3.2.1 Designed Interfaces	23
3.2.2 Data Analysis	25
3.3 Conclusion	31

4	Offline BCI Based Robotic Experiments Utilizing Posterior Probabilities	32
4.1	Designed BCI System	33
4.1.1	Continuous Output from the LDA	33
4.2	Designed Robotic System	34
4.3	Experiments	34
5	Online BCI Based Robotic Experiments Utilizing Posterior Probabilities	37
5.1	Designed BCI System	37
5.2	Designed Robotic System	38
5.3	Online Integration of BCI with ASSISTON-MOBILE	39
5.4	Experiments	40
5.5	Conclusions	43
6	Detection of Intention Level in Response to Task Difficulty from EEG	45
6.1	BCI System	45
6.2	EEG Experiments	46
6.2.1	EEG Data Collection	46
6.2.2	EEG Data Analysis	47
6.3	EEG and EMG Experiments	49
6.3.1	EEG Data Analysis	50
6.3.2	EMG Data Analysis	51
6.3.3	Correlation Analysis	52
6.4	Conclusions	53
7	Comparative Experimental Analysis of BCI-Assisted Robotic Rehabilitation	55
7.1	Experimental Paradigm	55
7.2	Training	58
7.2.1	Analysis of the Training Data	59
7.2.2	Building the Training Model	66
7.3	Testing	66
7.3.1	Analysis of the Testing Data	67
7.3.2	Classification	76
8	Conclusion	84
8.1	Summary	84
8.2	Future Works	85
8.2.1	BCI Based Robotic Experiments Utilizing Posterior Probabilities	86

8.2.2	Detection of Intention Level in Response to Task Difficulty from EEG	86
8.2.3	Comparative Experimental Analysis of BCI-Assisted Robotic Rehabilitation	87
	Bibliography	87

List of Figures

1.1	BCI-based robotic rehabilitation system.	2
1.2	Representative BCI-based robotic system.	3
2.1	(a) Apply electrode gel in holes. (b) Click active electrodes into holders. (electrodes and holders are color labelled.) [1,2]	9
2.2	The BioSemi pin-type active electrode has a sintered Ag-AgCl electrode tip, providing very low noise, low offset voltages and very stable DC performance and completely resistant to long term water enabling easy cleaning and disinfecting. [3]	10
2.3	Location of the electrodes which are placed according to International 10-20 system, proposed by American EEG society. [4]	10
2.4	Power spectrum density in the alpha frequency band.	11
2.5	log Power of the EEG signal recorded from channel C3 for resting and right arm motor imagery movement.	12
2.6	Posterior probabilities of samples for a two class classification problem. 13	
3.1	The classification results on the data set provided by University of Technology Graz, for BCI Competition 2003 for different timing windows.	22
3.2	Interface for entering the experimental information.	23
3.3	Training interface type I.	24
3.4	Testing interface type I.	24
3.5	Training interface type II.	25
3.6	Testing interface type II.	25
3.7	Timing scheme of experiment Type I.	26
3.8	Positions of the electrodes used in our experiments.	27

3.9	Classification results of experiment type I.	28
3.10	The mean classification accuracies across the subjects of experiment type I.	28
3.11	Timing scheme of experiment Type II.	29
3.12	Positions of the electrodes used in our experiments.	29
3.13	Classification results of right arm imagery movement or closed eyes. . .	30
4.1	Robotic system.	35
4.2	(a) Probability values and windowed probability values; (b) Kinetic energy of the robotic system.	36
5.1	A prototype of ASSISTON-MOBILE	39
5.2	Experimental setup consisting of the Biosemi ActiveTwo EEG mea- surement device and ASSISTON-MOBILE	41
5.3	(a) Moving window averaged probability of patient intention and (b) kinetic energy of the augmented system	42
5.4	Force readings during the exercise.	43
6.1	Timing scheme	46
6.2	Elbow flexion of 30° followed by extension.	49
6.3	EMG features and p-values of Subject D: (a) Maximum, (b) sum, (c) energy of the signal between the 3000 th – 5000 th samples, and (d) energy of the 1500 samples centered around the maximum point of the EMG in a trial.	52
6.4	Correlation analysis: (a) The mean correlation coefficients across the EMG features for each subject, (b) the mean correlation coefficients across the subject for each feature.	53
7.1	Representative experiment set-up.	56
7.2	Subject elimination (results of channel C_3).	58
7.3	(a) Training timing scheme (b) Testing timing scheme of C_1 , C_2 , C_4 , PA and PP (c) Testing timing scheme of C_3 and C_5	58
7.4	Averaged log PSDs for robot and non-robot assisted MI tasks.	60

7.5	PSD across time values of the electrode C_3 : Power spectra in movement periods and the rest periods for the electrode C_3 in the frequency band $6 - 15Hz$ for the training blocks with and without the robotic system guiding the subjects arm.	62
7.6	PSD across time values of the electrode C_z : Power spectra in movement periods and the rest periods for the electrode C_z in the frequency band $6 - 15Hz$ for the training blocks with and without the robotic system guiding the subjects arm.	63
7.7	PSD across time values of the electrode C_4 : Power spectra in movement periods and the rest periods for the electrode C_4 in the frequency band $6 - 15Hz$ for the training blocks with and without the robotic system guiding the subjects arm.	64
7.8	p -values of t-test ($PSD_{Resting} > PSD_{MI}$) for averaged PSDs in the alpha, as a function of time. The cue is shown at 0s. (a-b) C_3 , (c-d) C_z , (e-f) C_4	65
7.9	Averaged log PSDs for all conditions at C_3 channel.	69
7.10	PSD values across time for $C1$, $C2$, $C4$ conditions obtained from the C_3 channel.	71
7.11	PSD values across time for $C3$, $C5$ conditions obtained from the C_3 channel.	72
7.12	PSD values across time for $C1$, PA , PP conditions obtained from the C_3 channel.	73
7.13	PSD values across time for $C1$, $C3$ conditions obtained from the C_3 channel.	74
7.14	PSD values across time for $C4$, $C5$ conditions obtained from the C_3 channel.	75
7.15	Averaged classification results across subjects and trials in the time domain with one input channel C_3	78
7.16	Averaged classification results in the four timing windows obtained from the C_3 channel.	79
7.17	Averaged classification results in the four timing windows of every condition and their feature vectors.	80

7.18 The overall performance results. The obtained order of the PSD values from the three analysis and the classification accuracy order which is inversely proportional to the PSD values order. 82

List of Tables

3.1	LDA classification accuracies.	31
6.1	Classification accuracies of the first classification problem (load vs. relax) of the EEG based experiments.	48
6.2	Classification accuracies of the second classification problem of the EEG based experiments.	48
6.3	Classification accuracies of the third classification problem of the EEG based experiments. This is a three-class problem.	48
6.4	Classification accuracies of the first classification problem of the EEG-EMG based experiments.	50
6.5	Classification accuracies of the second classification problem of the EEG-EMG based experiments.	51
6.6	Classification accuracies of the third classification problem of the EEG-EMG based experiments. This is a three-class problem.	51
7.1	Experiment conditions.	57
7.2	p -values for $C1, C2, C4$	71
7.3	p -values for $C3, C5$	72
7.4	p -values for $C1, PA, PP$	74
7.5	p -values for $C1, C3$	75
7.6	p -values for $C4, C5$	75
7.7	Classification accuracies averaged across the trials for each condition and subject.	81

Chapter 1

Introduction

Neurological injuries are the leading cause of long-term disabilities that restrict activities of daily living (ADL) of millions of patients. Physical rehabilitation is the major form of treatment for neurological disabilities helping patients regain their motor control and actively take place in society. As rehabilitation therapies are known to be more effective when they are repetitive, intense, long term, and task specific; utilization of robotic devices not only eliminates the physical burden of movement therapy for the therapists, but also motivates patients to endure intense therapy sessions thanks to integration of multi-modalities, while simultaneously reducing the treatment costs.

Recently, there has been some interest in incorporating brain-computer interfaces (BCI) into robotic rehabilitation concepts (see Figure 1.1) to guide rehabilitation protocols to effectively induce activity-dependent brain plasticity and to restore neuromuscular function of patients with severe trauma due to stroke, cerebral palsy, or injury to spinal cord or brain. BCI has been an active area of research over the last two decades, mostly focusing on communication of patients with the outside world. Most BCIs rely on non-invasive electroencephalogram (EEG) signals, since collecting these electric potentials is more practical, less expensive, and safer for the patients, compared to invasive techniques.



Figure 1.1: BCI-based robotic rehabilitation system.

1.1 Scope

Our first objective in this thesis was to design and implement an end-to-end system for controlling a robotic system through the EEG signals collected from a human subject. This requires:

- The development of experimental scenarios for stimulating the appropriate neural mechanisms in the subject,
- The design of algorithms for machine learning as well as information extraction from the collected data,
- The construction of the robotic rehabilitation component,
- Combining the BCI component with the robotic system,
- The demonstration of successful control of the robotic system through experiments.

Once we had the first version of a working system as represented in Figure 1.2, our agenda for the remainder of the study was to conduct an experiment driven by some of the fundamental questions in this problem. This process led to changes

in our design of algorithms, hardware set up and as well as design of experimental scenarios.

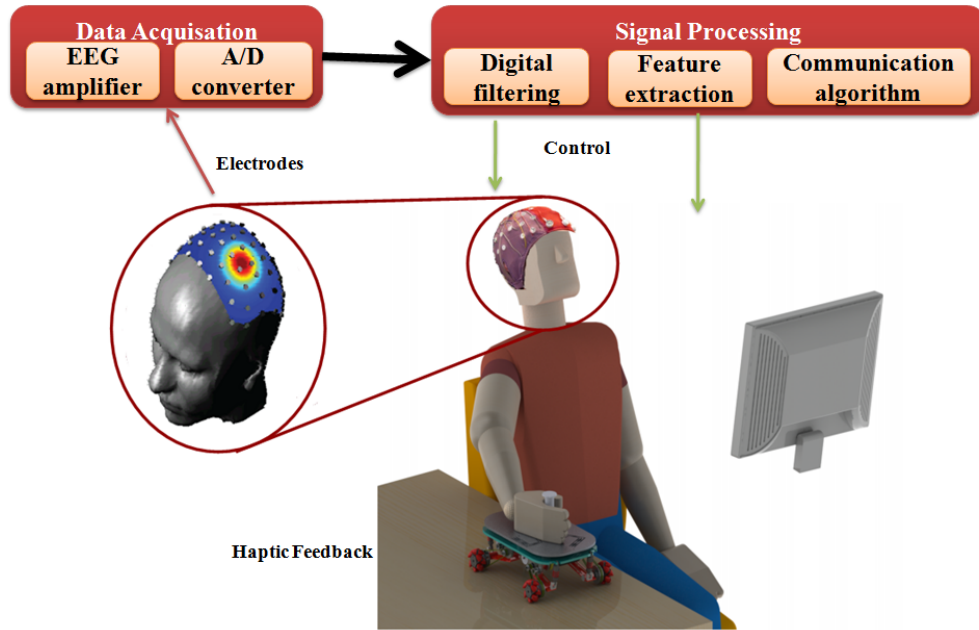


Figure 1.2: Representative BCI-based robotic system.

After building a new complete EEG-based BCI system that can control a rehabilitation robot, we have developed new procedures and mechanisms for the use of this integrated system in robotic rehabilitation. Afterwards, we examined challenging questions about potential impact of BCI on rehabilitation, the effect of robotic haptic feedback on BCI, and information contained in EEG about the rehabilitation process.

1.2 Motivation

BCI research deals with the problem of establishing direct communication pathways between the brain and external devices. The primary motivation is to enable patients with limited or no muscular control (including amyotrophic lateral sclerosis (ALS) and brainstem stroke patients) to use computers or other devices by automatically interpreting their intent based on measured brain electrical activity. Although this seems to be an extremely challenging problem, a variety of studies over the last 15-20 years have shown that non-invasively obtained electrical signals through the scalp-recorded EEG can be used as the basis for BCIs. This early suc-

cess has garnered much interest in BCI technology, raising anticipation (as well as some demonstration) for its use by healthy individuals as an additional communication pathway as well. This substantial progress has resulted in a growing interest in extending the application domain of BCIs from communication with a computer towards restoration of basic motor functions.

In a different area of research, studies have shown that physical rehabilitation therapy is responsible for most of the recovery experienced by patients with disabilities secondary to neurological injuries [5,6], and the therapies are more effective when they are task specific, intense, repetitive, and allow for active involvement of patients [7,8]. Using robotic devices in repetitive and physically involved rehabilitation exercises helps eliminate the physical burden of movement therapy for the therapists, and enables safe and versatile training with increased intensity. Robotic devices allow quantitative measurements of patient progress while enforcing, measuring, and evaluating patient movements, and with the addition of virtual environments and haptic feedback, they can be used to realize new treatment protocols. Therefore, these devices not only help increase the reliability, accuracy, and effectiveness of traditional physical rehabilitation therapies, but also help extend their applicability beyond the boundaries of clinics, realizing hospitals without borders.

Robotic rehabilitation has been shown to have a positive impact in post-stroke treatment for impaired patients [5, 6, 9, 10]. One key factor in the recovery of a patient is his/her mental involvement in the process and his/her effort during the treatment, since activity dependent plasticity requires that patients actively recruit their own muscles to the best of their ability. However, current robotic rehabilitation systems do not utilize any information about the mental state or intention of the patients, although they exploit their muscular involvement. For a patient in the early stages of recovery, muscular activity may be very limited.

In the proposed concept of a BCI-based rehabilitation system, the patient will be established as a mentally involved participant. It is important to stress that although muscle weakness is a problem for these patients, the most important goal of this therapy is to induce plastic recovery of neural control systems in brain and spinal cord.

This is a very new topic in the academic community with research efforts ini-

tiated in a number of laboratories around the world over the last 3-4 years that spans across multiple disciplines including neuroscience, signal processing (electronics engineering), machine learning (computer science), robotics (mechatronics), and rehabilitation (biomedical engineering). As a result, this is a vast open and extremely challenging area of research. Furthermore, this is a problem that has high potential for immediate application and might in turn help move BCI technology towards use in practical robotic control and rehabilitation systems.

1.3 Contributions

Our main goal of this thesis was to design, implement, and evaluate experimental protocols and real-time information extraction and robotic control strategies to increase the patient's involvement with the ultimate goal of improving the efficacy of the rehabilitation process. Some of the motivating questions for this thesis are listed as follows:

- How can BCI be used most effectively?
- Does the application of haptic feedback to a subject through a robotic system improve the performance of a BCI system?
- What is the effect of online velocity modification of the task according to BCI decisions compared to constant speed tasks?

For this purpose, firstly we have designed an EEG-based BCI system which has the potential to infer the passive state of the subject, including the level of intensity in response to task difficulty by examining whether the patterns in the EEG signal of the patient contain any information about the intention level. Secondly, we have built a complete EEG-based BCI system that can control a rehabilitation robot. Moreover, we have developed new procedures and mechanisms for the use of this system in robotic rehabilitation. Therefore the contributions of this thesis can be summarized as follows:

- We have built BCI based robotic systems, which uses posterior probabilities and conducted offline and online experiments.

- We have proposed an approach that enables detecting intention levels of subjects in response to task difficulty utilizing an EEG based BCI.
- We have designed an online BCI assisted protocol to continuously control the velocity of a robotic system.
- We have built an online experimental paradigm with different conditions using BCI-assisted/triggered, robotic/virtual reality systems to investigate the usage effect of the designed BCI and haptic feedback on the subject's active participation level to their imagery task .

Through the experimental analysis, our results verify that the motor imagery activity is stronger when the feedback is given as haptically to the subject rather than a virtual feedback. Moreover, when the subject continuously controls the velocity of a robotic system, rather than just triggering it, the subject becomes more involved to their tasks. Finally, our results verify the use of BCI in robotic rehabilitation may be preferable over conventional robotic rehabilitation systems in which movement is performed by the robot without considering the subject's involvement.

1.4 Outline

Chapter 2 presents the necessary background information about EEG signal processing and classification methods, brain-computer interfaces and rehabilitation systems by presenting a survey about published works, methods and results.

Chapter 3 covers the analysis of different EEG motor imagery movement data sets and includes the detailed description of the experimental paradigms and the steps followed to understand the underlying patterns in the EEG signal.

In Chapter 4, we have presented our offline experiments which involve integrating an EEG based BCI with a robotic system to target rehabilitation therapies of spinal cord injured patients.

Chapter 5 presents a systematic approach that enables online modification/adaptation of robot assisted rehabilitation exercises by continuously monitoring intention levels of patients utilizing an EEG based BCI.

In Chapter 6, we propose an approach that enables detecting intention levels of subjects in response to task difficulty utilizing an EEG based BCI.

Chapter 7 includes a series of online experiments with different conditions using BCI-assisted/triggered, robotic/virtual reality (VR) systems, their detailed data analysis and results.

Chapter 8 provides a summary of the contributions and the results of this thesis and suggests several potential future research directions.

Chapter 2

Background

This chapter intends to help the reader understand basic concepts about EEG signal processing and classification methods, brain-computer interfaces and rehabilitation systems by presenting a survey about published works, methods, and results.

2.1 Introduction

Brain-computer interfaces generate commands by measuring the brain signals. There exist two methods of measuring the brain activity: the invasive method in which the electrodes are placed under the scalp by a surgical operation, and the non-invasive method in which the brain signals are measured externally.

The invasive methods using "electrocorticography (ECoG)", "intracranial EEG (I-EEG)" or "subdural EEG (SD-EEG)" have an excellent resolution on the electrical activity of the brain, but are harder to implement and experiment with since they require surgical operation.

The non-invasive methods can be applied by using electroencephalography (EEG), magnetoencephalography (MEG), X-ray computed tomography (CT), positron emission tomography (PET), functional magnetic resonance imaging (fMRI) or functional near infrared spectroscopy (fNIRS).

Even though other methods have advantages on effective source localization and spatial resolution on the scalp over EEG, EEG is commonly favored for BCI applications, thanks to its portability, ease of use and low-cost. Moreover, EEG does not involve radioactivity and because it is silent, better rehabilitation therapies can be applied.

2.2 EEG Signals

Electroencephalogram (EEG) is a recording technique which measures the electrical activity of the brain. EEG signals can be acquired from the Ag/AgCl pin electrodes (see Figure 2.2) placed on an electrode cap which is worn by the subject and a conductive gel is applied to the subject's skin to decrease the skin resistance (see Figure 2.1). In Figure 2.3, the location of the electrodes which are placed according to International 10-20 system, proposed by American EEG society [11] is shown.

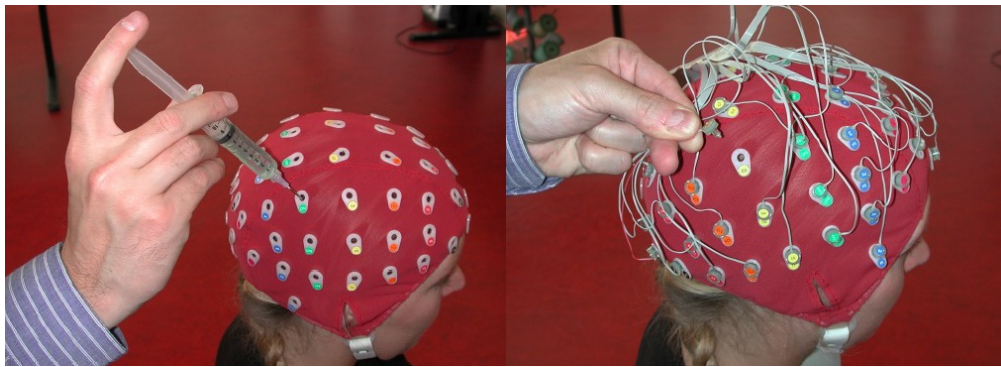


Figure 2.1: (a) Apply electrode gel in holes. (b) Click active electrodes into holders. (electrodes and holders are color labelled.) [1,2]



Figure 2.2: The BioSemi pin-type active electrode has a sintered Ag-AgCl electrode tip, providing very low noise, low offset voltages and very stable DC performance and completely resistant to long term water enabling easy cleaning and disinfecting. [3]

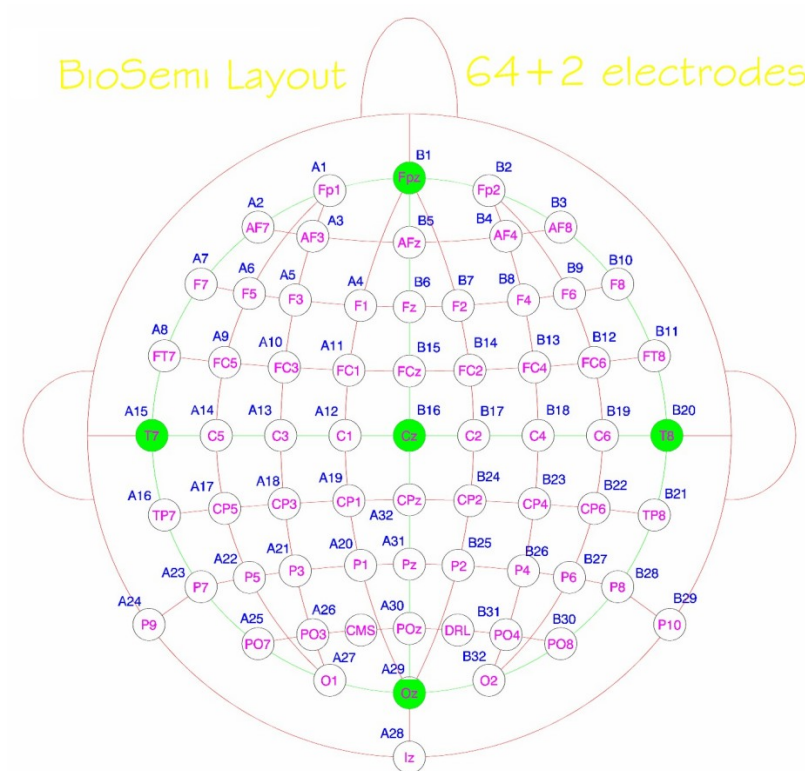


Figure 2.3: Location of the electrodes which are placed according to International 10-20 system, proposed by American EEG society. [4]

2.2.1 Sensorimotor Rhythms

The sensorimotor rhythms are the oscillatory brain wave rhythms of brain activity. Given EEG signals measured in BCI experiments designed to emphasize sensorimotor rhythms occurring in a correlated fashion with the user's intent, the goal is to process these signals and automatically recognize underlying patterns. EEG is typically characterized by its rhythmic activities. In 1990s, the phenomena of event-related synchronization (ERS) and desynchronization (ERD) [12, 13] patterns were introduced to identify motor imagery movements. In the case of execution of motor imagery movements, ERD or ERS occur and change the amplitude of the signal where ERD is related to imagination of the motor tasks (see Figure 2.4) and ERS is related to the passive state.

ERD and ERS are mainly characterized by the help of spectral powers computed in the typical EEG beta(β 16-24Hz), sigma (σ 12-16Hz) and alpha (α 8-12Hz) frequency bands related to the preparation of the imagery movements [12].

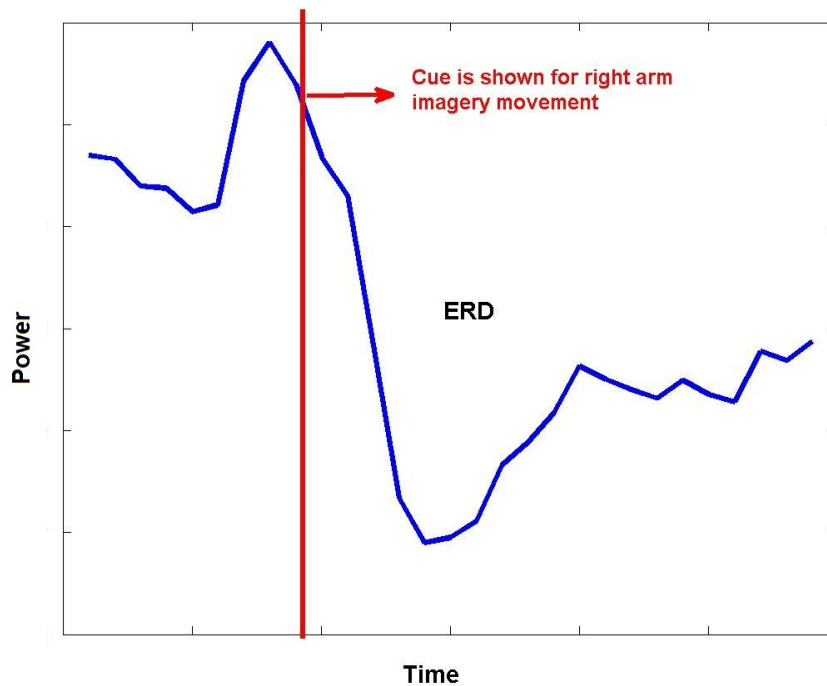


Figure 2.4: Power spectrum density in the alpha frequency band.

Spectral powers of specified frequency bands are measured by the power spectral density function (PSD) which computes the variations (energies) at frequencies. The

unit of PSD is energy per frequency (width) and averaged energy within a specific frequency band can be computed by integrating the PSD within that frequency band. In Figure 2.5, the logarithms of the averaged PSD values versus frequencies are shown for resting and right arm motor imagery movement. These results are obtained in the experiments we describe in detail in Chapter 7 of this thesis.

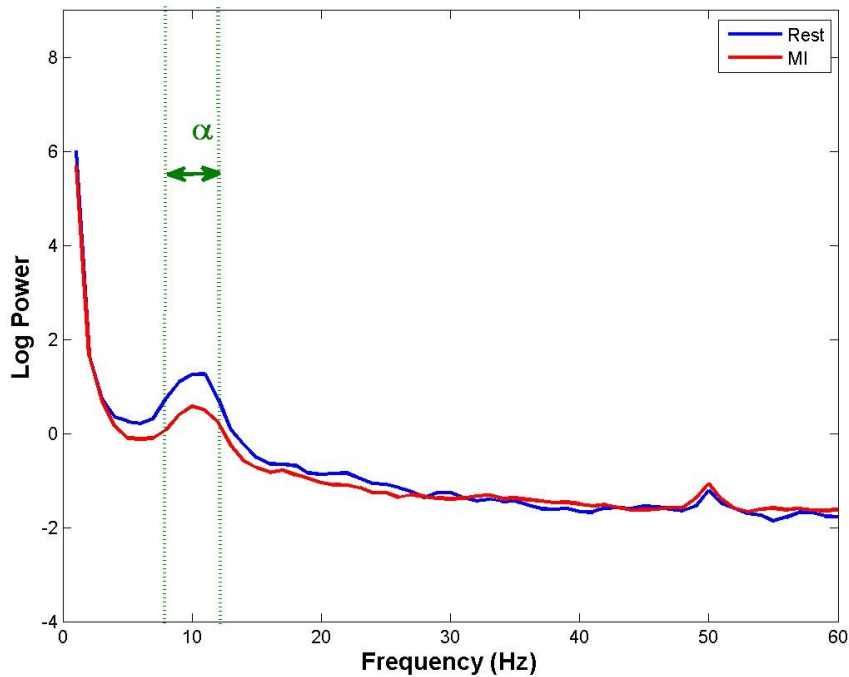


Figure 2.5: log Power of the EEG signal recorded from channel C3 for resting and right arm motor imagery movement.

2.2.2 Classification Methods

In the literature, linear and non linear methods have been proposed to classify motor imagery movements using ERD/ERS patterns as features [14]. Nevertheless, linear methods are commonly preferred, since they are generally more robust due to their lower complexity, stationarity structure, and consistency against overfitting [15]. Two of the most commonly used classifiers in BCI research are linear discriminant analysis (LDA) and support vector machines (SVM), which result in similar performances.

LDA is a classification method which separates classes by using hyperplanes obtained with the linear combination of the extracted features. In LDA, by assuming

two classes ($N = 2$) have normal density distributions, the classes are modelled to have the same covariance matrix but different mean vectors. Under this assumption a decision boundary is constructed based on the posterior probability values of each sample as shown in Figure 2.6.

In N -class problems ($N > 2$) several hyperplanes are used to separate the classes and the common approach is to make a classification between one class versus the remaining classes. SVM is also separates classes by using hyperplanes like LDA, but in SVM the distance between the hyperplanes and the nearest data points of every classes to the hyperplanes should be maximized. To make the data classes more separable, a mapping function may be used to present the data in an other space by using kernel functions.

Consequently, in this study, LDA which is a fast, stationary classification method that is known to produce good results in motor imagery based BCIs [16–20], is used to classify motor imagery movements using ERD/ERS patterns.

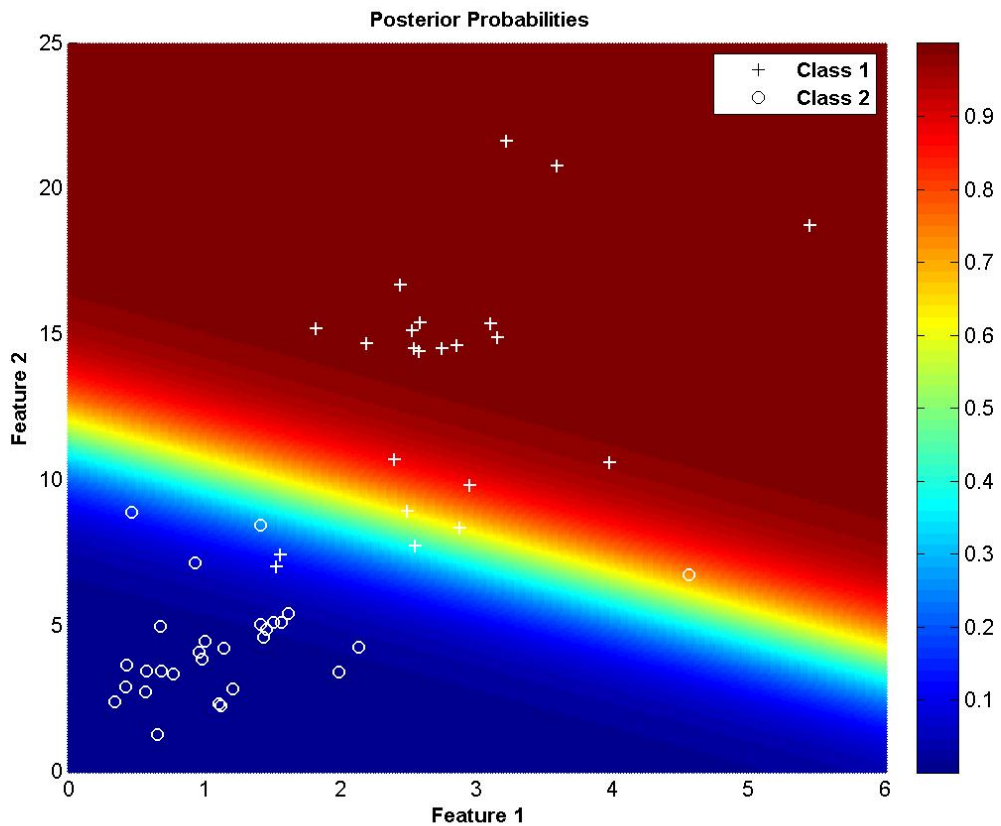


Figure 2.6: Posterior probabilities of samples for a two class classification problem.

2.3 EEG Based BCIs

The main purpose of non-invasive EEG-based BCI is to measure the electrical activity using EEG signals and to classify their patterns to extract user's intention. Up to now, various BCI applications have been designed using different EEG features: high-speed word spelling using virtual evoked potentials (c-VEPs)[21], Google search system by using motion onset VEP [22], brain painting system to draw different objects [23]. In [24] used event-related synchronization (ERS) and desynchronisation (ERD), to move forward in a Virtual Environment (VE).

Underlying patterns of EEG signals measured in experiments designed to emphasize sensorimotor rhythms related to the user's intent, can be automatically recognized by using ERD/ERS phenomena [12, 13], where ERD is related to the motor tasks and ERS is related to the passive states. The changes in the power of the alpha, sigma and beta frequency bands related to the preparation or planning of the imagery movements that displays ERD and ERS, give the opportunity to analyse EEG signals in the means of sensorimotor rhythms [12, 25]. Recognizing these patterns of sensorimotor rhythms gives the opportunity to control cue-based synchronous or self-paced asynchronous BCI systems, including prostheses [26, 27], wheelchairs [28], cursors [29], robots [30], and virtual environments [24]. Because EEG can be used in subjects who are incapable of making a motor response, this gives the opportunity to combine BCIs with rehabilitation systems.

2.4 Rehabilitation Systems

To improve the life quality of millions of patients suffering from neurological diseases and disabilities due to injuries, development of rehabilitation techniques is an active research area. Effective physical rehabilitation techniques designed for the treatment of neurological diseases has critical social and economical roles since they enable the active participation of the patients in the daily life and society by regaining their motor control skills.

Rehabilitation therapies are known to be more effective when they are repetitive, intense, long term and task specific. However, manual administration of such therapies are costly due to the physical burden and the manual labor involved.

Therefore, design methodologies for rehabilitation robots have matured in recent years. On the other hand, since active participation of patients in the therapies is known to be crucial for motor recovery, brain-computer interface (BCI) technology promises to become one of the main pathways to guide rehabilitation protocols to effectively induce activity-dependent brain plasticity and to restore neuromuscular function. Therefore under this section, rehabilitation systems are loosely categorized into two: Conventional robotic rehabilitation systems and BCI-based rehabilitation systems.

2.4.1 Conventional Robotic Rehabilitation Systems

Utilization of robotic devices for delivery of repetitive and physically involved rehabilitation exercises not only eliminates the physical burden of movement therapy for the therapists, but can motivate patients to endure intense therapy sessions thanks to integration of multi-modalities, while simultaneously reducing the treatment costs. Robot-assisted rehabilitation devices increase the reliability and accuracy of treatment, while also providing quantitative measurements to track the patient progress. Clinical trials investigating efficacy of robotic rehabilitation provide evidence that robotic therapy is effective for motor recovery and possesses high potential for improving functional independence of patients [5, 6, 9, 10].

In recent years, design methodologies for rehabilitation robots have matured and robotic systems for rehabilitation have become ubiquitous. Since active participation of patients in therapies is known to be crucial for motor recovery, state-of-art rehabilitation robots regulate the physical interaction between the patient and the device. These systems require patients to do positive work on the system such that movement exercises can be completed. These control techniques are commonly extended with “assist-as-needed” protocols to provide minimal assistance to the patient, since redundant amount of assistance is shown to be detrimental for recovery, while proper amount of assistance is necessary to ensure safety and progress.

In the literature, various techniques have been proposed to ensure active participation of patients in rehabilitation therapies by using surface electromyography (sEMG) signals as a means to provide driving signals to control rehabilitation devices. EMG signals are preferred as the human-robot interface for patients with

remaining muscle functions, since these signals can be directly correlated with human intention and provide fast enough reactions for adjusting amount of assistance [31–33]. In many implementations, the amount of assistance provided by the robotic device is taken to be directly proportional to the difference between the weighted functions of sEMG signals recorded from antagonistic muscle groups, reflecting the users’ movement intention [34, 35]. Moreover, the linear envelope of sEMG signals is used as an approximate estimation of joint torque, since it represents the muscle activation level and direction of intended movement coherent with the action of limb [36, 37]. Linear envelope of sEMG signals is advantageous since this method does not require much effort to precisely calibrate the relation between the EMG intensity and joint torque, as necessitated in the other approaches [34, 35], but instead it provides simple and sufficiently accurate means of torque estimation. Unfortunately, since remaining muscle function is a prerequisite for EMG based approaches, these techniques are not applicable to patients with severe disabilities. BCI-based systems provide a viable alternative.

2.4.2 BCI Based Rehabilitation Systems

Even though active rehabilitation devices can impose forces/movements to patients with all levels of impairment, it is not trivial to extend adaptive assistance protocols to patients with severe disabilities. In particular, severe motor disability of these patients preclude their voluntary muscle control and physical contribution to the task, on which most of the current “assist-as-needed” protocols depend. Bypassing the impaired neuromuscular system and enabling monitoring of the current state of brain activity, BCI technology promises an alternative pathway to guide rehabilitation protocols to effectively induce activity-dependent brain plasticity and to restore neuromuscular function. In the literature, it has been shown that stroke patients are capable of operating a motor imagery based BCI system as efficiently as healthy subjects [30, 38, 39]. Besides, [40] states that rehabilitation systems integrated with BCI are more effective when the patient’s intention to move are simultaneously adapted by the system itself.

Rehabilitation therapy using EEG-based BCI systems can be loosely categorized into two: systems that only represent movements corresponding to motor imagery,

typically in a virtual reality (VR) environment, and systems that physically interact with the patient to impose movement therapies corresponding to the motor imagery.

Belonging to the first category, in [41], 9 patients were asked to imagine reaching and grasping movements, while a BCI system classified patients' intentions into "no movement", "right arm movement" and "left arm movement" using Sensory Motor Rhythms with Linear Discriminant Analysis (LDA). The corresponding movements were presented to the patients in a simulated VR environment. The results of this study indicate that the users can control a virtual avatar in a motor training task that changes its difficulty according to the user capability. In [42], 19 healthy subjects were tested to perform reaching and grasping tasks with their right arm to three targets in a VR environment. To obtain the information about planning and execution of the movement, an advanced nonlinear analysis technique, mutual information, was used. Visual and audio feedback were provided to patients through a VR environment. This study argues that as well as the execution of the task, the preparation period also creates functional changes in the brain and reaching for the target may also be controlled using the data collected during the preparation period. In [43], 5 stroke patients were tested using an EEG-based BCI controlled VR ball-basket game. Intention of patients to move were extracted using event-related synchronization (ERS) and desynchronization (ERD) patterns associated with motor imagery from the EEG data. Results of the feasibility studies indicate a significant improvement in average mood of patients over the treatment sessions when motor imagery sessions are used in combination with conventional physical practice training. This study also shows feasibility of using BCI-based mental imagery tasks in post-stroke rehabilitation protocols together with traditional physical practice.

In [44], 6 healthy subjects were asked to imagine right or left arm movements to reach given targets. The BCI system categorized the EEG data as "right", "rest", "left" or "uncertainty" using a LDA based classifier on features extracted through the wavelet transform of the EEG signal. The uncertainty state was evaluated as a rest state. A FANUC LR Mate 200iB robot arm was used for visual feedback. The robot arm was never in contact with the subject, but classified EEG signals were used to direct the end-effector of the robot such that patients can control the robot

to track a desired trajectory. Such visualization was shown to improve the accuracy of the final decision about the mental task. In [45], a healthy subject was asked to concentrate on reaching three targets by focusing on right or left hand movements to move a 2 degrees of freedom (DoF) planar robotic arm, PupArm. Similar to [44], the robot arm was used for visualization and was never in contact with the subject. Normalized cross-correlation between EEG maps was utilized to classify mental tasks. Two control strategies were compared. In the first strategy, called hierarchical control, “up”, “down”, “right” and “left” commands were classified to let the user decide on the axis and the direction of movement of the robot arm. In the second strategy, called directional control, users were allowed to continuously choose the direction of the movement and control commands were generated periodically. The hierarchical control strategy is shown to be more reliable, but slower than the directional control approach.

In the EEG-based BCI system of [45], the user can control 2D movements of the robot arm PuParm - a force-controlled planar robot - to reach several goals without any physical interaction. In [46], two chronic stroke patients have participated EEG-based BCI system supported by a FES platform and had an error rate of less than 20%. However, it is not stated that BCI use resulted in any improvement in upper limb recovery.

In the second category, rehabilitation robots are integrated with BCI to impose necessary therapeutic exercises. In [38], 8 hemiparetic stroke patients were asked to imagine moving their affected hands without any actual movement. Naive Bayes Parzen Window was used to classify the ERD/ERS patterns as “move” and “rest”. This binary information was used to trigger or stop movements of a 2 DoF MIT-Manus robot for reaching tasks with 8 trajectories. The results of this study indicate that most of the stroke patients are capable of operating the BCI system effectively. In [30], 3 healthy subjects and 4 chronic stroke patients were asked to imagine moving their arm. The CSP filter was used to classify ERD/ERS as intention to “move” or “rest”. The BCI system was augmented with a Kinect to track 3-D objects in the workspace and an eye-tracker to allow patients to choose objects to reach, using their gaze. An online, fully synchronized bounded jerk trajectory planning method was utilized to provide the trajectory to the goal, and Light-Exos arm was triggered

to impose this trajectory to the subject’s arm. This study indicates that no performance difference has been observed between healthy subjects and stroke patients. In [47], 18 hemiparetic stroke patients out of 47 were selected as proper candidates for BCI based rehabilitation and were asked to imagine movements of their affected arm. Intention of patients to move was classified using the Filter Bank Common Spatial Pattern algorithm as “go” and “rest” states, and an MIT-Manus system was triggered to carry out the relevant movement with respect to the output state of the BCI system. [48] presents clinical results obtained using the same setup, but on 11 different hemiparetic stroke patients. These patients attended 12 therapy sessions over 4 weeks, each session lasting 1 hour. The results provide evidence that EEG-based BCI with robotic feedback neurorehabilitation can be operated by the majority of stroke patients and can be effective in restoring upper extremities motor function in stroke. In [49], 6 healthy subjects and 3 stroke patients were asked to imagine right hand movements of their (impaired) arm. Welch’s method was used to compute estimates for the power spectral density to classify the user’s intention to “go” or “rest”. 7 DoF Barrett WAM was triggered by these signals to impose flexion/extension movements to the users. Providing studies on both healthy subjects and stroke patients, this study provides further evidence for feasibility of successful integration of BCI with robotic systems for rehabilitation.

However, in the BCI-based rehabilitation systems mentioned above, patients’ intentions are only used to trigger the system, to start or to stop the movement without considering the continuity of patients’ focus during the course of the task. Consequently, these systems cannot ensure active participation of patients in the movement therapy because regardless of whether the patient spends more or less effort to be involved, the resulting movement is always the same. Hence, it is of interest to develop techniques that can infer the intention level of subjects in the course of a robotic rehabilitation routine.

Recently, [40] has advocated the importance of real-time adaptation of movement therapies to correspond with the patients’ intention captured by EEG-based BCI. Even though this study provides initial feasibility studies showing two stroke patients controlling a Barrett WAM robot attached to their impaired arm, the real-time adaptation of therapies based on BCI classification has been left as a part of their

future work. Similarly, in [49] intentions of the subjects are decoded by computing the PSDs of incrementally bigger time segments which includes previous time points. The state of the robot is updated either in a passive mode where the subjects are instructed to attempt a real/imaginary movement, or in an active mode where the subjects' movements are guided by the device, in every 300 ms. Updating the robot state every 300 ms enables the system to be synchronized with subjects' intentions. Welch's method has been used to compute estimates for the power spectral density to classify the user's intention as "go" or "rest".

Since active participation of patients in the therapies is known to be crucial for motor recovery, inferring the subject's level of mental stress, conditions or emotions from EEG signals, provides valuable information for "assist-as-needed" protocols. [50] proposes an approach to incorporate the user's attention state into game control, by computing the short window energy of the EEG signals that contrasts between attention conditions in which the subjects were asked to perform Stroop tasks and in-attentiveness conditions in which they were instructed to relax. [51,52] present a study to find a correlation between emotions and chronic mental stress levels measured by Perceived Stress Scale 14 (PSS-14) and EEG signals. [53] proposes a fast emotion detection approach from EEG, by showing neutral, positive and negative video clips to the subjects. Immediately after the played video, the subjects reported the induced emotions during watching the video clip. But these proposed approaches are very specific to the tasks executed in the experiments, strongly dependent on the patients or not suitable for real-time adaptation of robotic rehabilitation systems.

On the other hand, in rehabilitation therapies, as patients are always asked to finish a task by means of imagery or real movements, the velocity of the executed or imagined task may also be correlated with the patient's intention level during the task. In [54], each subject was asked to perform elbow flexion/extension motions for three minutes with arbitrary angles and speeds. The experimental results suggest that EEG signals with the tested decoding model can be used to continuously decode the elbow joint velocity. [55] shows an attempt to decode hand movement speeds from EEG signals during a drawing task. In [56], a linearly correlated relationship between speed and the EEG activity in the alpha and beta frequency bands during imagined and executed hand movements is found.

Chapter 3

Design and Evaluation of a Motor Imagery-based BCI System

This chapter describes the motor imagery-based BCI system we have designed and implemented. We evaluate this system on standard BCI competition data as well as on data recorded in our laboratory. This system serves as the basic BCI component in robotic rehabilitation work to be described in subsequent chapters.

3.1 Analysis of BCI Competition Data set

Firstly, the data set provided by The Department of Medical Informatics, Institute of Biomedical Engineering, University of Technology Graz, for BCI Competition 2003 [57] was used to understand the underlying patterns in motor imagery movements. This data set was recorded from a healthy subject who sat in a relaxing chair with armrests. The task of the subject was to control a feedback bar by means of imagery left or right hand movements. The order of left and right cues was random to prevent any systematic effect. EEG signals were measured over three bipolar EEG channels C_3 , C_z and C_4 with 128 Hz sampling rate. The training set contains 140 trials and the testing set contains another 140 trials. The length of a trial is 9 seconds. After the quiet two seconds, an acoustic stimulus is given and a cross ‘+’ is displayed for 1 second and then a right or left arrow appears as a cue for 6 seconds to indicate right or left arm imagery movement.

3.1.1 Feature Extraction

Activity of the EEG signal is mainly characterized by the help of the spectral powers computed in the typical EEG frequency bands. The relative powers in the

beta (β 16-24Hz), sigma (σ 12-16Hz) and alpha (α 8-12Hz) frequency bands have been selected as relevant features that are important for classification. Then Short Time Fourier Transform (STFT) was applied to each trial with a window which contains 512 samples and the window was shifted for 64 samples in each step of the transform.

The activity of the brain is observed after the cue is shown and the effect of the cue (imagination of the movement) on the EEG signal becomes smaller as the time passes. Hence, instead of analyzing the entire signal recorded in a trial, the timing windows which contain the data of $3.2 - 5$ s, $3.2 - 7$ s, $3.5 - 5.5$ s, $3.5 - 7$ s and $4 - 7$ s, were used. Afterwards, the averaged power spectral densities (PSDs) of selected frequency bands in that timing window, were calculated. As a result of this process, the extracted features of a trial consists of 9 dimensions (3 averaged PSDs for 3 channels) and were used as the input of the classifier.

3.1.2 Classification

Linear discriminant analysis and support vector machines (SVM) were used as classification methods. We used MATLAB's Statistical Toolbox and the libSVM toolbox. Classification accuracies are shown in the Figure 3.1.

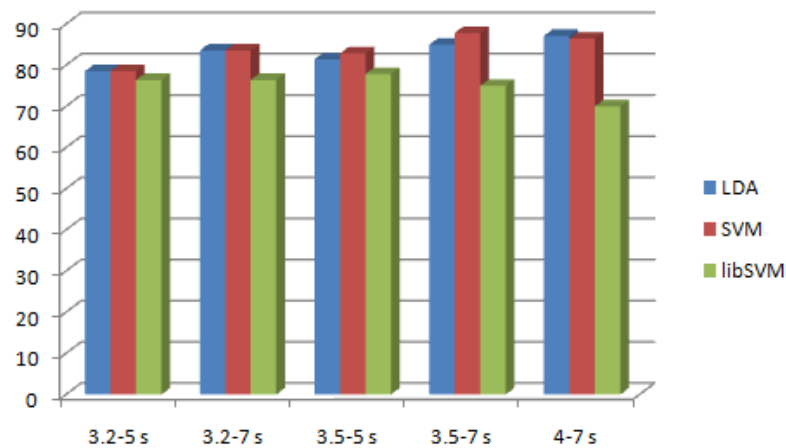


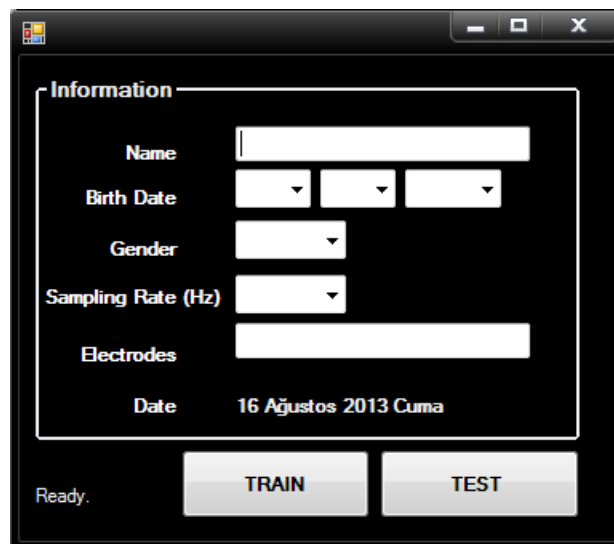
Figure 3.1: The classification results on the data set provided by University of Technology Graz, for BCI Competition 2003 for different timing windows.

3.2 Analysis of Data Sets Recorded in Our Laboratory

After obtaining an acceptable performance with the BCI competition data set, we have started to build our own data sets by designing different experimental paradigms. Firstly, we have tried to classify right versus left arm imagery movements. After obtaining accurate results, we have built a new classification problem which contains right arm imagery movement and resting classes. Because in rehabilitation therapies, distinguishing the movement periods from the resting periods is worthy to finish a rehabilitation task.

3.2.1 Designed Interfaces

The interfaces used in the experiments were implemented in Visual Studio, by using C#. In Figure 3.2, the first interface where the subject's and experimental informations are entered (subject's name, surname, birth date and gender; experiment's sampling rate, electrodes in use and experiment date) is shown. After clicking the "Train" button this information is logged in a text file and the interface built for the training session is opened. When the training session is finished this interface becomes visible again and by clicking the "Test" button, testing session's interface is displayed.



The image shows a software window titled "Information" with a dark background and white text. The window contains several input fields and buttons. At the top left, there is a small icon. The main content area is enclosed in a white border and contains the following elements:

- Name:** A text input field.
- Birth Date:** Three dropdown menus for day, month, and year.
- Gender:** A dropdown menu.
- Sampling Rate (Hz):** A dropdown menu.
- Electrodes:** A text input field.
- Date:** A label followed by the text "16 Agosto 2013 Cuma".

At the bottom of the window, there is a status bar with the text "Ready." on the left and two buttons labeled "TRAIN" and "TEST" on the right.

Figure 3.2: Interface for entering the experimental information.

Interface Type I: Right versus Left Arm Imagery Movement

Training: In the first interface type, a similar interface paradigm with the one used by the Graz [57] group was designed to build data sets that contain right/left arm imagery movement classes. A trial consists of a passive period followed by a cue period. At the beginning of a trial, a cross ‘+’ is displayed to indicate a passive period and then an acoustic stimulus indicates the beginning of a cue. Then, a right or left arrow appears as a cue for right or left imagery arm movements. The order of the cues is random.



Figure 3.3: Training interface type I.

Testing: Additionally, for online experiments, a cue based testing interface was designed. In the testing, the subject tries to move a virtual green ball located at the center of the screen to the right or left in means of right/left imagery movements according to the cues shown over the ball. Between these cues, there are passive periods. The signal recorded in the passive periods is not processed and analysed (see Figure 3.4). At the beginning of each trial the position of the ball is set to its initial position which is the center of the screen. The classification result of a trial is shown at the end of that trial.

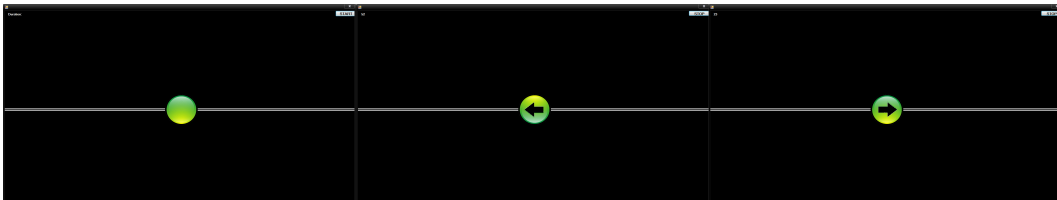


Figure 3.4: Testing interface type I.

Interface Type II: Right Arm Imagery Movement versus Resting

Training: In the second interface type, some modifications were made to the first interface type to record data sets which contain resting and right arm imagery

movement classes. The subjects were asked to relax or to imagine right arm movements.

For this experiment, an acoustic stimulus was added additionally to the first interface type to indicate a new cue will appear. The right arrow cue indicates the right arm movement periods and the “Relax” cue indicates the resting periods. Between these cues a ‘+’ stimulus was shown on the screen for passive periods. The order of the cues is random (see Figure 3.5).



Figure 3.5: Training interface type II.

Testing: The subjects are asked to move a virtual ball located on the left hand side of the screen by means of motor imagery right arm movements or to rest according to the cues shown on the ball. The passive periods are followed by an active period which contains a “right arm imagery movement” or a “Relax” cue (see Figure 3.6).

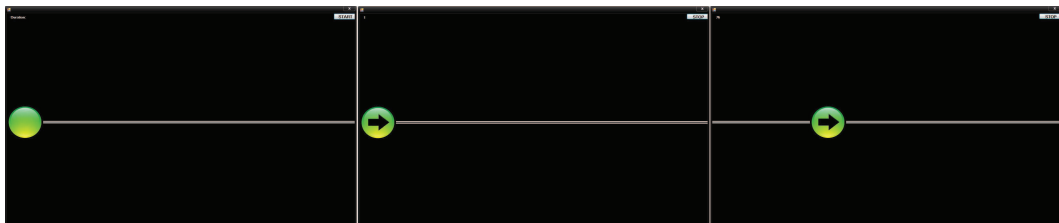


Figure 3.6: Testing interface type II.

3.2.2 Data Analysis

In this section, to build several data sets, the different types of experimental paradigms using only the training part of the interfaces described in Section 3.2.1 were designed. Afterwards, the data sets recorded in these experiments are divided into training and test data sets by applying two-fold cross validation. The offline data analysis results are fully detailed and explained.

Experiment Type I

In the experiment type I, the training part of the interface type I was used and the subjects were asked to imagine right or left arm imagery movements according to the cues shown on the screen. At the beginning of a trial, a cross ‘+’ is displayed for 3 seconds then, a right or left arrow appears as a cue for 6 seconds. Therefore, the length of a trial is 9 seconds as shown in Figure 3.7. A run consists of 40 trials (20 trials for right/left movement) and an experiment consists of 3 or 4 runs to avoid fatigue. Six healthy subjects participated in this experiment. The signals were sampled by 2 kHz (2048 samples) and were downsampled to 512 Hz to reduce the amount of data to be processed.

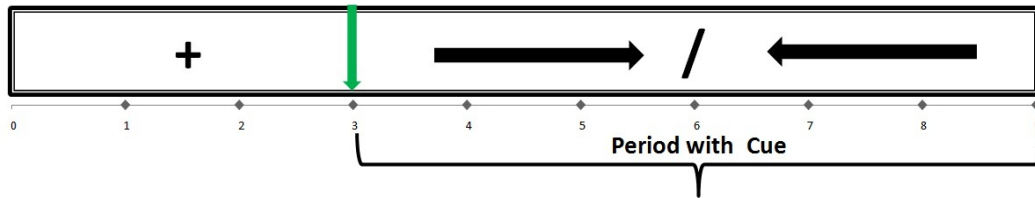


Figure 3.7: Timing scheme of experiment Type I.

The recordings were done over 35 channels that are presented in red colour in the Figure 3.8. But all 35 channels do not give important information about the motor imagery movements. In the literature, it has been shown that ERD is spread mainly over the central areas which include the central (C_3, C_z, C_4), frontal (FC_1, FC_2) and postcentral (CP_1, CP_2) channels [12, 58, 59]. To find the most informative channels, the classification results of the features obtained from different channels (3 electrodes: C_3, C_z, C_4 and 7 electrodes: $C_3, C_z, C_4, FC_1, FC_2, CP_1, CP_2$) with two different referencing methods were compared.

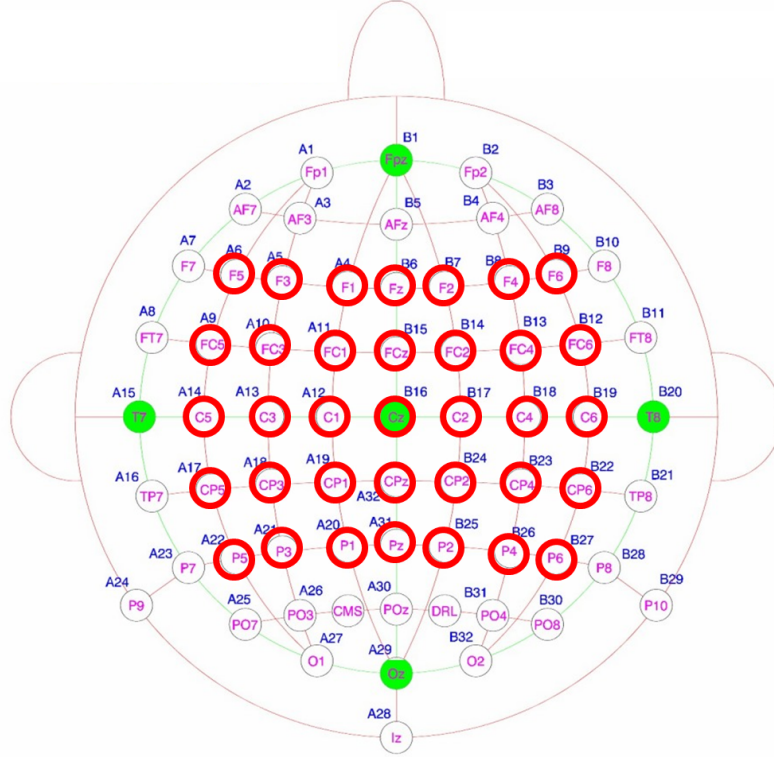


Figure 3.8: Positions of the electrodes used in our experiments.

In the first referencing method, 4 channels positioned around a channel (upper, lower, right, left neighbors) are used as the references of that main channel which is located at the center. This method is called the Laplace Method. The second referencing method is to take the upper and lower neighbors (anterior and posterior) of a main channel as its references. The mean of the data acquired from these references is subtracted from the main channel and a referenced channel is obtained.

The averaged PSDs of specified frequency bands (alpha, sigma and beta) were selected as features. LDA and SVM were used as classification methods.

To eliminate data recorded before the subject has had enough time to concentrate on the task, the first trial of each run was eliminated. Therefore, 117 or 156 trials are obtained from one subject in 3 or 4 runs. The performance of the classifier was measured by applying two-fold cross validation for 100 times to obtain different training and test datasets consisting of the 75% and the 25% of the entire data set, respectively. Overall classification accuracy was obtained by averaging over these 100 classification results (see Figure 3.9). The mean accuracies across the subjects are presented in Figure 3.10. The averaged LDA accuracies of 3 electrodes with 2

references and 7 electrodes with 4 references are close to each other. If we make the recordings over many channels, then the amount of the data will be increased and this will increase the analysis time. Therefore, we may say that the EEG signals which are measured over 3 channels with 2 references is sufficient for the LDA classifier.

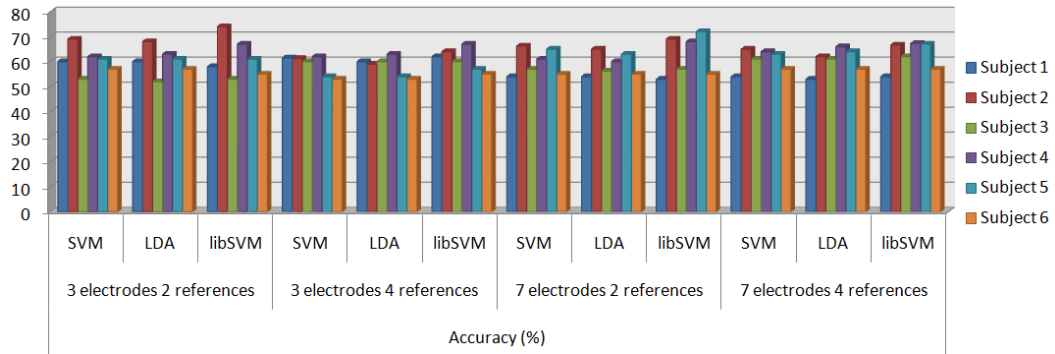


Figure 3.9: Classification results of experiment type I.

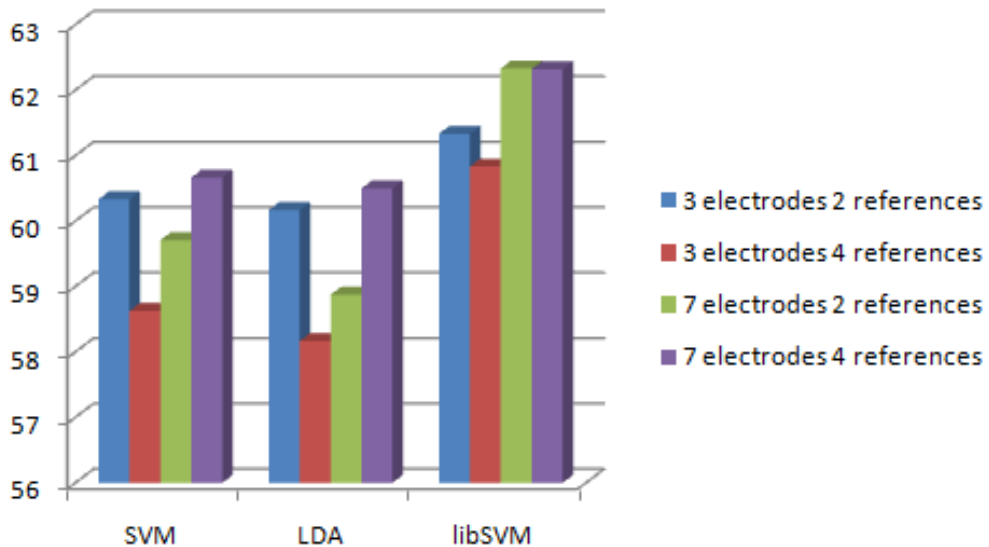


Figure 3.10: The mean classification accuracies across the subjects of experiment type I.

Experiment Type II

In the experiment type II, the training part of the interface type II was used. The data set of this experiment was recorded from three healthy subjects. While subjects sat quietly during data collection, without visible arm movements, their task was

to close their eyes for resting or to imagine right arm movements. A run consists of 60 trials (30 trials for right arm imagery movement and 30 trials for resting) and an experiment consists of 3 or 4 runs to avoid the fatigue. “+” is displayed for 3 seconds then, a right arrow or “Relax” appears as a cue for 6 seconds. Therefore, the length of a trial is 9 seconds as shown in Figure 3.11. The signals were sampled by 2 kHz (2048 samples) and were downsampled to 512 Hz. To eliminate data recorded before the subject has had enough time to concentrate on the task the first trial of each run was eliminated. Therefore, 177 or 236 trials are obtained from one subject in 3 or 4 runs.

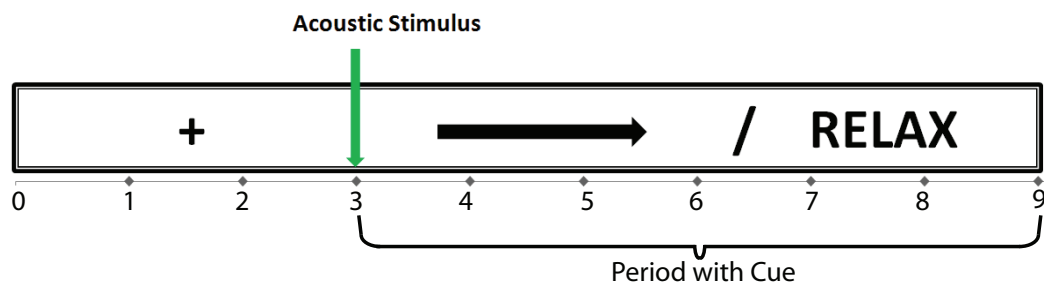


Figure 3.11: Timing scheme of experiment Type II.

The recording configuration shown in Figure 3.12 uses Ag-Cl electrodes at C_3 , C_z , C_4 locations of the international 10-20 electrode placement system, at 512 Hz sampling rate. Their anterior and posterior channels are used as references. By subtracting the average of the data received from upper and lower neighbor channels of a main channel, three referenced main channels are obtained.

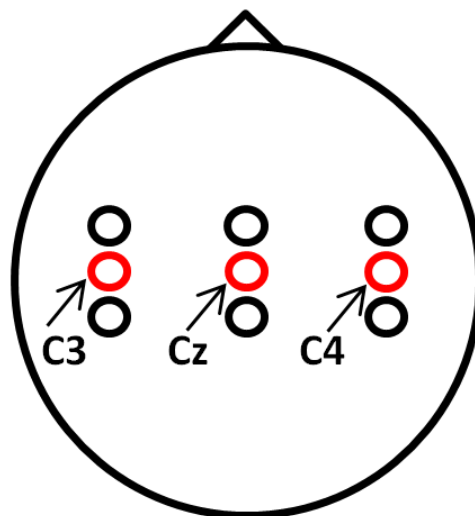


Figure 3.12: Positions of the electrodes used in our experiments.

The averaged PSDs in a specified timing window for each subject were classified by LDA and SVM. The performance of the classifiers was measured by applying two-fold cross validation for 100 times to obtain different training and test datasets consisting of the 75% and the 25% of the entire data set, respectively. Overall classification accuracy was obtained by averaging over these 100 classification results (see Figure 3.13). The results are greater than 90% for *Subject 1* and *Subject 2* where as *Subject 3*'s performance is greater than 70%.

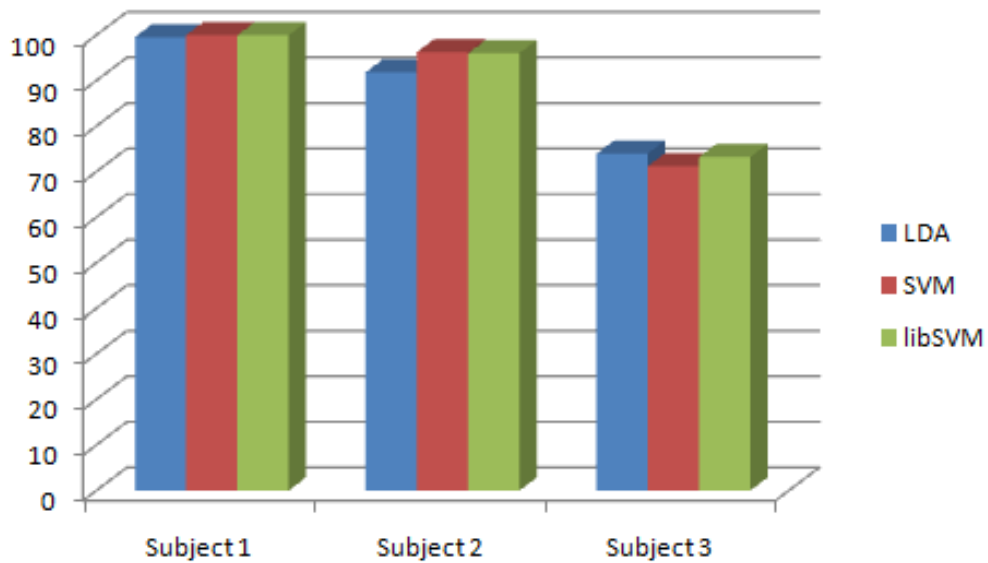


Figure 3.13: Classification results of right arm imagery movement or closed eyes.

Experiment Type III

In the experiment type III, the interface type II was used. To examine if closing eyes in resting periods affects the performance of the classifier, in this experiment, subjects were asked to rest without closing their eyes or to imagine right arm movements. In resting periods, the subjects were asked to focus on the cue shown on the screen and just relax. The data set of this experiment was recorded from nine healthy subjects. The recording configuration uses Ag-Cl electrodes at C_3 , C_z , C_4 locations and averaged PSDs of the alpha, sigma and beta frequency bands in a specified timing window for each subject were used as the features.

The performance of the LDA classifier was measured by applying two-fold cross validation for 300 times to obtain different training and test datasets consisting of the 75% and the 25% of the entire data, respectively. Overall classification accuracy

was obtained by averaging over these 300 classification experiments. Classification accuracy values vary between 84% and 63% across the subjects (see Table 3.1). The results show that the performance of motor imagery movement based BCIs, depend on the subject, his/her fatigue level and concentration. The level of accuracy we obtain is comparable to results reported in the BCI literature.

Subject No	Accuracy (%)
1	70.1622
2	83.9504
3	64.0922
4	69.5714
5	70.3694
6	63.0357
7	79.8810
8	74.6047
9	72

Table 3.1: LDA classification accuracies.

3.3 Conclusion

In this chapter we have described the BCI system that we have developed for classification of motor imagery. We have demonstrated the performance of the system on a number of sets and experimental protocols. These experiments have shown that our system achieves classification accuracies similar to other methods in the literature (see, e.g., [41, 42, 44, 45, 49, 57]). This system is used as the BCI component of the robotic control and rehabilitation work to be presented in the rest of this thesis.

Chapter 4

Offline BCI Based Robotic Experiments Utilizing Posterior Probabilities

In this chapter, an electroencephalogram (EEG) based Brain-Computer Interface (BCI) is integrated with a robotic system designed to target rehabilitation therapies of spinal cord injured patients such that patients can control the rehabilitation robot by imagining movements of their right arm. In particular, the power density of frequency bands are used as features from the EEG signals recorded during the experiments and they are classified by Linear Discriminant Analysis (LDA). As one of the novel contributions of this chapter, the posterior probabilities extracted from the classifier are directly used as the continuous-valued outputs, instead of the discrete classification output commonly used by BCI systems, to control the velocity of the therapeutic movements performed by the robotic system. Since, the probabilistic outputs may correspond to the instantaneous intention levels of motor imagery and this information can be used to determine the amount of assistance for “assist-as-needed” protocols. Adjusting the exercise velocity of patients online, as proposed in this study, according to the instantaneous levels of motor imagery during the movement, has the potential to increase efficacy of robot assisted therapies by ensuring active involvement of patients. The proposed BCI-based robotic rehabilitation system has been successfully implemented on physical set ups in our laboratory and sample experimental data are presented.

4.1 Designed BCI System

4.1.1 Continuous Output from the LDA

In this study, the data set recorded in the experiments presented in Section 3.2.2 was used. A classification problem which contains two classes (right arm imagery movement and rest period), was built and LDA which separates classes by using hyperplanes, was used as a classifier. The assumption made for the training data is, its two classes have multivariate normal density distributions. Training set classes are modelled to have the same covariance matrix but different mean vectors. These are estimated from the training data as shown in Eqns. (4.1) and (4.2).

$$\hat{\mu}_k = \frac{\sum_{i=1}^N M_{ik} x_i}{\sum_{i=1}^N M_{ik}} \quad (4.1)$$

$$\hat{\Sigma}_k = \frac{\sum_{i=1}^N \sum_{k=1}^2 M_{ik} (x_i - \hat{\mu}_k)(x_i - \hat{\mu}_k)^T}{N - 2} \quad (4.2)$$

If a sample x_i belongs to class k , the value of M_{ik} is 1, otherwise it is 0. A testing sample is classified by minimizing the expected cost value as shown in Eqn. (4.3).

$$\hat{y} = \arg \min_{y=1,2} \sum_{k=1}^2 P(k|x)C(y|k), \quad (4.3)$$

where C is the cost function, \hat{y} is the assigned class of the sample and k is its true class. If a testing sample is classified falsely, then the cost function is equal to 1, otherwise it is equal to 0. This cost function results in the maximum a posteriori (MAP) decision rule, hence each sample is assigned to the class providing the maximum posterior probability for that sample.

The binary \hat{y} output of the LDA classifier was used to calculate the classification accuracies which are presented in Section 3.2.2. In this chapter, the posterior probability values which are calculated using Eqns. (4.4) and (4.5), were used as continuous-valued outputs and used to control the velocity of the robot instead of the binary classification output commonly used by BCI systems. Since the probabilistic outputs may correspond to the instantaneous intention levels of motor imagery and this information can be used to determine the amount of assistance for “assist-as-needed” protocols. The analysis of the relationship between the posterior probabilities and the intention levels, is presented in detail in Chapter 6.

$$P(x|k) = \frac{1}{(2\pi|\Sigma_k|)^{1/2}} \exp\left(-\frac{1}{2}(x - \mu_k)\Sigma_k^{-1}(x - \mu_k)^T\right) \quad (4.4)$$

$$P(k|x) = \frac{P(x|k)P(k)}{P(x)} \quad (4.5)$$

4.2 Designed Robotic System

For the physical experiments in this chapter, a robotic system which was designed for upper limb rehabilitation therapies (see Figure 4.1). The posterior probabilities obtained from the offline analysis of the data set presented in Section 3.2.2, were used to control the velocity of the robot that follows a fixed contour. During the physical therapy exercises, to ensure the safety of robot-human interaction Passive Velocity Field Control (PVFC) [60–62] was used.

PVFC has multiple advantages for rehabilitation purposes: First of all, PVFC provides passivity with respect to the external forces. This property guarantees that the system causes no harm to patients during the contour tracking task, even if they fail the tracking at any given time. Furthermore, by monitoring the applied forces; the amount of assistance as well as the complexity of the task can easily be modified in order to prevent slacking continuous decrease in the levels of the muscle activation during repetitive motions as the movement error becomes slow - a fundamental property of human motor control. The BCI-based rehabilitation system has the same idea; except the controller does not use the muscle activity to detect slacking but the EEG data provided by BCI system. BCI-based rehabilitation system with PVFC control motivates the patients to intend to perform the task at all times. PVFC guarantees that no harm is done to patients at all times. Moreover, the patients can simultaneously change the behavior - speed, contour, etc. - of the robot with their intention levels so that they can relate their motor tasks to physical outcome better.

4.3 Experiments

In this chapter, our aim was to obtain continuous outputs which correspond to the instantaneous intention levels of motor imagery, from the classifier rather than to solve a classification problem. In order to control the velocity of the robot, *Subject 2*'s data were used. Two-fold cross validation was applied to obtain training and test data sets consisting of the 60% and the 40% of the entire data set, respec-

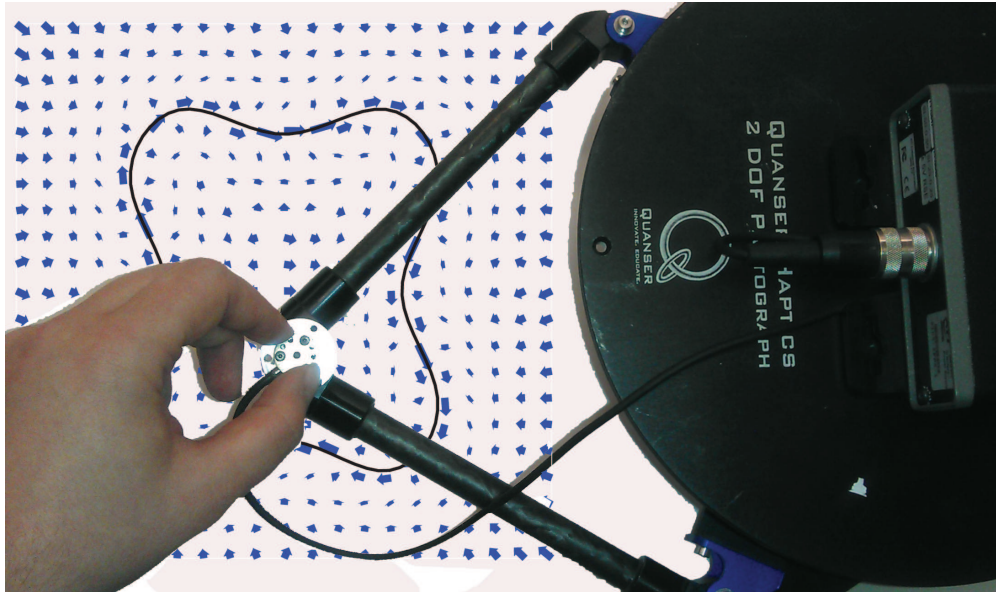


Figure 4.1: Robotic system.

tively. Because the goal of rehabilitation therapies is to be able to execute real movements, the trials which contain resting periods were eliminated for this study. Besides, the posterior probabilities of the misclassified right arm imagery movements are set to zero. Therefore, it is known that only right arm motor imagery cues are given and it is possible to automatically detect the incorrect classifications. The posterior probability values assigned to the correctly classified right arm imagery movements and the posterior probabilities of misclassified right arm imagery movements which are set to zero were used to adjust the velocity of the robot.

The energy of the system was calculated by PVFC and according to the energy, the instantaneous velocity of the robot was determined. Thus, the probabilistic outputs which may correspond to the instantaneous intention levels of motor imagery, are used to guide the speed of the contour following task by directly adjusting the speed coefficient $\rho = 0.7$ of PVFC. Therefore, the robot can follow the task with minimum 0.7 and maximum 1.7 times greater than its velocity field.

PVFC was implemented with a sampling frequency of 500 Hz through a desktop computer equipped with a PCI I/O card. To have smooth movements at the robotic system, a 4-second window contains 2000 samples, was shifted along the data and the mean of the posterior probabilities in the temporal window was calculated and fed to the input of the robotic system. The zero values were excluded from the window as they present misclassification. The robot was moved with its new determined

velocity for 2 seconds.

Figure 4.2 depicts a sample plot for the kinetic energy of the system, as well as the windowed probability values provided to PVFC. Kinetic energy of the overall system is directly proportional to the tracking speed in the given desired velocity field.

In this chapter, we have proposed a method to obtain instantaneous intention levels of motor imagery from the LDA classifier. We have used the posterior probabilities to control the velocity of the robot. We have demonstrated the integration of the BCI and the robotic system was implemented successfully as shown in Figure 4.2. Our agenda for the remainder of this study is to achieve real-time control of a rehabilitation robot, by utilizing posterior probabilities, which is presented in Chapter 5.

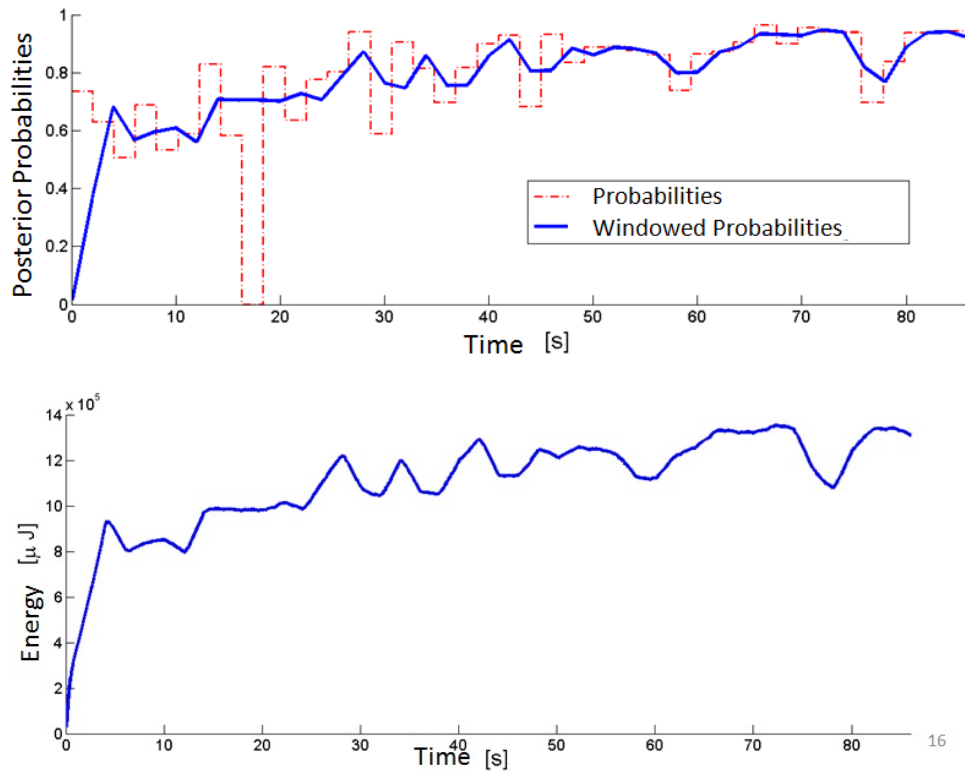


Figure 4.2: (a) Probability values and windowed probability values; (b) Kinetic energy of the robotic system.

Chapter 5

Online BCI Based Robotic Experiments Utilizing Posterior Probabilities

In this chapter, we present a systematic approach that enables online modification/adaptation of robot assisted rehabilitation exercises by continuously monitoring intention levels of patients utilizing an EEG based BCI. In particular, we use LDA to classify event-related synchronization (ERS) and desynchronization (ERD) patterns associated with motor imagery; however, instead of providing a binary classification output, we utilize posterior probabilities extracted from LDA classifier as the continuous-valued outputs to control a rehabilitation robot as described in detail in Chapter 4.

The experimental procedure we describe in this chapter corresponds to the BCI-based robotic control paradigm we propose for rehabilitation experiments. This chapter simply describes the approach and demonstrates its implementation to achieve real-time control of a rehabilitation robot. Since giving patients real-time control over the speed of the task, the proposed approach ensures active involvement of patients throughout exercise routines and has the potential to increase the efficacy of robot assisted therapies. Chapter 7 contains a detailed analysis of this protocol and its comparison with other rehabilitation protocols.

5.1 Designed BCI System

An experiment consists of an offline session which is similar to the experimental paradigm presented in Section 3.2.2 and an online session. For online sessions the testing interface presented in Section 3.2.1 was used. The task of the subject is to move a virtual green ball by means of imagery right arm movements.

During online sessions, the posterior probabilities assigned to right arm imagery movement class are considered to control the velocity of the robot. As it is known that the true class is always right arm imagery movement, only true positive (TP) and false negative (FN) right arm imagery movements are analyzed. Therefore, if data are classified as a rest period, than it is a FN decision and the value of the posterior probability assigned to right arm imagery movement class is equal or less than 0.5 where for TP decisions it is equal or greater than 0.5. For that reason, FN posterior probabilities assigned to right arm imagery movement class, are used as a decreasing effect where TP right arm imagery movement posterior probabilities have an increasing effect on the speed of the robot. Moreover, to have smooth movements at the robotic system, the mean of the posterior probabilities in the temporal window is calculated and fed to the input of the robotic system. A 3-second window is shifted along the data and the classifier produces a posterior probability output for every second using the model built in the offline session.

The recording configuration uses Ag-Cl electrodes at C_3 , C_z , C_4 locations of the international 10-20 electrode placement system, at 512 Hz sampling rate. Their anterior and posterior channels are used as references. By subtracting the average of the data received from upper and lower neighbor channels of a main channel, three referenced main channels are obtained.

5.2 Designed Robotic System

ASSISTON-MOBILE, a 3 DoF series elastic actuator, is used for assisting patients while completing therapeutic table-top exercises. ASSISTON-MOBILE consists of a 3-DoF planar, compliant parallel mechanism coupled to an omni-directional Mecanum-wheeled mobile platform. The deliberate introduction of a multi-DoF compliant element between the mobile multi-DoF actuation unit and the patient transforms the non-backdriveable active holonomic platform into a multi-DoF series elastic actuator.

In addition to administering active, passive, and resistive therapeutic exercises, ASSISTON-MOBILE can assist-as-needed [60], that is, it can interactively adjust the amount of assistance, to help increase the training efficiency by ensuring active participation of patients. ASSISTON-MOBILE can also easily be integrated with

BCI using PVFC as detailed in the next section. A picture of ASSISTON-MOBILE is presented in Figure 5.1.



Figure 5.1: A prototype of ASSISTON-MOBILE

5.3 Online Integration of BCI with ASSISTON-MOBILE

Contour following tasks are preferable in rehabilitation, since these exercises emphasize coordination and synchronization between various DoF during therapeutic exercises, while allowing patients to take control of exact timing along the path. Trajectory following controllers cannot guarantee that patients are always on the pre-determined path due to the radial reduction phenomena [63, 64]. Hence, we utilize PVFC to administer contour following tasks.

Employment of PVFC is advantageous in rehabilitation exercises, since with this controller in place, the task and the speed of the task can be decoupled from each other. Consequently, patients can be allowed to proceed with their preferred pace, while assistance can still be provided as determined by the therapist. In PVFC, the task is embedded in a predefined velocity field, while the speed of the task depends on the instantaneous energy of the closed loop system. In particular, PVFC mimics the dynamics of a flywheel; therefore, it cannot generate energy, but can only store and release the energy supplied to it. As a result, the controller renders the closed-loop system passive *with respect to externally applied forces*. This is one of the unique features of PVFC, as classical passivity-based robot control laws [65–67] cannot guarantee passivity when external forces (other than joint motor torques)

are considered as the input. Passivity with respect to external forces is crucial in human-machine interaction, since it enhances safety by limiting the amount of energy that can be released to the operator, especially in case of an unexpected system failure.

In PVFC, the pace of the task is determined by the total energy present in the system. This energy is due to the initial conditions and the work done by the external forces, that is, the energy provided/subtracted by the patient and disturbance forces acting on the system. However, the speed of the contour following task can also be controlled by regulating the total energy of the system by the actuators through an exogenous control term appended to the original PVFC controller. This extra control term features a speed coefficient r that allows easy modification of the task speed. The reader is referred to [61, 68, 69] for theory and implementation details of PVFC.

For BCI experiments, to enable online adaptation of robot assisted rehabilitation exercises with the intention of the patients, the posterior probabilities extracted from the LDA classifier are used as the continuous-valued outputs to PVFC. These outputs correspond to the instantaneous levels of motor imagery during the movement, and are used to guide the speed of the contour following task by directly adjusting the speed coefficient r in PVFC. With increased level of “intention”, a higher speed to complete the task is supplied to the patient providing feedback to encourage active participation of the patient.

5.4 Experiments

We have performed a feasibility study with a healthy subject for a single session in order to validate the applicability of the proposed control scheme. The subject (Subject 9 in Table 3.1) whose offline session data had 72% averaged classification accuracy, participated in the experiment involving control of ASSISTON-MOBILE.

The experimental setup consists of a Biosemi ActiveTwo EEG System and ASSISTON-MOBILE robot as shown in Figure 5.2. PVFC is implemented in real-time with a sampling frequency of 500 Hz through a desktop computer equipped with a PCI I/O card.

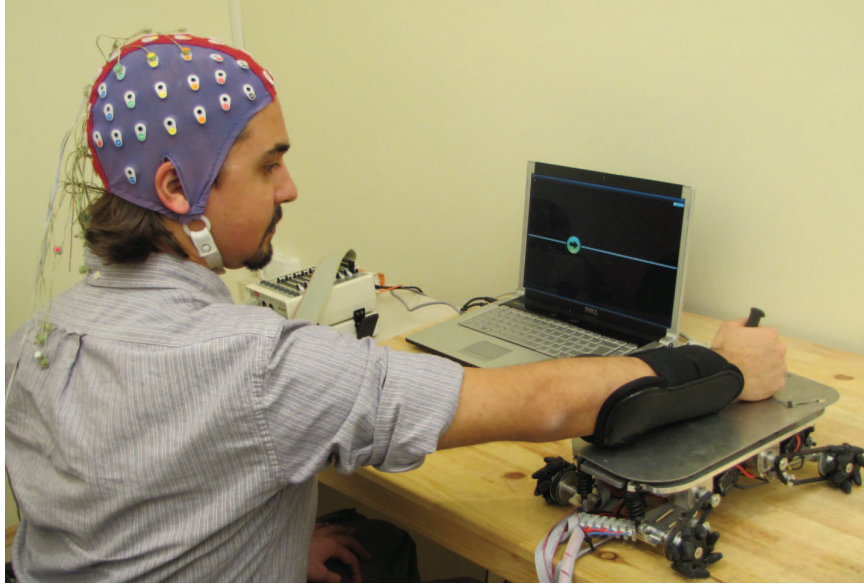


Figure 5.2: Experimental setup consisting of the Biosemi ActiveTwo EEG measurement device and ASSISTON-MOBILE

The experiment starts by introducing EEG-based BCI system to volunteers using the test algorithms detailed in Section 5.1. Once the subject is ready, the first phase of the experiment is initiated to familiarize the subject with the online modification of the speed of the contour following task. In this phase, the subject is instructed to control ASSISTON-MOBILE via motor imagery of his/her right arm movements tracing the contour, without causing any actual movement with the arms. At this phase, there is no physical interaction with the robot, but the subject is placed in front of ASSISTON-MOBILE so that he/she can observe the result of the intended movement.

In the second phase, the subject is attached to ASSISTON-MOBILE and asked not to make any voluntary arm movements, while he/she controls the robot via motor imagery of his/her right arm movements tracing the contour using the proposed control framework. In order to avoid sudden variations in the contour tracking speed, instantaneous signals provided by the BCI classifier at each second are averaged over 3 seconds using a moving window for a smoother therapy experience.

This phase of the experiment starts with ASSISTON-MOBILE in idle condition and the user is instructed to imagine moving his/her right arm to follow the desired contour, which is taken as a straight line for simplicity. With increased level of intention, a higher speed to complete the task is supplied to the patient providing

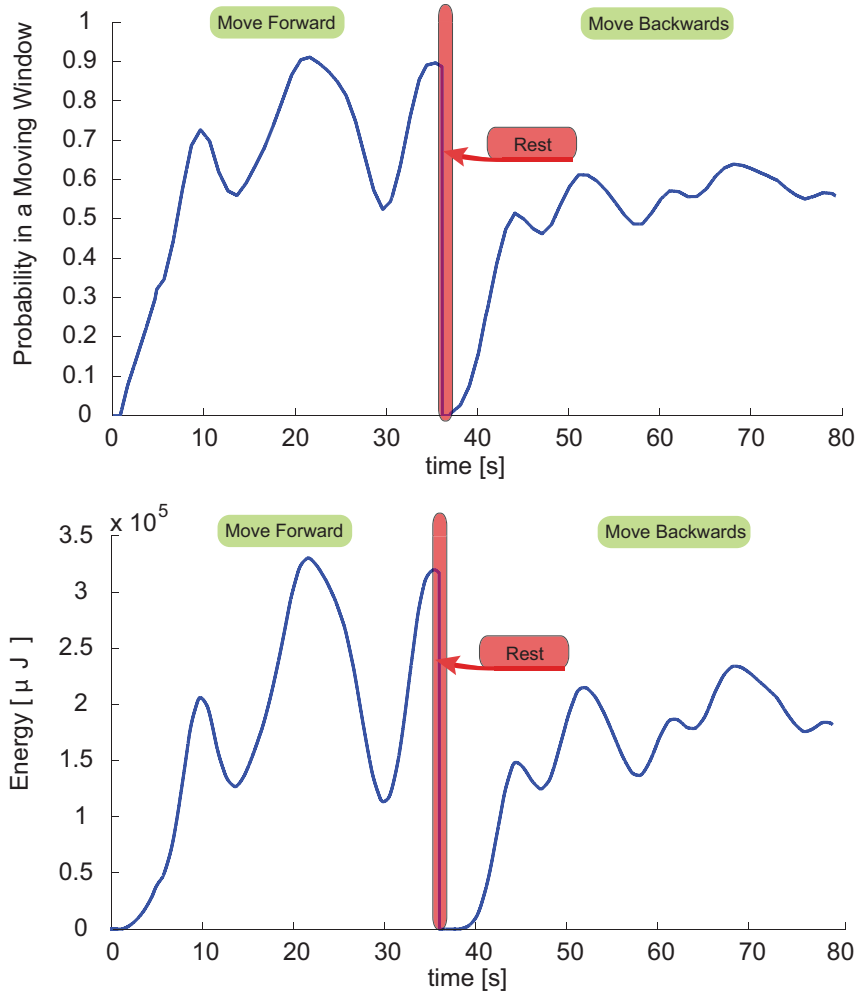


Figure 5.3: (a) Moving window averaged probability of patient intention and (b) kinetic energy of the augmented system

positive feedback to encourage the active participation of the patient. Once the contour is traversed in forward direction, motion of the device is deliberately stopped and the subject is instructed to rest for a few seconds. Then, the contour is traversed backwards.

Figure 5.3 depicts a sample plot for the kinetic energy of the system, as well as the windowed probability values provided to PVFC at each second throughout the exercise. As detailed in Section 5.2, PVFC can regulate the speed of the contour tracking task by providing/extracting energy to/from the system through its control parameters depending on the intention level of subjects. Therefore, kinetic energy of the overall system presented in Figure 5.3(a) is directly proportional to the tracking speed in the given desired velocity field [70]. Comparing Figure 5.3(a) and (b), it

can be observed that PVFC can successfully administer the contour following task at the speed levels dictated by the BCI signals.

Figure 5.4 presents the magnitude of the resultant interaction forces between the subject and ASSISTON-MOBILE during the same trial. During a large portion of the exercise, the subject applies no apparent external forces, while some unintentional movements can be observed at several instances. Note that residual movements, such as involuntary contractions, can also be applied by patients on the device. Thanks to inherent passivity of our contour tracking controller with respect to external forces, the coupled human-robot system stays passive and faithfully tracks the desired contour even under such forces.

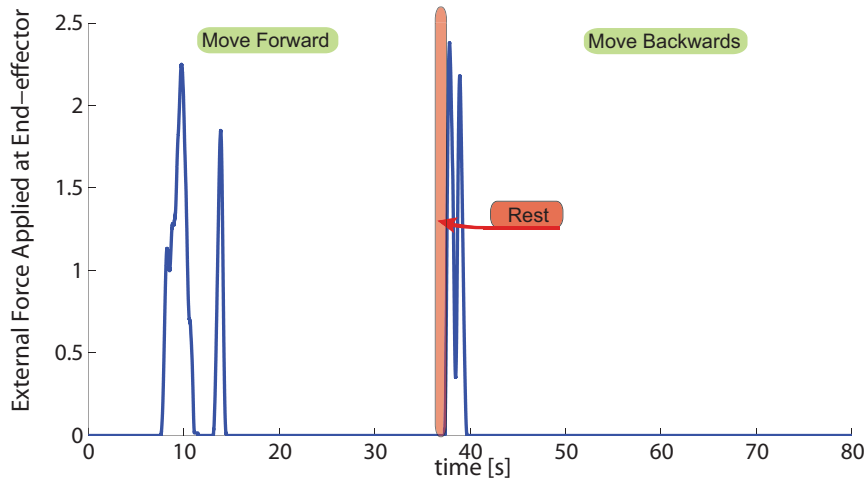


Figure 5.4: Force readings during the exercise.

5.5 Conclusions

In this chapter, we have proposed and implemented a BCI-based robotic rehabilitation system that enables online control of the robot’s velocity with the implicative probabilities of intention extracted from the LDA classifier. The control scheme was successfully implemented on the ASSISTON-MOBILE, where the speed of contour tracking was increased with increased intention level classified by BCI. Since this rehabilitation system was primarily designed for patients with little to no motion capability, increased intention to move the injured limb will be rewarded by faster task execution. On the contrary, lower intention levels will be penalized by slowing down the movement and halting it at the worst case. This real-time

modification/adaptation of the robot's velocity, ensures the active participation of the patient to his/her task. The proposed framework with contour tracking exercises has been shown to enable seamless on-line modification of task speed without endangering the safety of the patient, especially due to externally applied forces.

Chapter 6

Detection of Intention Level in Response to Task Difficulty from EEG

In Chapter 4 and 5, we have proposed a method which uses the posterior probabilities as the instantaneous intention levels of motor imagery but we have not analyzed the relationship between them. Hence, in this chapter, we present an approach that enables detecting intention levels of subjects in response to task difficulty utilizing an EEG based BCI. In particular, we use LDA to classify event-related synchronization (ERS) and desynchronization (ERD) patterns associated with right elbow flexion and extension movements, while lifting different weights. We observe that it is possible to classify tasks of varying difficulty based on EEG signals. Additionally, we also present a correlation analysis between intention levels detected from EEG and surface electromyogram (sEMG) signals. Our experimental results suggest that it is possible to extract the intention level information from EEG signals in response to task difficulty and indicate some level of correlation between EEG and EMG. With a view towards detecting patients' intention levels during rehabilitation therapies, the proposed approach has the potential to ensure active involvement of patients throughout exercise routines and increase the efficacy of robot assisted therapies.

6.1 BCI System

The training part of the Interface Type II (see Section 3.2.1) was used as the BCI component of this study to build datasets which contain resting and movement periods. A trial consists of a passive period followed by an active period with a cue. At the beginning of a trial, an acoustic stimulus indicates the beginning of a

trial and then a cross ‘+’ is displayed for 6 seconds which indicates a passive period. Then, a right arrow or ‘Relax’ text appears as a cue for 6 seconds. Therefore, the length of each trial is 12 seconds as shown in Figure 6.1. The order of the cues is random and a session consists of 3 runs with 20 trials (10 trials for right arm movement and 10 trials for relax).

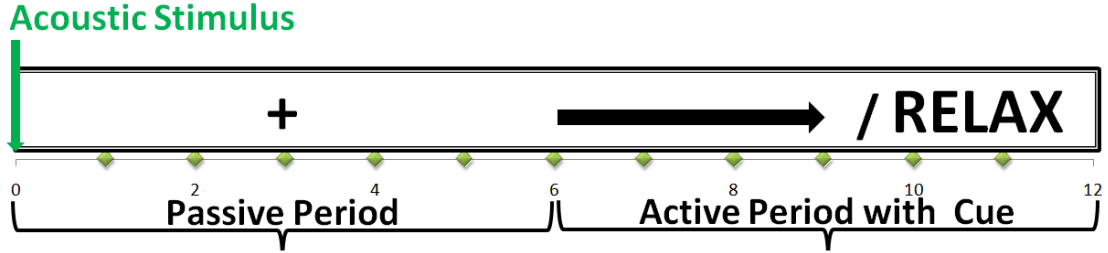


Figure 6.1: Timing scheme

6.2 EEG Experiments

A cue-based synchronous offline experiment consisting of 3 consecutive sessions with resting periods between each them to avoid fatigue, was designed to detect the intention level in response to task difficulty, from EEG signals. The task of the subjects is to relax or execute right elbow in fully flexed position followed by extension movements while lifting loads of different weights by their right hands according to the cues shown in the interface. The first session involves flexion and extension movements without any load. In the second session, the subject lifts a dumbbell when asked to execute right arm movements. For the third session, the weight of the dumbbell is increased. The weight of the lifted loads varies between 1280 – 7280 g depending on the subject’s skeletal muscles’ maximum power output.

6.2.1 EEG Data Collection

For EEG recordings, a Biosemi ActiveTwo EEG System is used. The recording configuration uses Ag-Cl electrodes at C_3 , C_z , C_4 locations of the international 10-20 electrode placement system, at 512 Hz sampling rate. Their anterior and posterior channels are used as references. By subtracting the average of the data received from anterior and posterior channels of a channel, three referenced main channels are obtained.

6.2.2 EEG Data Analysis

In this study, ERD and ERS are mainly characterized by the help of spectral powers computed in the typical EEG *alpha* (α , $8-13Hz$), *sigma* (σ , $14Hz-18Hz$), *beta* (β , $16-24Hz$) and *beta*₂ (β_2 , $24-30Hz$) frequency bands related to the preparation of the movements. To analyze these frequency bands the Short Time Fourier Transform is applied to each trial. The activity of the brain can be observed after the cue is shown. Hence, instead of analyzing frequency bands of the entire signal, a timing window is used. Afterwards, the average power spectral densities of the 4 selected frequency bands are calculated and selected as features. Therefore, 4 different spectral power densities are calculated for 3 different electrodes resulting in a 12-dimensional feature vector.

The performance of the LDA classifier is measured by applying two-fold cross validation for 300 times to obtain different training and test data sets which consists of the 75% and the 25% of the entire data, respectively. Overall classification accuracy is obtained by averaging over these 300 classification experiments.

The first classification problem is built separately for each session to classify right arm movement periods vs. resting periods. In the second classification problem, each session is classified against each other (load 1 vs load 2, load 1 vs. load 3, load 2 vs. load 3). Finally, the third classification problem contains 3 classes (load 1, load 2, load 3) and tries to find which load was being lifted during the trial. We note that load 1 indicates no load; load 2 is the lighter load, and load 3 is the heavier load.

Right handed 2 subjects, aged 23 and 25, have participated in this study. The classification accuracies obtained are listed in Tables 6.1, 6.2 and 6.3. For this experiment, β is found as the most informative frequency band. Therefore, the classification results where only the power spectral density of β is used as the feature, are also presented. The results show that movement periods can be detected successfully and the intention level of the subject in response to task difficulty may be extracted from the EEG signals with promising accuracy. Note that results in Tables 6.1 and 6.2 correspond to a two-class problem, whereas those in Table 6.3 correspond to a three-class problem.

Session	Frequency	Subject A	Subject B
1	<i>all</i>	79.64	83.43
	β	82.10	78.55
2	<i>all</i>	83	79.60
	β	85.38	78.29
3	<i>all</i>	88.22	87.36
	β	89.60	86.21

Table 6.1: Classification accuracies of the first classification problem (load vs. relax) of the EEG based experiments.

Load	Frequency	Subject A	Subject B
1 vs. 2	<i>all</i>	58.64	55.31
	β	64.62	63.90
1 vs. 3	<i>all</i>	88.31	79.05
	β	94.32	73.19
2 vs. 3	<i>all</i>	80.90	78.95
	β	89.45	79.52

Table 6.2: Classification accuracies of the second classification problem of the EEG based experiments.

Frequency	Subject A	Subject B
<i>all</i>	62.92	60.59
β	69.83	61.11

Table 6.3: Classification accuracies of the third classification problem of the EEG based experiments. This is a three-class problem.

6.3 EEG and EMG Experiments

EEG classification experiments in Section 6.2.2 have provided evidence that the EEG signals contain information about motor task difficulty. In this section, we consider a slightly different experimental set up, and not only run similar classification experiments to Section 6.2.2, but also provide an alternate evaluation mechanism to explore the same question. In particular, we exploit (and also verify) the well-known direct relationship between rectified sEMG signals and the weight of the load, and evaluate the correlation between simultaneously recorded EEG and sEMG signals. In this experiment, subjects are asked to execute flexion and extension movements where the elbow flexion is limited to 30° as shown in Figure 6.2. The angular limit in the elbow flexion plays an important role in the accuracy of the sEMG signal validation.

In this experiment, sEMG signals are collected simultaneously with EEG signals, from the biceps brachii, which is the muscle that lies on the upper arm between the shoulder and the elbow, with the aid of surface electrodes of a sEMG signal acquisition device (Delsys-Bagnoli-8). In particular, raw sEMG signals sampled at 1 kHz (using NI USB 6251) are filtered against inherent environmental noise and artifacts with a band-pass filter with a passband of 20-500 Hz. Then, these signals are full-wave rectified. The full-wave rectified signals are later utilized to extract the relation between the force exerted by the muscle and the intensity of sEMG signals.



Figure 6.2: Elbow flexion of 30° followed by extension.

6.3.1 EEG Data Analysis

Right handed 3 subjects (1 male, 2 females), aged 23-31, have participated in the EEG-EMG experiments. The same classification problems presented in Section 6.2.2 are analyzed and the accuracy results are shown in Tables 6.4, 6.5 and 6.6. The results support the inferences of Section 6.2.2 and demonstrate that elbow flexion which is limited to 30° periods, can be detected successfully and the intention level of the subject in response to task difficulty may be extracted from the EEG signals.

Since we have obtained promising accuracies when the average power spectral densities of *alpha* (α , $8-13Hz$), *sigma* (σ , $14Hz-18Hz$), *beta* (β , $16-24Hz$) and *beta*₂ (β_2 , $24-30Hz$) frequency bands were used as the features of the LDA classifier, we present a correlation analysis in Section 6.3.3 between these EEG features and the intention level features detected from sEMG.

Session	Frequency	Subject C	Subject D	Subject E
1	<i>all</i>	62.43	53.64	69.17
	β	59.38	53.64	65.62
2	<i>all</i>	71.72	60.45	74
	β	76.67	72.21	59.86
3	<i>all</i>	84.69	61.95	66.64
	β	83.23	64.69	71.03

Table 6.4: Classification accuracies of the first classification problem of the EEG-EMG based experiments.

Load	Frequency	Subject C	Subject D	Subject E
1 vs. 2	<i>all</i>	60.98	75.19	67.14
	β	70.74	77.31	64.12
1 vs. 3	<i>all</i>	84.46	76.36	76.26
	β	78.64	77.82	73.82
2 vs. 3	<i>all</i>	75.69	78.90	65.67
	β	60.74	74.21	68.15

Table 6.5: Classification accuracies of the second classification problem of the EEG-EMG based experiments.

Frequency	Subject C	Subject D	Subject E
<i>all</i>	54.65	63.37	49.85
β	52.017	68.45	49.84

Table 6.6: Classification accuracies of the third classification problem of the EEG-EMG based experiments. This is a three-class problem.

6.3.2 EMG Data Analysis

The RMS value of the sEMG signal is correlated with the level of physiological activities in the motor unit during muscle contraction. Hence, four different features were extracted from the RMS value of sEMG signals to reflect the properties of the muscle activation level depending on the executed task [71]. In particular, the maximum, sum and energy of the data inside the window containing the 3000th – 5000th samples (5.9 – 9.8s) and the energy of the 1500 samples centered around the maximum point of the EMG in a trial were used as the EMG features. In Figure 6.3, the means and the standard deviations of each feature calculated from the sEMG of *Subject D* and their p-values obtained from a t-test are shown. The increasing value of these features as a function of task difficulty indicates the positive correlation between the two, which is an expected behavior.

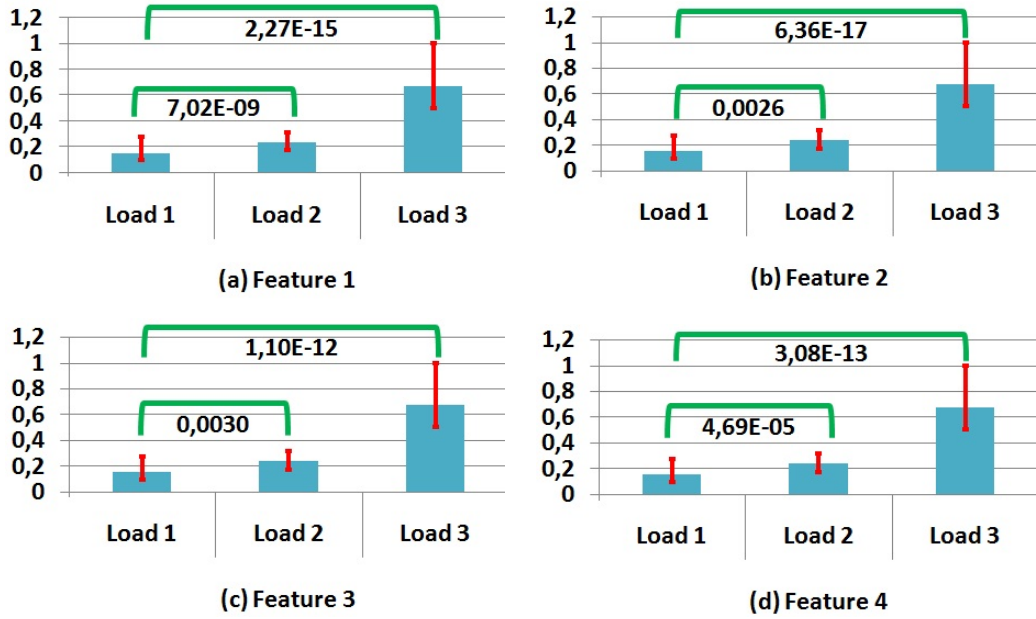


Figure 6.3: EMG features and p-values of Subject D: (a) Maximum, (b) sum, (c) energy of the signal between the 3000th – 5000th samples, and (d) energy of the 1500 samples centered around the maximum point of the EMG in a trial.

6.3.3 Correlation Analysis

Given the well-known relationship between the EMG signals and task difficulty, we are now interested in analyzing the correlation between features extracted from EEG and EMG signals. This analysis is aimed at supplementing our EEG classification experiments, which have already demonstrated that EEG signals are informative about intention levels of the subjects in response to task difficulty. The EEG-EMG correlation study provides an alternate analysis. The correlation coefficients for each of the EMG features were calculated for each frequency band, electrode and subject. The mean correlation coefficients across the EMG features for each subject are shown in Figure 6.4(a) and across the subjects for each EMG feature are presented in Figure 6.4(b). We observe that the correlation between the EMG features and the EEG features from the C_3 and C_z channels are consistent for each subject and for each EMG feature. Moreover, the correlation coefficients calculated in the C_4 channel are less than C_3 and C_z , when we use the all and alpha frequency bands as the EEG feature vector. Because for movement and imagery right arm tasks, a more intense response is obtained in C_3 than in C_4 , indicating

laterality in the motor cortex [12, 58, 59].

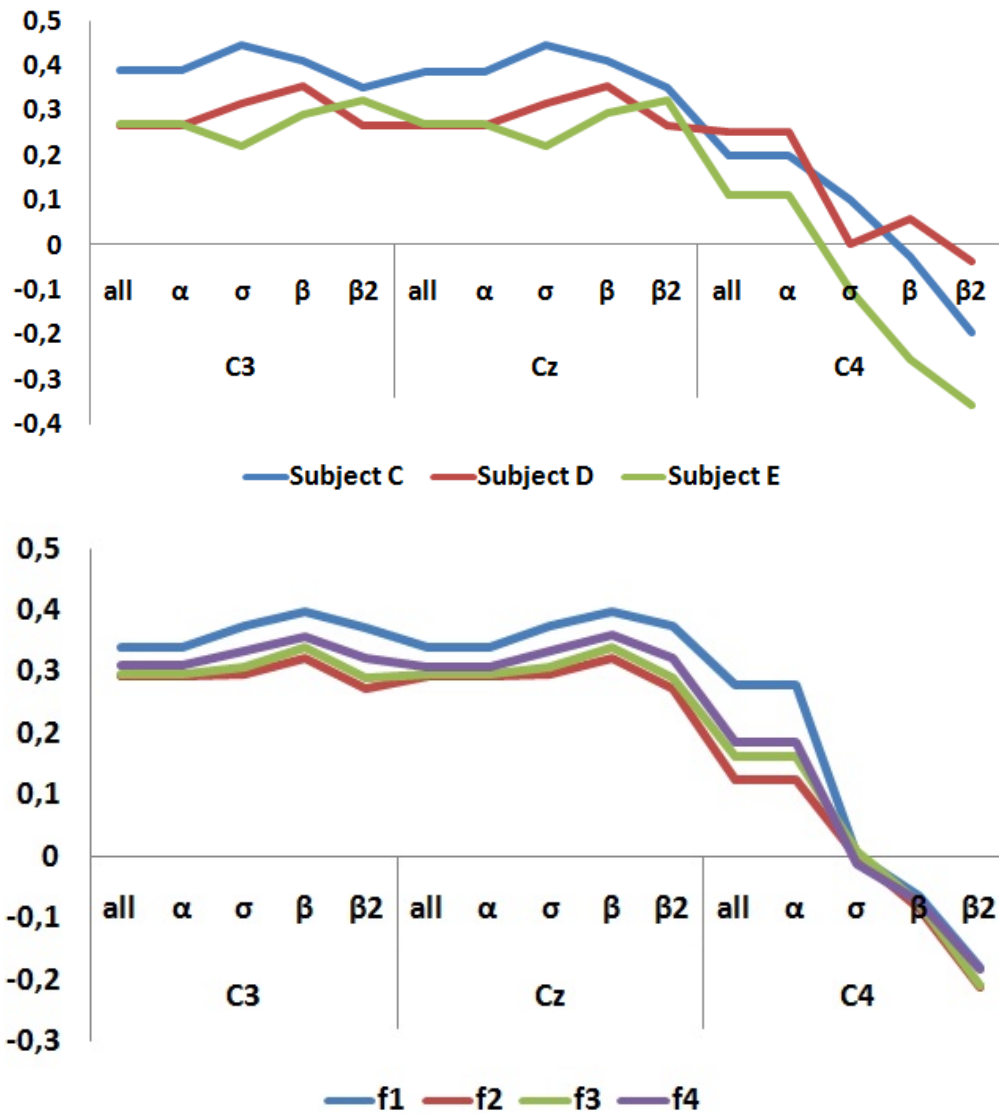


Figure 6.4: Correlation analysis: (a) The mean correlation coefficients across the EMG features for each subject, (b) the mean correlation coefficients across the subject for each feature.

6.4 Conclusions

In this chapter, we considered the question of whether EEG signals can provide information about the intention level of a subject in a motor task experiment in response to task difficulty. This is motivated by the desire to exploit information about the level of intention of patients in BCI-based robotic rehabilitation. We designed two distinct data collection experiments involving different levels of elbow

flexion and extension movements. Each experiment contained sessions dedicated to lifting loads of different weights, leading to varying levels of task difficulty. We collected EEG data using a cue-based synchronous set up, where subjects were asked to rest or to execute right elbow extension and flexion movements while lifting various weights. We used LDA to classify the ERD/ERS patterns. We posed several two-class and three-class classification problems, where classes correspond to task difficulty (weight of the load lifted) or indicate a relaxation interval. Our experimental results suggest that it is possible to extract information from EEG signals about the intention level of the subjects in response to task difficulty. In the second experiment, we collected EMG data in synchrony with the EEG data as well. Since EMG data are known to capture information about task difficulty in a motor task execution experiment, we also examined the information content of the EEG signals about task difficulty by analyzing the correlation between features extracted from EEG and EMG signals. Our results indicate some level of correlation between the two types of signals. On the other hand, the experiments presented in this chapter have some limitations which can be summarized as follows:

- During each following session, the weight of the loads gets heavier (e.g. In the first session, the subjects have not lifted any load and in the last session, they have lifted the heaviest load.). This may cause fatigue, and we may classify the fatigue state rather than the intention levels from the EEG. On the contrary, when there is fatigue, the task will be more difficult for the subject and therefore we may still detect the intention levels in response to task difficulty. Consequently, it will be worth to conduct these experiments with different order of sessions.
- Because of real arm movements, there will be some EMG artifacts in the EEG signals. There are several published works to eliminate the muscle artifacts from the EEG, by using linear filtering, regression, blind source separation, principal component analysis etc. [72]. An additional step which uses one of these methods may be added to be sure if the EEG features are classified or not.

Chapter 7

Comparative Experimental Analysis of BCI-Assisted Robotic Rehabilitation

Up to now, we have built an online EEG-based BCI system which has the potential to infer the motor imagery states of the subject to control a rehabilitation robot (see Chapter 5) and we have investigated the intention level information in the EEG as described in Chapter 6. Our agenda for the remainder of this thesis, is to present a series of online experiments to analyze the motivating key points of this study, which are listed as follows:

- Impact of robotic haptic feedback on BCI performance
- Comparison of using BCI continuously throughout robotic movement versus just for triggering the robotic movement
- Impact of the presence of BCI within the rehabilitation protocol on the motor cortical activity of the subject.

For this purpose, in this chapter, we present the new procedures and mechanisms we have developed for the use of the designed EEG-based BCI system in robotic rehabilitation, analyze the subject's active involvement levels, and present the detailed results with their conclusions.

7.1 Experimental Paradigm

In the state-of-art BCI-based rehabilitation systems the patients are asked to control a robotic device to which their arms are attached or to control a virtual system without obtaining any haptic feedback. In Chapters 4-5, we have implemented

offline and online robotic experiments but we have not analyzed the effect of online modification of the robot's velocity. Moreover, we have not conducted any online experiment to control a virtual ball presented in the testing part of the Interface Type II in Section 3.2.1. Therefore, we have not analyzed the effect of haptic or visual feedback on the active participation of the subject.

Consequently, an experiment in which the subject is asked to control a virtual ball of a VR shown on the screen or a robotic system, in particular ASSISTON-MOBILE, by means of right arm imagery movements, was designed to analyze the key issues listed at the beginning of this chapter.

A representative set-up of the experiments is shown in Figure 7.1.

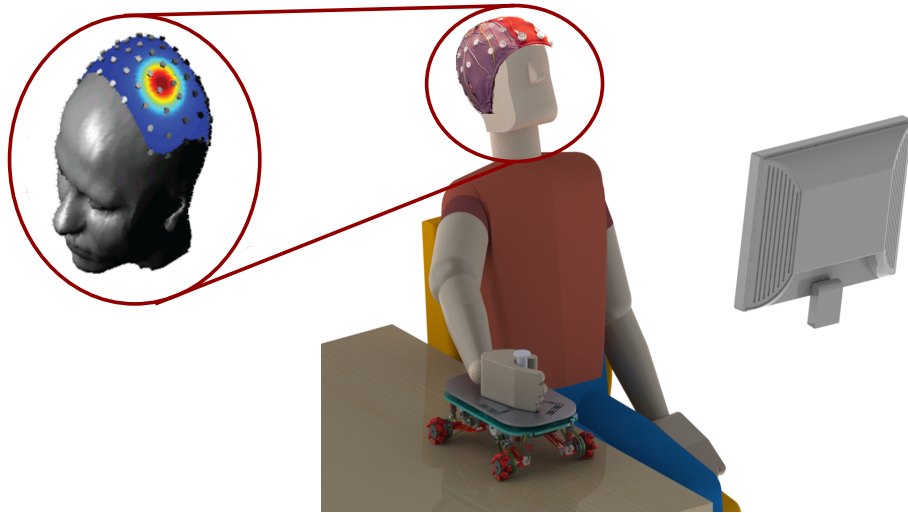


Figure 7.1: Representative experiment set-up.

An experiment consists of one session recorded in a day with consecutive 7 conditions ($C1, C2, C3, C4, C5, PA, PP$) where each condition includes its own training and testing blocks as briefly shown in Table I. The order of the conditions was randomized and there were resting breaks between each condition to prevent fatigue and any systematic effect.

Conditions	Training	Testing
$C1$	Robot moves	BCI assisted robot
$C2$	Robot does not move	BCI assisted robot
$C3$	Robot moves	BCI triggered robot
$C4$	Robot does not move	BCI assisted VR
$C5$	Robot does not move	BCI triggered VR
PP	-	Patient passive
PA	-	Patient active

Table 7.1: Experiment conditions.

The EEG signals were measured over C_3 , C_z , C_4 locations of the international 10-20 electrode placement system, at 2048 Hz sampling rate. Their anterior and posterior channels are used as references (CP_3 , FC_3 for C_3 , CP_z , FC_z for C_z and CP_4 , FC_4 for C_4). By subtracting the average of the data received from anterior and posterior channels of a channel, three referenced main channels are obtained. We note that the $C3$ and $C4$ notation indicates the condition 3 and 4, whereas the C_3 and C_4 notation indicates the name of the channels.

13 right-handed healthy subjects participated in this study voluntarily. All subjects participated in all conditions of an experiment. Before the experiments, all subjects have attended in a session in which they experience all the conditions of an experiment. Moreover, the subjects gave informed consent by signing a form.

Among 13 subjects, the results given in this study are based on 6 of them, since the remaining 7 subjects' data are inconsistent for each condition. Low classification accuracies (below 50% for at least 2 conditions) were obtained for these subjects. Therefore they were extracted from the data analysis part. The remaining 6 subjects are five males and one female with ages between 24 and 29 years.

In Figure 7.2, one of the excluded subject's and one of the included subject's averaged data across the trials of the $C2$ condition are shown. In the excluded subject's data, resting and MI periods cannot be separated and the classification accuracy of this condition is 46.2%. In the included subject's data, the resting and the MI periods are separated and the PSD values of the MI are smaller than the

resting periods as it is expected. Moreover, testing and training data are similar, since they both include MI periods.

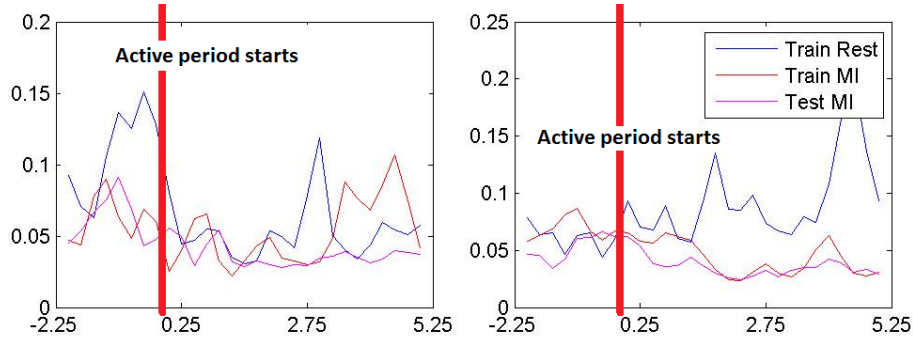


Figure 7.2: Subject elimination (results of channel C_3).

7.2 Training

We use separate training blocks for each condition. Each training block contains 10 trials (5 MI, 5 resting task) where a trial consists of 8 s of a passive period followed by 5 s of an active period with a cue. Therefore, the length of each trial is 13 s as shown in Figure 7.3(a). The training Interface Type II (see Section 3.2.1) was used. The first trial always contains a MI task to remind the condition protocol and is eliminated for the analysis of the data to have equal size of trials for each task.

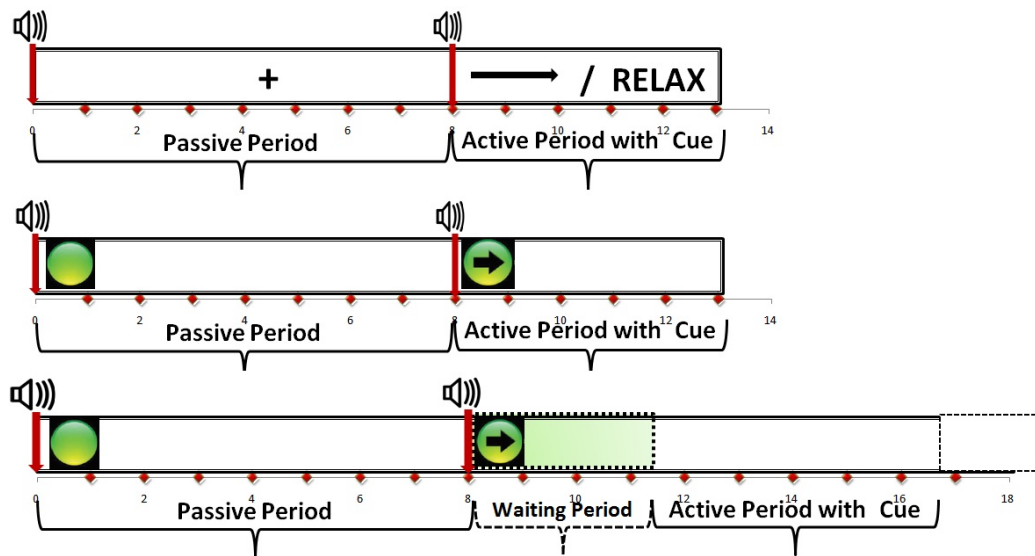


Figure 7.3: (a) Training timing scheme (b) Testing timing scheme of C_1 , C_2 , C_4 , PA and PP (c) Testing timing scheme of C_3 and C_5

In the passive periods the signals are not analyzed to give the opportunity to the subjects to execute little movements to prevent fatigue before the active periods. In the active periods, the subjects are asked to rest or imagine right arm movements according to the cues shown on the screen. In $C1$ and $C3$, the robotic system on which the subjects' arm is attached, moves forward with a constant velocity during the right arm imagery movement tasks to assist the subject to be more involved in their tasks. The robotic system returns to its initial position in 5 s in the passive periods. In $C2$, $C4$ and $C5$, there is no robotic movement in the training phase. The subject is asked either to perform MI or rest. The recorded labelled EEG data are used to train the classifiers, just like in a BCI experiment (such as the ones described in Chapter 3) without any robotic movement.

7.2.1 Analysis of the Training Data

In Figure 7.4 the logarithm of the averaged PSD values between the second and the third seconds of the active period, versus the frequency band $0 - 30Hz$ are presented for C_3 , C_z , C_4 channels. Looking at the figures, the difference between the log power values of the resting and MI periods in the alpha frequency band are greater than the log power values in the other frequency bands. This significant difference indicates that the alpha frequency band may be used to infer the MI periods. Moreover, the log power values of the resting periods are greater than the log power values of the MI periods for all electrodes, since ERD occurs during MI and the PSD values become smaller.

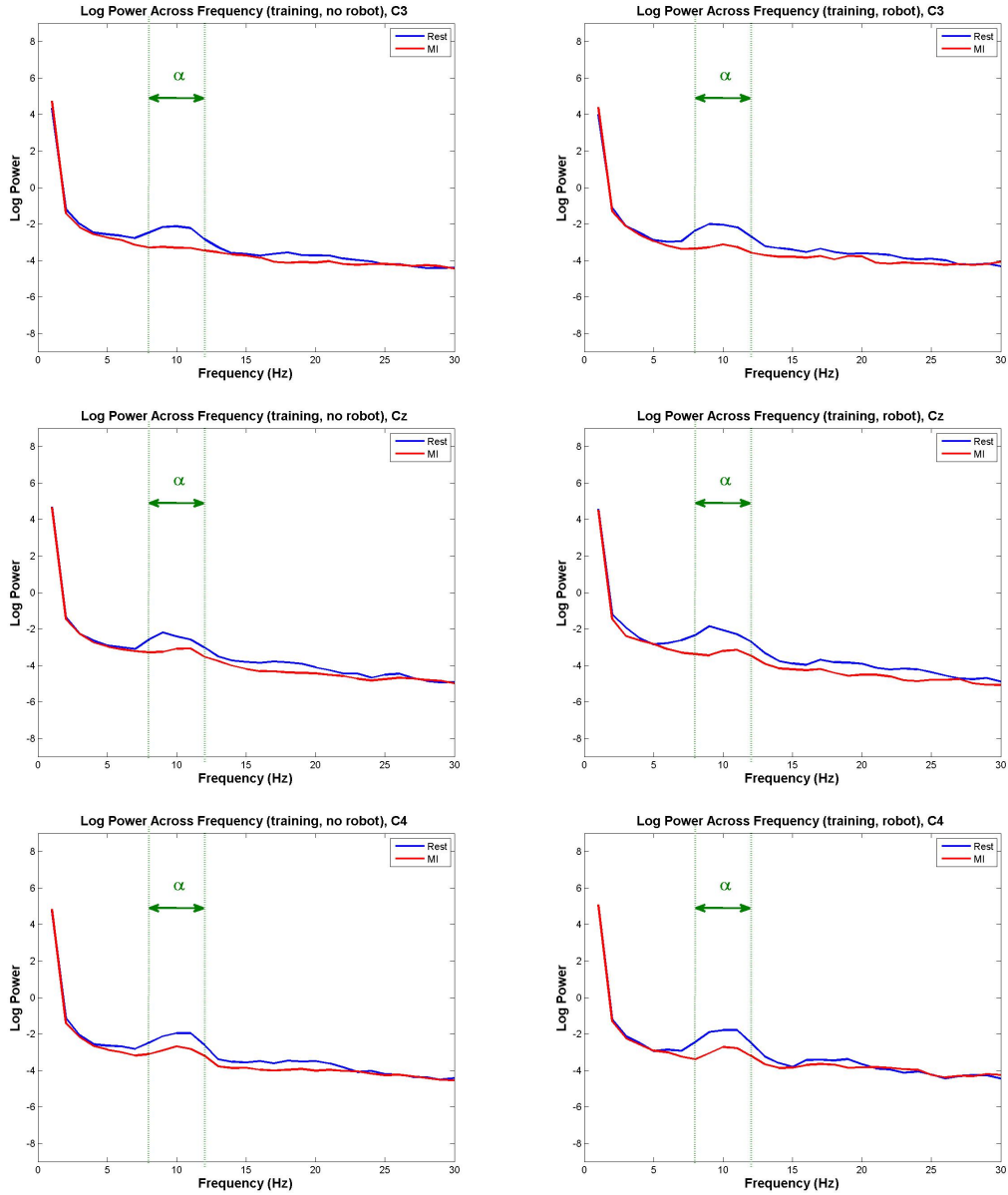


Figure 7.4: Averaged log PSDs for robot and non-robot assisted MI tasks.

The training blocks are very important for BCI based systems, since the quality of the training data directly affects the performance of the classifier and consequently the efficacy of the BCI systems. In particular, we are interested in understanding whether such haptic feedback improves the separability of MI and rest classes in the measured EEG data. To this end, the averaged results over robot-assisted ($C1$, $C3$) and non-robot assisted ($C2$, $C4$, $C5$) conditions are analyzed.

In Figures 7.5 to 7.7, the averaged power spectrum densities across the subjects as a function of time are shown for the C_3 , C_z and C_4 electrodes. Our key observations concluded from these figures can be listed as follows:

- The PSD values of motor imagery (MI) task are smaller than the resting task as expected in the active period. Consequently, the ERD in the case of motor imagery (MI) task is more intense.
- The PSD values of MI periods are smaller in channel C_3 than C_z and C_4 . Because of the laterality in the motor cortex, during the right arm MI tasks, the left side of the brain becomes more intense [12, 58, 59].
- The resting periods are similar for robot assisted and non-robot assisted protocols, since there isn't any robot movement in the resting periods of the robot assisted protocols either.
- We observe that the PSD values of resting periods in channel C_z are greater than the values in the C_3 and C_4 channels. Since we focused on the MI tasks to analyze the involvement level of the subject in different protocols in this chapter, the reason of this observation will be investigated in a future study.
- For **the C_3 channel**, the suppression in the PSD values of the robot assisted training tasks is more continuous than the non-robot assisted training tasks. The PSD values of the robot assisted training tasks are suppressed prior to non-robot assisted tasks.
- For **the C_z channel**, the suppressions in the PSD values of the robot assisted and non-robot assisted training tasks are not continuous.
- For **the C_4 channel**, the PSD values of the robot assisted training tasks are continuously suppressed where the PSD values of the training tasks without robot assistance increases at 3 s after the cue is shown.
- We may say that the robot assisted training protocols provide more intense MI tasks for the C_3 and C_4 channels and the PSD values are more suppressed in the C_3 channel for the robot and non-robot assisted training tasks.

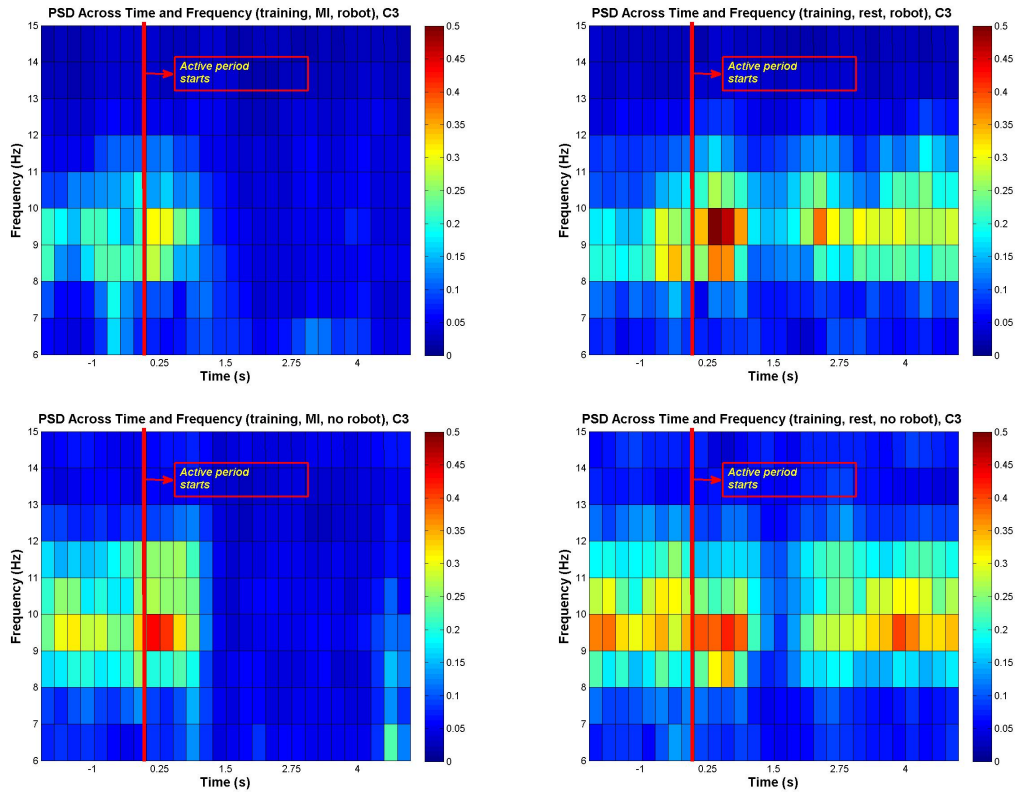


Figure 7.5: PSD across time values of the electrode C_3 : Power spectra in movement periods and the rest periods for the electrode C_3 in the frequency band $6 - 15Hz$ for the training blocks with and without the robotic system guiding the subjects arm.

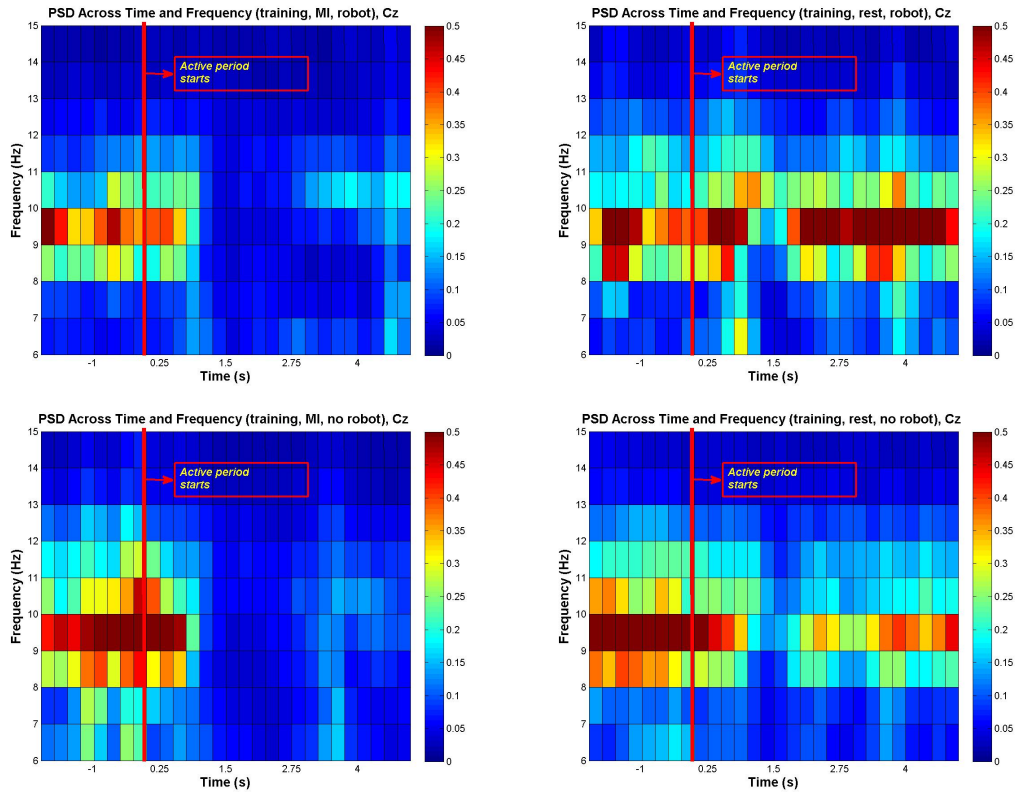


Figure 7.6: PSD across time values of the electrode C_z : Power spectra in movement periods and the rest periods for the electrode C_z in the frequency band $6 - 15Hz$ for the training blocks with and without the robotiv system guiding the subjects arm.

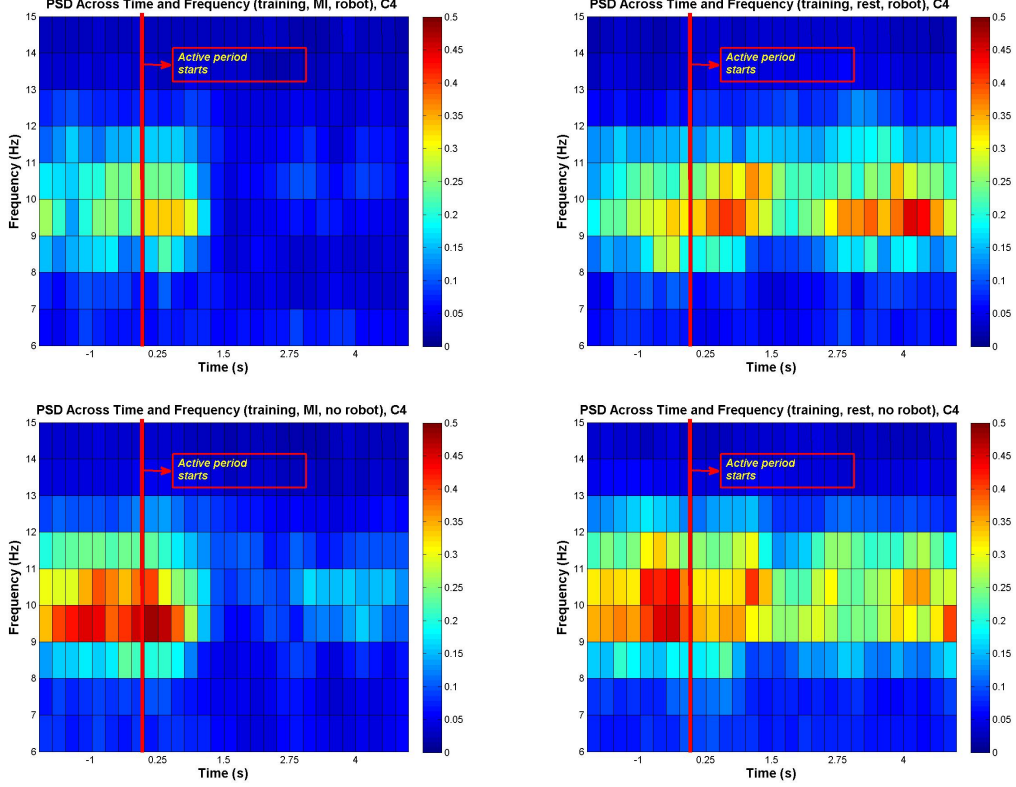


Figure 7.7: PSD across time values of the electrode C_4 : Power spectra in movement periods and the rest periods for the electrode C_4 in the frequency band $6 - 15Hz$ for the training blocks with and without the robotic system guiding the subjects arm.

A one tailed t-test which tests if the averaged PSDs in the alpha frequency band of the resting periods are significantly ($p = 0.05$) greater than the motor imagery periods ($PSD_{Resting} > PSD_{MI}$) was applied and the p -values are graphically presented for robot assisted and non-robot assisted training protocols in Figure 7.8. We can list our key points as follows:

- For the robot assisted training protocols, the $PSD_{Resting}$ becomes significantly greater than the PSD_{MI} 1 s after the cue is shown till the end of the trial.
- The p -values are mostly smaller for the MIs with robot movements than the MIs without robot movements. This point supports the inference that the robot assisted training protocols provide more intense MI tasks.
- For all three electrodes, we obtained small p -values. Therefore, we may say that the feature obtained from C_3 , C_z and C_4 can be used for right arm imagery movement and resting tasks discrimination.

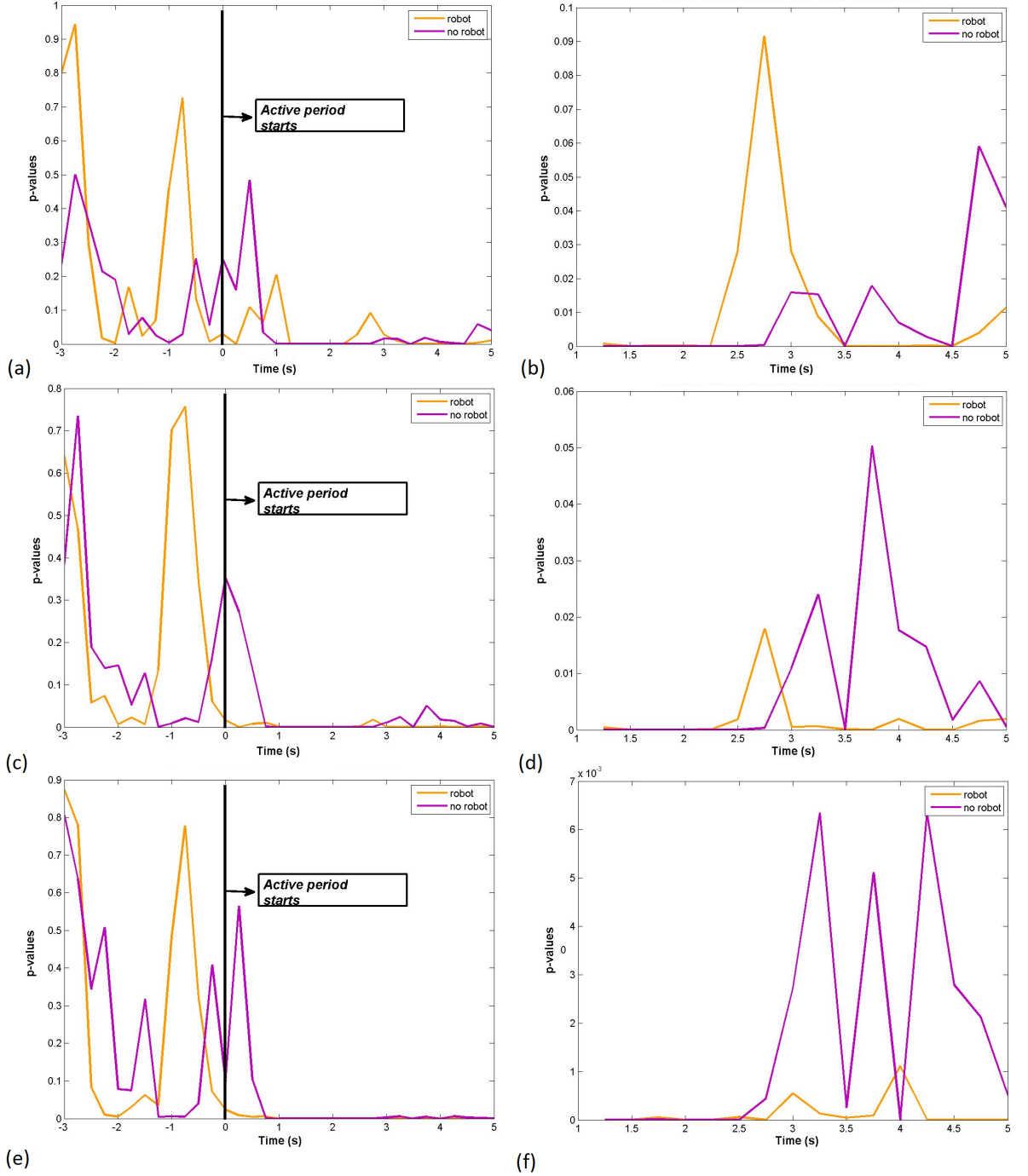


Figure 7.8: p -values of t-test ($PSD_{Resting} > PSD_{MI}$) for averaged PSDs in the alpha, as a function of time. The cue is shown at 0s. (a-b) C_3 , (c-d) C_z , (e-f) C_4

In conclusion, we may say that we can build the training model with better quality by using the robot-assisted training protocols which measures the EEG over C_3 , C_z and C_4 channels and uses the averaged PSDs of alpha frequency band as the features. For this study, we have mainly focused on the C_3 channel to analyze the participation level of the subjects, because of the laterality of the brain.

7.2.2 Building the Training Model

ERD and ERS are characterized by the help of spectral powers computed in the typical EEG alpha band ($8 - 13Hz$) for the C_3 channel. To analyze this frequency band the Short Time Fourier Transform is applied to each trial. The activity of the brain can be observed after the cue is shown. Hence, instead of analyzing frequency bands of the entire signal, a timing window between 2 and 3 seconds is used. Afterwards, the average power spectral densities of the alpha frequency band are calculated and selected as features. Therefore, spectral power densities of alpha are calculated for 3 different electrodes resulting in a 3-dimensional feature vector.

7.3 Testing

A testing block contains 15 trials where a trial consists of 8 s of a passive period followed by 5 s of an active period in which the subjects are asked to execute imagery or real right arm movements (see Figure 7.3(b)). At the beginning of each period, an acoustic stimulus indicates the beginning of a trial. The feedback to the subject is given with a virtual ball presented in the testing part of the Interface Type II (see Section 3.2.1) or ASSISTON-MOBILE robotic system in the active periods. The feedback system returns to its initial position during the passive period during which the signals are not analyzed and waits for the next trial. There are four kinds of testing blocks which are defined as follows:

- **BCI-assisted Conditions:** The subjects are asked to execute right arm imagery movements to move a virtual ball or the ASSISTON-MOBILE robotic system as fast as they can. The velocity is updated every 250 ms according to the outputs obtained from the LDA classifier of BCI, aiming to reflect the intention level of the subject. In $C1$ and $C2$, ASSISTON-MOBILE provides haptic feedback, and in $C4$, the virtual reality system provides a feedback with a virtual ball.
- **BCI-triggered Conditions:** In the triggered conditions there is an additional period between passive and active periods which is called the waiting period. In this period, the subjects are asked to execute right arm imagery

movements to trigger a virtual ball or the ASSISTON-MOBILE robotic system movement with a constant velocity. When an intention of movement is detected, the waiting period ends and the active period starts. The maximum and the minimum duration of a waiting period is 10 s and 500 ms long since the first 250 ms of a waiting period is not analyzed and the first intention can be detected in the second 250 ms (see Figure 7.3(c)). In the active period, the feedback system moves with a fixed velocity without considering the LDA classifier outputs. Therefore even if the subject is not actively involved in the task during the active period and has a decrease in his/her intention level, the system gives the same feedback. In *C3* and *C5*, the subjects were asked to trigger the ASSISTON-MOBILE and the virtual ball, respectively, by executing right arm imagery movements.

- **Patient Active:** In the *PA* condition, the subjects are asked to move ASSISTON-MOBILE by applying forces. The velocity of the robot is updated based on the applied force magnitude. Therefore, in this condition the subjects are actively involved in the task.
- **Patient Passive:** In the *PP* condition, ASSISTON-MOBILE moves forward with a constant velocity and guides the subject's arm to complete the movement without considering the EEG signals. Therefore, in this condition the subjects do not control the system and they do not have to execute right arm imagery movements. This protocol is the conventional robotic rehabilitation protocol for the patients whose severe motor disabilities preclude their voluntary muscle control and physical contribution to their task.

7.3.1 Analysis of the Testing Data

The aim of this study was to compare the active participation level of the subjects in their tasks in different conditions to find the most efficient rehabilitation concept. We measure this participation level with the PSD values. Since it is known that during MI, ERD occurs and the PSD values become smaller, then the active participation level may be measured by the values of PSDs. Hence, our objective is to find a therapy protocol in which the PSD values are continuously the smallest. For

this analysis, because of the laterality of the brain we have presented the results obtained from the C_3 channel. Therefore, we analyzed the data with 4 small timing windows ($0 - 1, 1.25 - 2.25, 2.5 - 3.5, 3.75 - 4.75$ s).

The logarithm of the averaged PSD values between the second and the third seconds of the active period are shown in Figure 7.9 as a function of frequency band $0 - 30Hz$. Looking at the figures, we observe the peaks in the alpha frequency band. Our key observations, which we subsequently justify through quantitative analysis in this chapter, are as follows:

- **The impact of haptic feedback through robotic movement on cortical activity (hence BCI performance):**

When we examine the results of the BCI-assisted protocols, the log power values in the alpha frequency band of the $C4$ in which the virtual ball was controlled are greater than the values obtained in the condition $C1$ in which the haptic feedback was provided to the subject by the robotic system. Moreover the log power values of the condition $C2$ which also provides haptic feedback but has a non-robot assisted training protocol, are close to $C4$ in the alpha frequency band.

For BCI-triggered protocols, the $C3$ protocol in which the robotic system was controlled has smaller log power values in the alpha frequency band than C_5 . This difference may be caused because of the haptic feedback which has the potential to make the subjects more involved in their tasks.

- **The impact of adding BCI to a robotic rehabilitation protocol:**

In $C1$ and PA in which the subjects are the active participant of the protocol, we observe lower PSD values in the alpha frequency band than values of the PP condition in which the subject is not an active participant of the protocol. Consequently, we may say that more intense MIs can be observed in $C1$ and PA conditions than PP .

The log Power values computed from the C_3 channel are similar for the $C1$ and the PA conditions. As it known that PA is a protocol which guarantees the active participation of the subject, we may say that the impact of adding

BCI in $C1$ to the robotic rehabilitation protocol has the potential to increase the subject's active participation level.

Overall, these observations suggest that BCI-assisted robotic therapy can enable motor cortical activity, which is

1. similar to a scenario in which the subject could actually execute the motion,
2. much stronger than the activity produced in a conventional patient-passive rehabilitation protocol.

- **Comparison of two different ways to use BCI (continuous use during movement versus just to trigger movement):**

The BCI-triggered robotic condition $C3$ has larger log Power values than the BCI-assisted robotic condition $C1$. The BCI-triggered VR condition $C5$ has larger log Power values than BCI-assisted robotic condition $C4$. These observations favor the continuous use of the BCI during the MI.

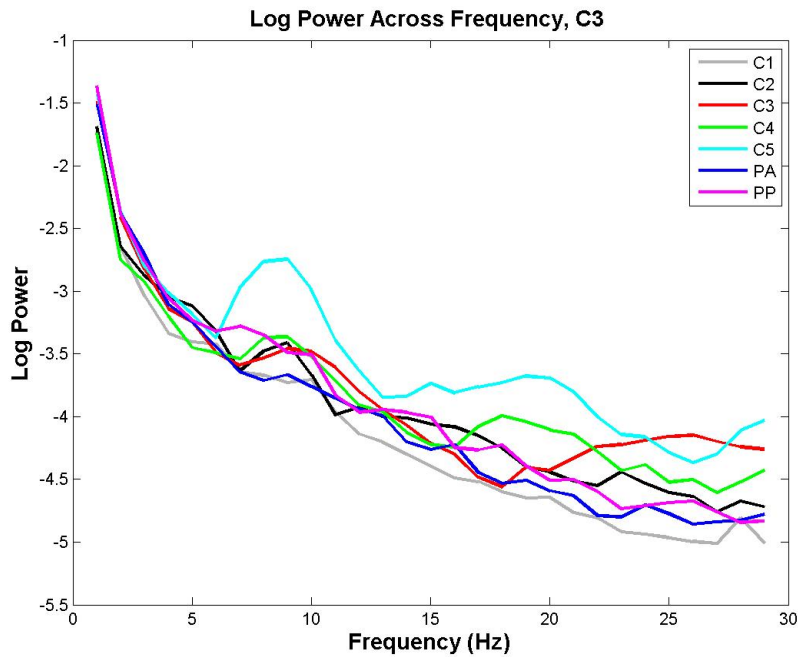


Figure 7.9: Averaged log PSDs for all conditions at C_3 channel.

We applied three different types of analysis to investigate these motivating observations in detail. For this purpose, we present the figures of averaged PSD values

across the subjects for each condition with their conclusions and we provide the t-test results of these analysis. In these t-tests, the p -value has been chosen as 0.05 for the statistical significance level.

Analysis 1: The impact of haptic feedback through robotic movement on cortical activity (hence BCI performance)

In Figure 7.10, the averaged PSD values across the subjects are given for $C1$, $C2$ and $C4$ conditions for the C_3 channel. We can observe from the figure that the PSD values of $C1$ are more intense than the PSDs of $C4$. Since $C1$ provides haptic feedback where $C4$ provides virtual feedback. Moreover, the PSD values in $C1$ are more suppressed and more continuous than the values in the $C2$. The suppression in the $C2$ begins prior to the $C4$ and it is more intense at the beginning of a trial, but it is not continuous. As the time passes these two conditions become similar.

One tailed and two tailed t-tests were applied to investigate the difference of the PSD values in these conditions The t-test results given in Table 7.2 and Figure 7.10 show that:

- In the first timing window, the PSD values of $C1$ are not significantly smaller than $C2$ but the p -value is very close to 0.05. As the time passes, for the other timing windows they become significantly smaller than the values in $C2$. Since the $C1$ has a robot-assisted training protocol, the subject's performance is better than $C2$ because of the quality of training model.
- The PSD_{C1} is significantly smaller than the PSD_{C4} for all timing windows. $C1$ has a larger ERD than $C4$ since the feedback was given haptically instead of virtually.
- At the beginning of the trials (in the first timing window), $C2$ is more intense than $C4$. But in the following timing windows, these two conditions become similar and they are not significantly different.

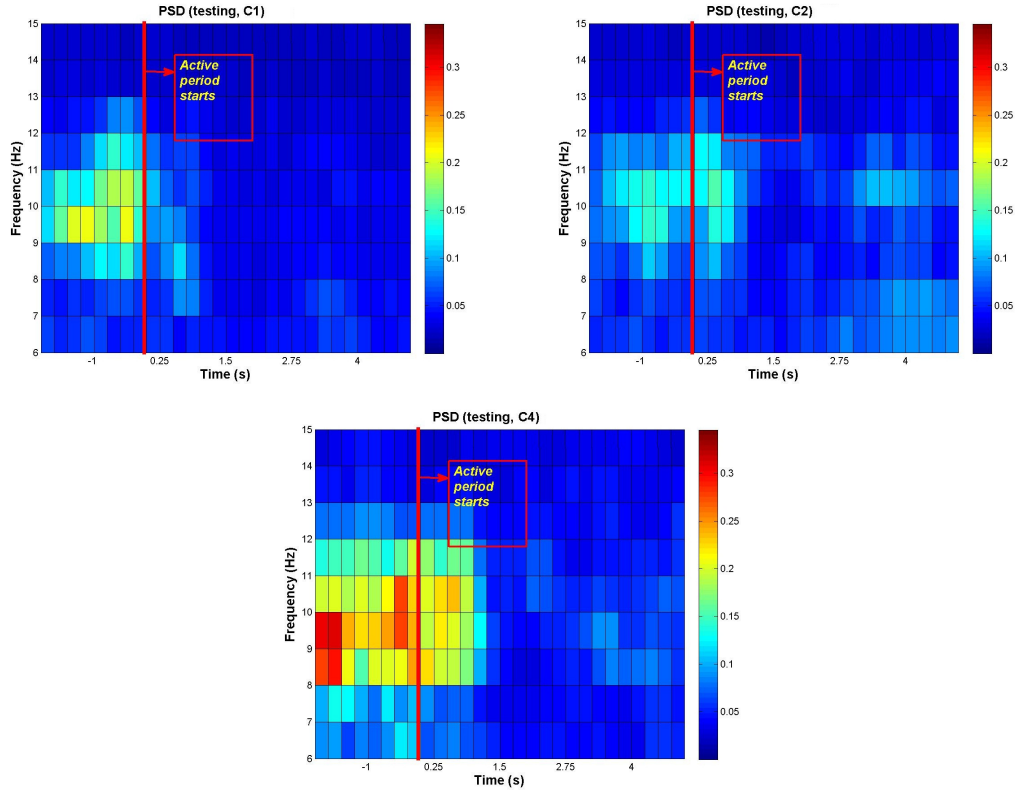


Figure 7.10: PSD values across time for C_1 , C_2 , C_4 conditions obtained from the C_3 channel.

Table 7.2: p -values for C_1 , C_2 , C_4 .

	0–1	1.25–2.25	2.5–3.5	3.75–4.75
$C_1 < C_2$	0.056017	0.037798	0.02194	0.008087
$C_1 < C_4$	2.17E-05	0.000801	0.008295	0.000103
$C_2 < C_4$	0.000963	0.15447	0.532643	0.537954
C_1 / C_2	0.112034	0.075596	0.04388	0.016174
C_1 / C_4	4.33E-05	0.001601	0.016589	0.000206
C_2 / C_4	0.001927	0.308939	0.934713	0.924093

In Figure 7.11, the averaged PSD values across the subjects are given for C_3 and C_5 conditions which contain the triggered protocols. From this figure, it can be observed that the ERD in C_3 is greater than C_5 . This may be because of the haptic feedback provided in C_3 . One tailed and two tailed t-tests results are given in Table 7.3. The significant p -values in every timing window indicates that the

PSD_{C3} is smaller than the PSD_{C5} . Therefore, the haptic feedback through robotic movement appears to enhance the MI activity observed in the motor cortex. This suggests the potential of haptic feedback to improve BCI performance.

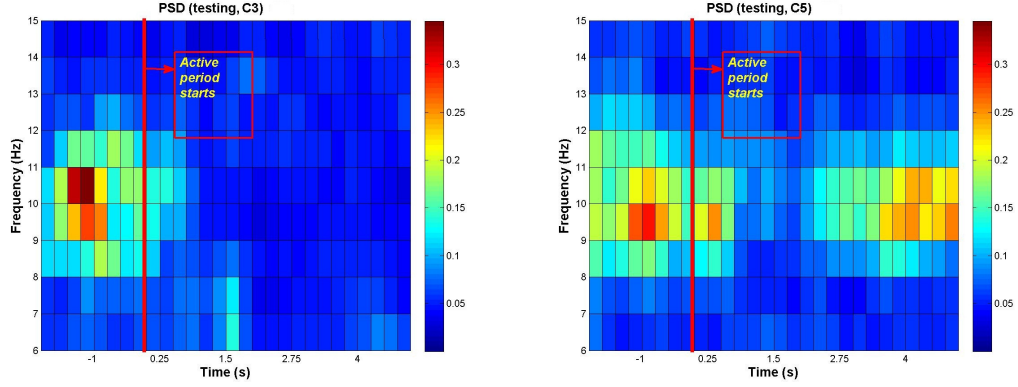


Figure 7.11: PSD values across time for $C3$, $C5$ conditions obtained from the C_3 channel.

Table 7.3: p -values for $C3$, $C5$.

	0–1	1.25–2.25	2.5–3.5	3.75–4.75
$C3 < C5$	0.016046	6.64E-05	4.7E-08	5.2E-09
$C3/C5$	0.032093	0.000133	9.41E-08	1.04E-08

Analysis 2: The impact of adding BCI to a robotic rehabilitation protocol.

In Figure 7.12, the averaged PSD values across the subjects are given for $C1$, PA and PP . In PA , the subject is the active participant, whereas in PP , the subject is passive. $C1$ is the condition which has a robot assisted training protocol that gives the opportunity to build training models with better quality and in the testing block $C1$ uses the BCI as the continuous controller of the robot’s velocity. We compared $C1$ with PA and PP conditions to investigate the impact of adding BCI to a robotic rehabilitation protocol.

Examining Figure 7.12, we may say that PSD_{PP} is greater than PSD_{C1} and PSD_{PA} . This is an expected behaviour, since in PA , it is known that the patient actively moves his/her arm, whereas in PP the robot moves the subject’s arm when

the subject is passive, and finally in $C1$ the subject tries to actively imagine right arm movement. Moreover, we cannot differentiate PA and $C1$ by looking their PSD plots.

One tailed and two tailed t-test results are given in Table 7.4. The significant p -values in every timing window indicates that the PSD_{C1} is smaller than the PSD_{PP} . PSD_{PA} is significantly smaller than PSD_{PP} for all timing windows except the last one. Moreover, according to the results, PSD_{C1} and PSD_{PA} are not significantly different except the last timing window. This result is promising for BCI-based rehabilitation, since having a rehabilitation system for stroke patients which helps them to imagine movements as strong as the active movements, may increase the effectiveness of the therapy. Therefore, we may make an $PSD_{PA} \cong PSD_{C1} < PSD_{PP}$ order to measure the participation level of the subjects.

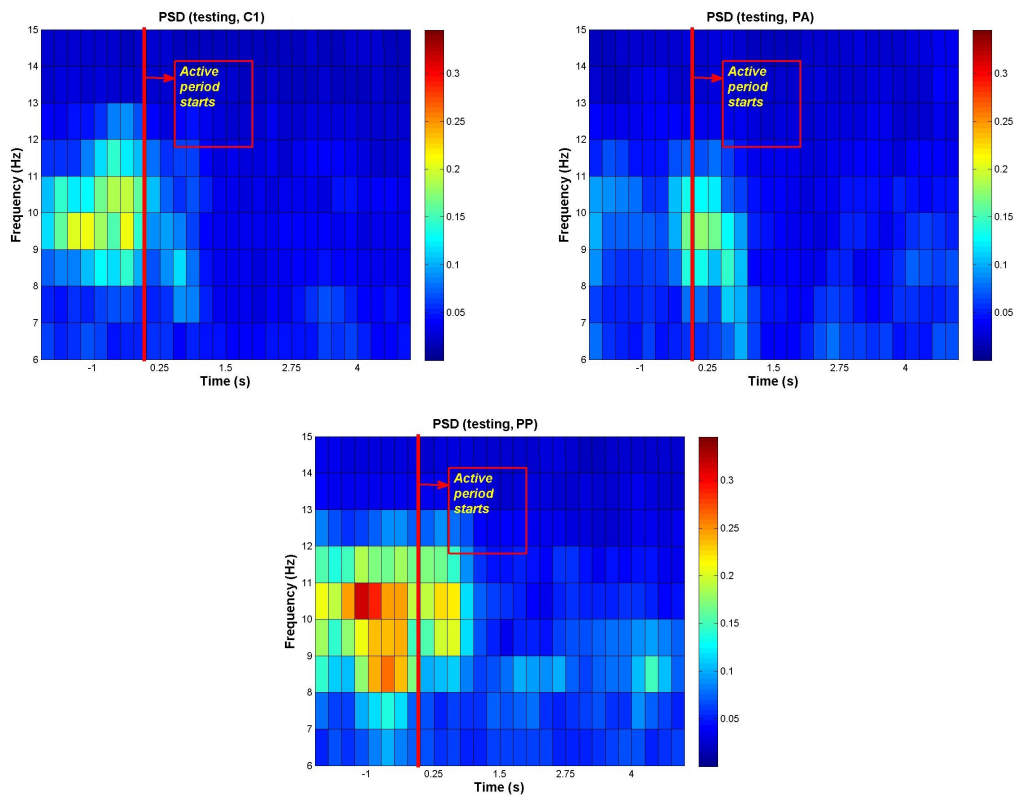


Figure 7.12: PSD values across time for $C1$, PA , PP conditions obtained from the C_3 channel.

Table 7.4: p -values for $C1$, PA , PP .

	0–1	1.25–2.25	2.5–3.5	3.75–4.75
$C1 < PA$	0.176782	0.202874	0.234988	0.021459
$C1 < PP$	0.002824	0.001112	0.00206	0.003573
$PA < PP$	0.040901	0.001749	0.008047	0.094319
$C1/PA$	0.353564	0.405747	0.469977	0.042918
$C1/PP$	0.005648	0.002225	0.004119	0.007147
PA/PP	0.081802	0.003498	0.016093	0.188638

Analysis 3: Comparison of two different ways to use BCI for robotic control (continuous use during movement versus just to trigger movement.):

In Figure 7.13, the averaged PSD values across the subjects are given for BCI-assisted and BCI-triggered robotic control conditions $C1$ and $C3$. From this figure, it can be observed that the ERD in $C1$ is more intense than in $C3$. One tailed and two tailed t-tests results are given in Table 7.5. At the beginning of a trial the difference between these two conditions are not significant. But in the following timing windows, PSD_{C1} becomes significantly smaller than PSD_{C3} .

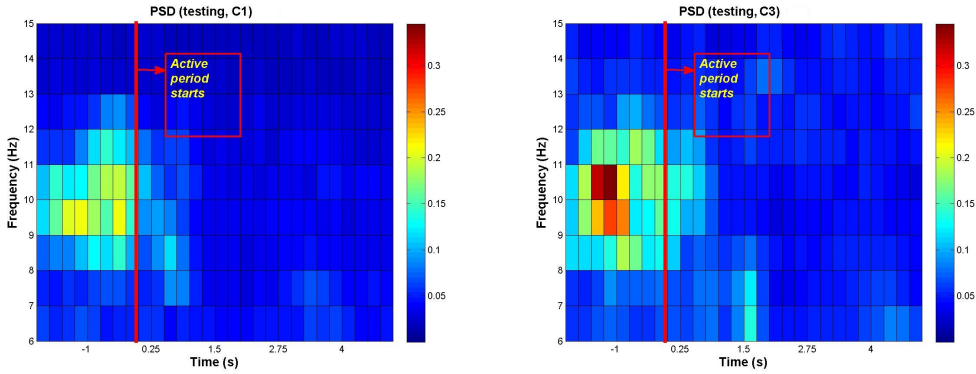


Figure 7.13: PSD values across time for $C1$, $C3$ conditions obtained from the C_3 channel.

In Figure 7.14, the averaged PSD values across the subjects are given for BCI-assisted and BCI-triggered VR conditions $C4$ and $C5$. From this figure, we see that the ERD in $C5$ is not continuous and the PSD_{C5} values are getting larger than $C4$ as the time passes. From the one tailed and two tailed t-tests results given in Table

Table 7.5: p -values for $C1$, $C3$.

	0–1	1.25–2.25	2.5–3.5	3.75–4.75
$C1 < C3$	0.12701	0.001001	0.012594	0.001346
$C1 / C3$	0.25402	0.002002	0.025187	0.002693

7.6, we see that in the first timing window these two conditions are not significantly different but in the other three timing windows PSD_{C4} is significantly smaller than PSD_{C5} .

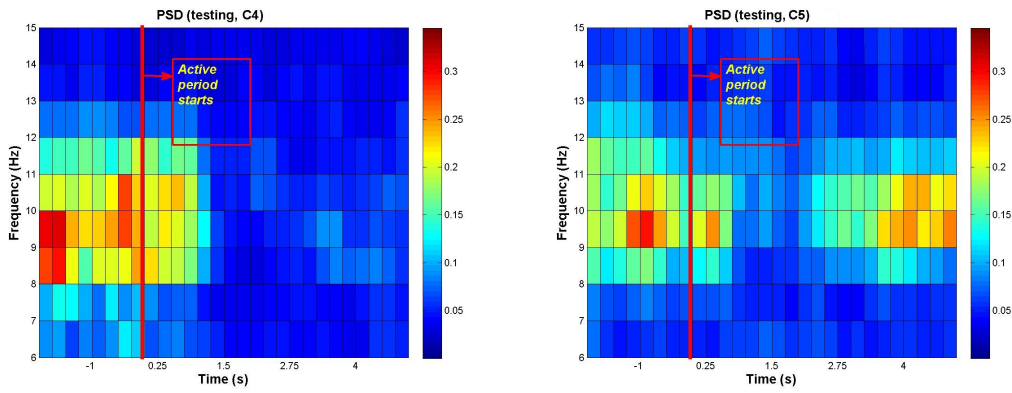


Figure 7.14: PSD values across time for $C4$, $C5$ conditions obtained from the $C3$ channel.

Table 7.6: p -values for $C4$, $C5$.

	0–1	1.25–2.25	2.5–3.5	3.75–4.75
$C4 < C5$	0.951512	0.000143	5.15E-06	1.06E-07
$C4 / C5$	0.096975	0.000286	1.03E-05	2.11E-07

In conclusion, in this analysis we compared the two different ways to use BCI for robotic control (continuous use during movement versus just to trigger movement.). We may conclude that the continuous use of BCI may help the subject remain continuously involved in their tasks.

7.3.2 Classification

In the previous sections of this chapter, we have analyzed the structure of the training and the testing data. We have concluded that adding BCI to a robotic rehabilitation system has a potential to help the patient imagine movements as strong as the active movements and increase the effectiveness of the therapy. The efficacy of the BCI is very important for the robotic rehabilitation systems, to provide “assist-as-needed” protocols. Therefore in this section, we compare the performance of the ways (triggered/assisted) to use BCI and the methods (haptic/visual) to provide feedback. For this purpose, we analyzed the MI detection performance of the LDA classifier for $C1$, $C2$, $C3$, $C4$ and $C5$ conditions.

In the training blocks, we have collected data of two classes (right arm imagery movement and resting task). On the other hand, in the testing blocks the subjects were asked to imagine only right arm movements. Therefore, we have built a detection problem for MI periods rather than a classification problem. Two different values were used to present the two classes. 2 is used to indicate MI tasks where the resting tasks are indicated by 1. In the testing block, the LDA classifier uses the power spectrum densities in the alpha frequency band as the feature and produces an output in each 250 ms . The first 500 ms and the last 250 ms of an active period are not analyzed. Therefore by using Equation 7.1, there are 17 window samples for each trial and 255 for a condition. The outputs are averaged in a moving window of 1 s and form a continuous input for the feedback system for online velocity modification.

$$\frac{5\text{ s} - 750\text{ ms}}{250\text{ ms}} = 17\text{ windows.} \quad (7.1)$$

As the power spectral densities of one frequency band (alpha) are calculated for 3 different electrodes, we obtain a 3-dimensional feature vector. In the online experiments, we have used the features obtained from C_3 , C_z , C_4 electrodes. But for the offline analysis of the data, we have focused on the C_3 channel. Because during the right arm MI tasks, the left side of the brain becomes more intense [12, 58, 59]. Consequently, we present our results obtained by only using the C_3 channel which is located on the left hand side of the brain.

The training blocks for each condition are independent and separate classifiers are learned from such training data. Therefore, although both $C1$ and $C3$ have

robot assisted training protocols, they have their own training blocks. In the same way, C_2 , C_4 and C_5 have their own training blocks.

In Figure 7.15, three vectors which are averaged across the subjects and normalized by using Equation 7.2 to visualize their relationship are presented in the time domain for the C_3 channel:

$$Vector_{normalized} = \frac{Vector - \min(Vector)}{\max(Vector) - \min(Vector)}. \quad (7.2)$$

1. PSD vector: The PSD values obtained from the C_3 channel which are the inputs of the classifier. As the PSD values decrease the subject becomes more involved to his/her tasks.
2. Feature vector: The vector obtained by multiplying the PSD vector with the weights assigned by the classifier's training model.
3. Class vector: The classifier's outputs. As they are normalized values, 1 indicates the classes detected as MI periods where 0 indicates the detected resting periods (before the normalization they were 2 and 1). Therefore if a class value is close to 1, this means the classification accuracy in that time point is close to 100%.

The inversely proportional relationship between the PSD vector and the class vector can be seen in this figure. The active period starts at 0 in the time domain by showing the cue on the screen. For all conditions after that time point, the smaller PSD values and consequently larger classification accuracies are obtained.

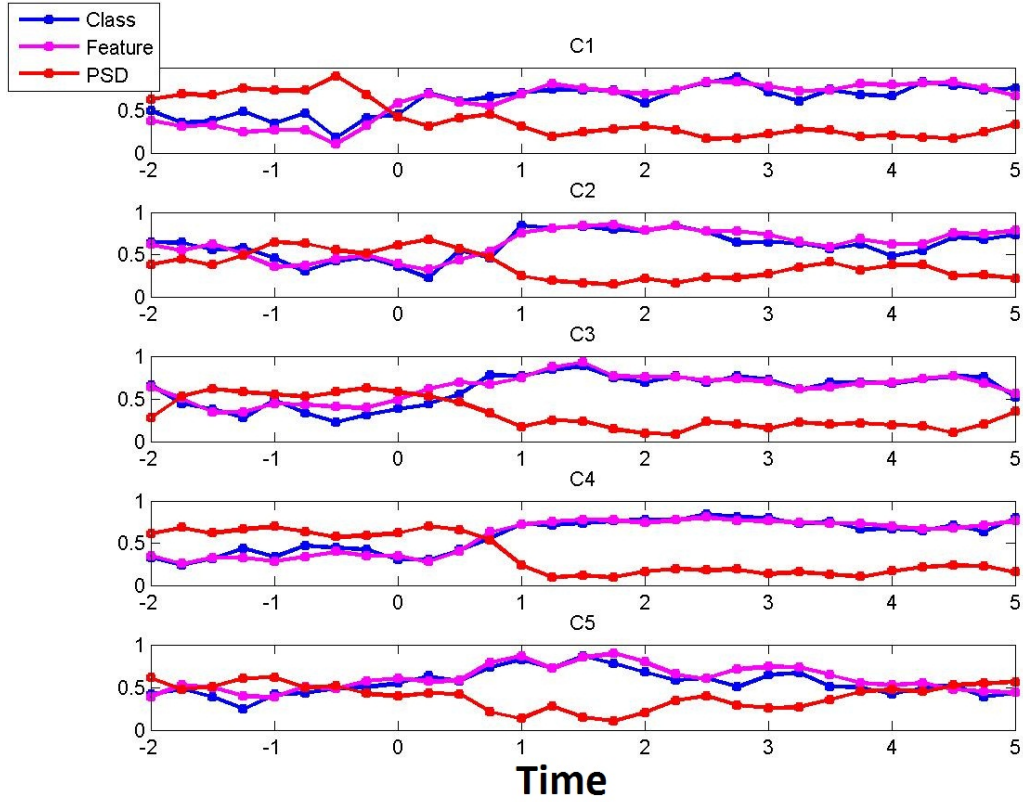


Figure 7.15: Averaged classification results across subjects and trials in the time domain with one input channel C_3 .

In Figure 7.16, we present the averaged feature, class and PSD vectors in the 4 small timing windows ($0 - 1, 1.25 - 2.25, 2.5 - 3.5, 3.75 - 4.75$ s) which are also used for the t-test of the testing data. The class vector is directly proportional to the feature vector and inversely proportional to the PSD vector.

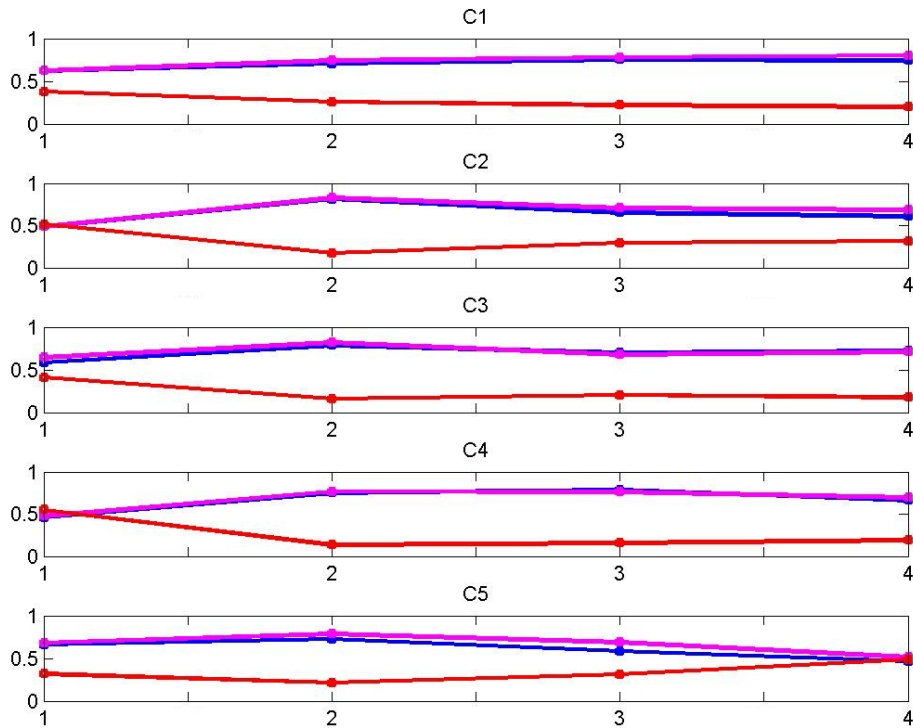


Figure 7.16: Averaged classification results in the four timing windows obtained from the C_3 channel.

To see the differences among the conditions, in Figure 7.17, we present the normalized results of each condition in the same plot. For this purpose, the vectors were divided by the maximum value of the three vectors to obtain the normalized data. The class and the PSD vectors are inversely proportional.

- The impact of haptic feedback through robotic movement on cortical activity:** According to the averaged class vector results across the subjects and the trials, the classification accuracies of C_1 which provides haptic feedback are greater than C_4 for every timing window. Moreover, for BCI-triggered conditions, C_3 in which the feedback is given haptically has a better accuracy than C_5 which provides visual feedback. This may be because the robotic system assists the subjects during the training and testing blocks.
- Comparison of two different ways to use BCI (continuous use during movement versus just to trigger movement.):** In the classification results shown in Figure 7.17, the performance of C_3 which is a BCI-triggered

condition, decreases across the time where the performance of $C1$ which is a BCI-assisted condition stays consistent and has higher performance than $C3$. This may be because of the continuous assistance of the BCI system. Besides, although $C5$ gives a better performance than $C4$ in the first timing window, as the time passes by its accuracies become smaller and $C4$ becomes better than $C5$. $C4$ provides BCI-assisted control where $C5$ provides BCI-triggered control and does not use the BCI output to control the feedback system.

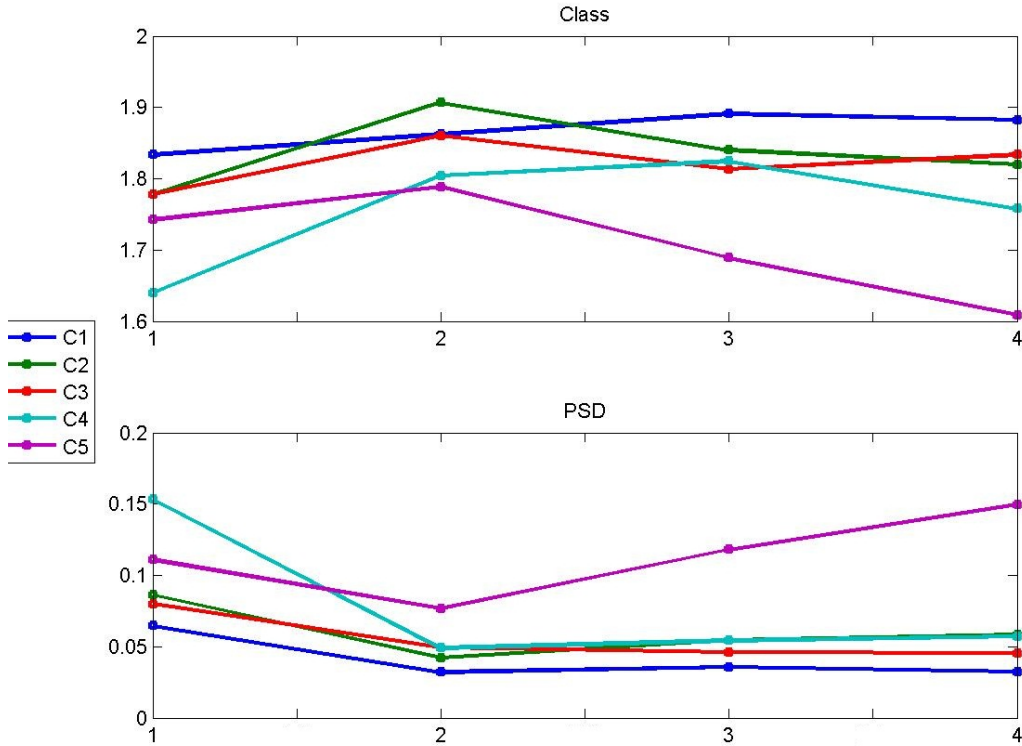


Figure 7.17: Averaged classification results in the four timing windows of every condition and their feature vectors.

In Table 7.7, the classification accuracies of the experiment for each subject and each condition are presented. The independent training data was used to build the training model and the C_3 electrode is selected as the input channel.

The averaged classification accuracies across the subjects can be listed as $ACC_{C1} > ACC_{C2} > ACC_{C3} > ACC_{C4} > ACC_{C5}$. Since the accuracy results given in this table, contain all timing points, we cannot differentiate the accuracy change in the time domain (e.g. the performance decrease of the $C3$ and $C5$ in the time domain

Table 7.7: Classification accuracies averaged across the trials for each condition and subject.

Classification Accuracy					
	c1	c2	c3	c4	c5
S1	94.5098	83.52941	93.72549	92.15686	61.56863
S2	98.03922	84.31373	97.64706	92.94118	68.23529
S3	84.70588	88.23529	43.13725	85.09804	81.96078
S4	95.29412	80.78431	90.19608	34.90196	71.76471
S5	84.70588	98.82353	99.21569	93.72549	71.76471
S6	68.23529	77.64706	78.82353	74.5098	70.58824
average	87.5817	85.55556	83.79085	78.88889	70.98039

cannot be observed from this table.). Therefore, these results are used to support our previous results.

To sum up, in Figure 7.18, the overall analysis results have been shown. From the logarithm of PSD values as a function of frequency band $0 - 30Hz$, we have extracted our motivating observations to apply three different analysis (see Figure 7.9):

1. Analysis 1: The impact of haptic feedback through robotic movement on cortical activity. $C1$ vs. $C2$ vs. $C4$
2. Analysis 2: The impact of adding BCI to a robotic rehabilitation protocol. $C1$ vs. PA vs. PP
3. Analysis 3: Comparison of two different ways to use BCI for robotic control (continuous use during movement versus just to trigger movement.) $C1$ vs. $C3$ and $C4$ vs. $C5$.

According to the peak values in the alpha frequency band shown in Figure 7.9, we have defined an order of PSD values, which is not based on a statistical analysis. Afterwards, we have presented the PSD value plots of each condition in the time domain (see Figures 7.10 to 7.14), and we have analyzed the figures with these pre-defined three analysis. Moreover, we have conducted a t-test over the conditions for

every subject and we have obtained similar analytical results with our observations (see Tables 7.2 to 7.6). Then, we have demonstrated the relationship between the PSD, weighted feature and the classification accuracy values in the time domain in Figures 7.15 to 7.17. By using the inversely proportional relationship between the PSD values and the classification performance, we have concluded in the similar PSD order of the conditions. Finally, we have presented the accuracies for each subject and condition, and provided the averaged overall classification accuracies in Table 7.7. These averaged accuracies support our previous statements.

Method	ANALYSIS 1		ANALYSIS 2	ANALYSIS 3	
Log Power Plot	$C1 < C2 \sim C4$	$C5 > C3$	$PP > C1 \sim PA$	$C3 > C1$	$C5 > C4$
PSD Plot	$C1 < C2 \sim C4$	$C5 > C3$	$PP > C1 \sim PA$	$C3 > C1$	first timing window: $C5 \sim C4$, others $C5 > C4$
T-test	first timing window: $C1 \sim C2 < C4$, others $C1 < C2 \sim C4$	$C5 > C3$	$PP > C1 \sim PA$	first timing window: $C3 \sim C1$, others $C3 > C1$	first timing window: $C5 \sim C4$, others $C5 > C4$
Classification in the Time Domain	second timing window: $C2 < C1 < C4$, others $C1 < C2 < C4$	$C5 > C3$	X	second timing window: $C3 \sim C1$, others $C3 > C1$	first timing window: $C5 \sim C4$, others $C5 > C4$
Averaged Classification Accuracy	$C1 < C2 < C4$ $ACC_{C1} > ACC_{C2} > ACC_{C4}$	$C5 > C3$ $ACC_{C5} < ACC_{C3}$	X	$C3 > C1$ $ACC_{C3} < ACC_{C1}$	$C5 > C4$ $ACC_{C5} < ACC_{C4}$

Figure 7.18: The overall performance results. The obtained order of the PSD values from the three analysis and the classification accuracy order which is inversely proportional to the PSD values order.

According to the performance order presented in Figure 7.18, we may group the conditions as follows:

- PA , $C1$ and $C2$: robot movement based on subject's continuous intent
- $C3$, PP : robot movement without subject's involvement during the movement
- $C4$, $C5$: no robotic movement

In this study we have demonstrated that robotic haptic feedback increases the BCI performance. Moreover, we have provided evidence that using BCI continuously versus just for triggering the feedback system should be preferred to make the subjects more involved to their tasks. Furthermore, our results suggest that the presence of BCI within the rehabilitation protocol, provides a similar impact on the motor cortical activity of the subject to actual movements in which the subject is the active participant of the task. Despite the promising outputs of this experiment,

it is important to note that the presented results might have some sensitivity to the choice of electrodes or timing windows, and this variation suggests that further experiments and analysis are necessary to build more confidence on the findings of our preliminary study.

Chapter 8

Conclusion

8.1 Summary

In this thesis, we have proposed, designed, implemented and evaluated a new approach for BCI based robotic rehabilitation. In particular, we have developed several experimental scenarios for stimulating the appropriate neural mechanisms in the subject and designed algorithms for machine learning as well as information extraction from the collected EEG data. Once we have demonstrated the performance of the BCI system on a number of sets and experimental protocols, we have combined the BCI component with the robotic system and demonstrated the successful control of the robotic system through experiments.

Afterwards, we have proposed a method to obtain continuous outputs from the LDA classifier to control the velocity of the robot. For this purpose, the posterior probabilities of the LDA classifier were extracted and used as the instantaneous intention levels of motor imagery. We have demonstrated that the offline/online integration of the BCI and the robotic system was implemented successfully. The online modification/adaptation of the robot's velocity ensures the active participation of the patient to his/her task.

Moreover, we have proposed an approach that enables detecting intention levels of subjects in response to task difficulty utilizing an EEG based BCI. We have designed two distinct data collection experiments involving different levels of elbow flexion and extension movements. Each experiment contained sessions dedicated to lifting loads of different weights, leading to varying levels of task difficulty. Our experimental results suggest that it is possible to extract information from EEG signals about the intention level of the subjects in response to task difficulty.

Besides, we have collected EMG data in synchrony with the EEG data as well. Since EMG data are known to capture information about task difficulty in a motor task execution experiment, we have also examined the information content of the EEG signals about task difficulty by analyzing the correlation between features extracted from EEG and EMG signals. Our results indicate some level of correlation between the two types of signals.

Lastly, we have built an online experimental paradigm with different conditions using BCI-assisted/triggered, robotic/virtual reality systems to investigate the impact of haptic feedback through a robotic system on the BCI performance, adding BCI to a robotic rehabilitation protocol and providing continuous use of BCI for robotic control. Our results indicate that the motor imagery activity is stronger when the haptic feedback is provided rather than a visual feedback. Moreover, when the subject continuously controls the velocity of a robotic system, rather than just triggering it, the subject becomes more involved to their tasks. Finally, our results verify the use of BCI in robotic rehabilitation may be preferable over conventional robotic rehabilitation systems in which movement is performed by the robot without considering the subject's involvement.

8.2 Future Works

In this thesis, we have built several EEG based BCIs and integrated them with robotic systems. In the context of rehabilitation experiments, we have observed that our proposed BCI-based protocols lead to stronger activity during motor tasks. We view this as partial evidence that the proposed protocol keeps the subjects more involved in their tasks and hence could strengthen the efficacy of robot-assisted rehabilitation. However, we are still a long way from claiming that such a protocol could help in the motor learning and rehabilitation process of a stroke patient. One might raise a number of questions related to our current protocol some of which motivate its potential extensions. One question is whether inclusion of the possibility of controlling a robot through EEG in the rehabilitation protocol would cause patients to stop trying to perform actual movements of their extremities, and whether this would hurt the rehabilitation process. This question motivates further studies on how the BCI piece should be positioned within the overall robotic

rehabilitation protocol. Secondly, an important question is whether the BCI-based rehabilitation protocol can enhance the motor learning process. All we have shown up to this point is that it leads to stronger motor cortex activity, as compared to other protocols. However a related but more important question is to determine its potential in improving the motor capabilities of subjects. In order to answer that question one needs to perform motor task performance experiments before and after the use of our BCI-based protocol. A further question is how one could bring in carefully designed neurofeedback mechanisms (in addition to the visual and haptic feedback already present) into the rehabilitation protocol to ensure motor learning. These questions motivate future work built on top of the contributions of this thesis.

8.2.1 BCI Based Robotic Experiments Utilizing Posterior Probabilities

Future work includes the comparison of the posterior probabilities with the features of the LDA classifier which are the power spectrum densities of specified frequency bands. This comparison includes the analysis of each electrode and each frequency bands in details by obtaining classifier weights.

8.2.2 Detection of Intention Level in Response to Task Difficulty from EEG

During each following session, the weight of the loads gets heavier. This may cause fatigue, and we may classify the fatigue state rather than the intention levels from the EEG. On the contrary, when there is fatigue, the task will be more difficult for the subject and we may still detect the intention levels in response to task difficulty. Consequently, it will be worth to conduct these experiments with different order of sessions. Besides, because of real arm movements, there will be some EMG artifacts in the EEG signals. An additional step can be added to be sure if the EEG features are classified or not. Moreover, a larger scale experiment with healthy volunteers are planned to test consistency of the proposed approach.

8.2.3 Comparative Experimental Analysis of BCI-Assisted Robotic Rehabilitation

Future work for this study includes a larger scale experiment with healthy volunteers and clinical trials with spinal cord injured patients to further test efficacy and effectiveness of the proposed results. Furthermore, the proposed online method for building the training model can be specialized for each subject. Lastly, a better threshold can be found for the waiting periods of the triggered protocols.

Bibliography

- [1] Biosemi, the preparations for an EEG measurement. [Online]. Available: http://www.biosemi.com/pics/apply_cap2_large.jpg
- [2] Biosemi, the preparations for an EEG measurement. [Online]. Available: http://www.biosemi.com/pics/apply_cap3_large.jpg
- [3] Biosemi, pin-type active-electrodes. [Online]. Available: http://www.biosemi.com/pics/pin_bundle2_large.jpg
- [4] Biosemi, 64 channels surgical medium/small (red/yellow) 10/20 layout. [Online]. Available: http://www.biosemi.com/pics/cap_64_layout_medium.jpg
- [5] G. Kwakkel, B. J. Kollen, and H. I. Krebs, “Effects of robot-assisted therapy on upper limb recovery after stroke: A systematic review,” *Neurorehab. and Neural Repair*, vol. 22, no. 2, pp. 111–121, 2008.
- [6] K. Nykanen, “The effectiveness of robot-aided upper limb therapy in stroke rehabilitation: A systematic review of randomized controlled studies,” Master’s thesis, University of Jyväskylä, Institute of Health Sciences, Physiotherapy, 2010.
- [7] N. A. Bayona, J. Bitensky, K. Salter, and R. Teasell, “The Role of Task-Specific Training in Rehabilitation Therapies,” *Topics in Stroke Rehabilitation*, vol. 12, no. 3, pp. 58–65, Jun. 2005.
- [8] C. Bütefisch, H. Hummelsheim, P. Denzler, and K. H. Mauritz, “Repetitive training of isolated movements improves the outcome of motor rehabilitation of the centrally paretic hand.” *Journal of the neurological sciences*, vol. 130, no. 1, pp. 59–68, May 1995.

- [9] G. B. Prange, M. J. Jannink, C. G. Groothuis-Oudshoorn, H. J. Hermens, and M. J. IJzerman, “Systematic review of the effect of robot-aided therapy on recovery of the hemiparetic arm after stroke,” *Journal of Rehabilitation Research & Development*, vol. 43, no. 2, pp. 171–184, 2006.
- [10] J. Mehrholz, T. Platz, J. Kugler, and M. Pohl, “Electromechanical and robot-assisted arm training for improving arm function and activities of daily living after stroke,” *Stroke*, vol. 40, 2009.
- [11] E. Niedermeyer and F. H. L. da Silva, *EEG Recording and Operation of the Apparatus*, 5th ed. Lippincott Williams and Wilkins, 2005.
- [12] G. Pfurtscheller and F. H. Lopes da Silva, “Event-related EEG/MEG synchronization and desynchronization: Basic principles.” *Clinical neurophysiology*, vol. 110, no. 11, pp. 1842–1857, 1999.
- [13] G. Pfurtscheller, “Brain-Computer Interfaces: A new communication device for handicapped persons,” *Journal of Microcomputer Applications*, vol. 16, no. 3, pp. 293–299, 1993.
- [14] F. Lotte, M. Congedo, A. Lécuyer, F. Lamarche, and B. Arnaldi, “A review of classification algorithms for EEG-based Brain-Computer Interfaces.” *Journal of neural engineering*, vol. 4, no. 2, pp. R1–R13, 2007.
- [15] K. Muller, C. Anderson, and G. Birch, “Linear and nonlinear methods for Brain-Computer Interfaces,” *IEEE Transactions on Neural Systems and Rehabilitation Engineering*, vol. 11, no. 2, pp. 165–169, 2003.
- [16] C. Vidaurre, M. Kawanabe, P. von Buunau, B. Blankertz, and K. Muller, “Toward unsupervised adaptation of LDA for Brain-Computer Interfaces,” *IEEE Transactions on Biomedical Engineering*, vol. 58, no. 3, pp. 587–597, 2011.
- [17] D. D’Croz-Baron, J. Ramirez, M. Baker, V. Alarcon-Aquino, and O. Carrera, “A BCI motor imagery experiment based on parametric feature extraction and fisher criterion,” in *International Conference on Electrical Communications and Computers*, 2012, pp. 257–261.

- [18] G. Pfurtscheller and C. Neuper, “Motor imagery and direct Brain-Computer Communication,” *Proceedings of the IEEE*, vol. 89, no. 7, 2001.
- [19] G. Pfurtscheller, C. Neuper, C. Guger, W. Harkam, H. Ramoser, A. Schlogl, B. Obermaier, and M. Pregenzer, “Current trends in graz Brain-Computer Interface (BCI) research,” *IEEE Transactions on Rehabilitation Engineering*, vol. 8, no. 2, pp. 216–219, 2000.
- [20] D. Xiao, Z. Mu, and J. Hu, “A linear discrimination method used in motor imagery EEG classification,” in *International Conference on Natural Computation*, vol. 2, 2009, pp. 94–98.
- [21] G. Bin, X. Gao, Y. Wang, Y. Li, B. Hong, and S. Gao, “A high-speed BCI based on code modulation VEP,” *Journal of Neural Engineering*, vol. 8, pp. 1–5, 2011.
- [22] T. Liu, L. Goldberg, S. Gao, and B. Hong, “An online Brain Computer Interface using non-flashing visual evoked potentials,” *Neural Engineering*, vol. 7, no. 3, pp. 36003–360012, 2010.
- [23] J. I. Muenssinger, S. Halder, S. C. Kleih, A. Furdea, V. Raco, A. Hoesle, and A. Kubler, “Brain painting: First evaluation of a new Brain-Computer Interface application with ALS patients and healthy volunteers.” *Frontiers in Neuroscience*, vol. 4, no. 182, 2010.
- [24] G. Pfurtscheller, R. Leeb, C. Keinrath, D. Friedman, C. Neuper, C. Guger, and M. Slater, “Walking from thought,” *Brain Research*, vol. 1071, no. 1, pp. 145–152, 2006.
- [25] S. S and C. J. A, *EEG Signal Processing*. Chichester: Wiley, 2007.
- [26] A. Murguialday, V. Aggarwal, A. Chatterjee, Y. Cho, R. Rasmussen, B. O’Rourke, S. Acharya, and N. Thakor, “Brain-Computer Interface for a prosthetic hand using local machine control and haptic feedback,” in *IEEE International Conference on Rehabilitation Robotics*, 2007, pp. 609–613.

- [27] C. Guger, W. Harkam, C. Hertnaes, and G. Pfurtscheller, “Prosthetic control by an EEG-based brain-computer interface (BCI),” in *European Conference for the Advancement of Assistive Technology*, 1999, pp. 1–6.
- [28] D. Huang, K. Qian, D.-Y. Fei, W. Jia, X. Chen, and O. Bai, “Electroencephalography (EEG)-based brain computer interface (BCI): A 2-D virtual wheelchair control based on event-related desynchronization/synchronization and state control,” *IEEE Transactions on Neural Systems and Rehabilitation Engineering*, vol. 20, no. 3, pp. 379–388, 2012.
- [29] D. Huang, P. Lin, D.-Y. Fei, X. Chen, and O. Bai, “EEG-based online two-dimensional cursor control,” in *IEEE International Conference on Engineering in Medicine and Biology Society*, 2009, pp. 4547–4550.
- [30] A. Frisoli, C. Loconsole, D. Leonardis, F. Banno, M. Barsotti, C. Chisari, and M. Bergamasco, “A new gaze-BCI-driven control of an upper limb exoskeleton for rehabilitation in real-world tasks,” *IEEE Transactions on Systems, Man, and Cybernetics, Part C: Applications and Reviews*, vol. 42, no. 6, pp. 1169–1179, 2012.
- [31] J. Stein, K. Narendran, J. McBean, R. Krebs, and R. Hughes, “Assistive control system using continuous myoelectric signal in robot-aided arm training for patients after stroke,” vol. 86, no. 4, pp. 255–261, 2007.
- [32] T. Hayashi, H. Kawamoto, and Y. Sankai, “Control method of robot suit HAL working as operator’s muscle using biological and dynamical information,” in *IEEE/RSJ Int. Conf. on Intelligent Robots and Systems*, 2005, pp. 3063–3068.
- [33] R. Gopura, K. Kiguchi, and Y. Li, “SUEFUL-7: A 7DOF upper-limb exoskeleton robot with muscle-model-oriented EMG-based control,” in *Int. Conf. on Intelligent Robots and Systems*, 2009, pp. 1126–1131.
- [34] H. Cheng, M. Ju, and C. Lin, “Improving elbow torque output of stroke patients with assistive torque controlled by EMG signals,” vol. 125, no. 6, pp. 881–886, 2003.

- [35] R. Song, K. Tong, and L. Li, “Assistive control system using continuous myoelectric signal in robot-aided arm training for patients after stroke,” vol. 16, no. 4, pp. 371–379, 2008.
- [36] T. Lenzi, S. De Rossi, N. Vitiello, and M. Carrozza, “Control method of robot suit HAL working as operator’s muscle using biological and dynamical information,” in *Conf Proc IEEE Eng Med Biol Soc.*, 2011, pp. 628–631.
- [37] T. Lenzi, S. D. Rossi, N. Vitiello, and M. Carrozza, “Intention-based EMG control for powered exoskeletons,” in *IEEE Transactions on Biomedical Engineering*, vol. 59, 2012, pp. 628–631.
- [38] C. Wang, K. S. Phua, K. K. Ang, C. Guan, H. Zhang, R. Lin, K. Chua, B. T. Ang, and C. Kuah, “A feasibility study of non-invasive motor-imagery BCI-based robotic rehabilitation for stroke patients,” in *IEEE/EMBS Conference on Neural Engineering*, 2009, pp. 271 –274.
- [39] K. K. Ang, C. Guan, K. Chua, B. Ang, C. K. Kuah, C. Wang, K. Phua, Z. Chin, and H. Zhang, “A clinical evaluation of non-invasive motor imagery-based brain-computer interface in stroke,” in *IEEE Int. Conf. on Engineering in Medicine and Biology Society*, 2008, pp. 4178 –4181.
- [40] T. Meyer, J. Peters, D. Brtz, T. Zander, B. Scholkopf, S. Soekadar, and M. Grosse-Wentrup, “A Brain-Robot Interface for studying motor learning after stroke,” in *IEEE/RSJ International Conference on Intelligent Robots and Systems*, 2012, pp. 4078 –4083.
- [41] S. Bermudez i Badia, H. Samaha, A. G. Morgade, and P. F. Verschure, “Exploring the synergies of a hybrid BCI - VR neurorehabilitation system,” in *International Conference on Virtual Rehabilitation*, 2011, pp. 1 –8.
- [42] A. Faith, Y. Chen, T. Rikakis, and L. Iasemidis, “Interactive rehabilitation and dynamical analysis of scalp EEG,” in *IEEE International Conference on Engineering in Medicine and Biology Society*, 2011, pp. 1387 –1390.
- [43] G. Prasad, P. Herman, D. Coyle, S. McDonough, and J. Crosbie, “Applying a Brain-Computer Interface to support motor imagery practice in people with

- stroke for upper limb recovery: A feasibility study,” *Neuroengineering and rehabilitation*, vol. 7, no. 60, pp. 1–17, 2010.
- [44] E. Ianez, J. M. Azorin, A. Ubeda, J. M. Ferrandez, and E. Fernandez, “Mental tasks-based Brain Robot Interface,” *Robotics and Autonomous Systems*, vol. 58, no. 12, pp. 1238 – 1245, 2010.
- [45] A. Ubeda, E. Ianez, J. Badesa, R. Morales, J. M. Azorin, and N. Garcia, “Control strategies of an assistive robot using a Brain-Machine Interface,” in *IEEE/RSJ International Conference on Intelligent Robots and Systems*, 2012, pp. 3553 –3558.
- [46] F. Meng, K.-Y. Tong, S. tak Chan, W. wa Wong, K. him Lui, K. wing Tang, X. Gao, and S. Gao, “BCI-FES training system design and implementation for rehabilitation of stroke patients,” in *IEEE International Joint Conference on Neural Networks*, 2008, pp. 4103 –4106.
- [47] K. K. Ang, C. Guan, K. Sui Geok Chua, B. T. Ang, C. Kuah, C. Wang, K. S. Phua, Z. Y. Chin, and H. Zhang, “A clinical study of motor imagery-based Brain-Computer Interface for upper limb robotic rehabilitation,” in *IEEE International Conference on Engineering in Medicine and Biology Society*, 2009, pp. 5981 –5984.
- [48] K. K. Ang, C. Guan, K. Chua, B. T. Ang, C. Kuah, C. Wang, K. S. Phua, Z. Y. Chin, and H. Zhang, “Clinical study of neurorehabilitation in stroke using EEG-based motor imagery Brain-Computer Interface with robotic feedback,” in *IEEE International Conference on Engineering in Medicine and Biology Society*, 2010, pp. 5549 –5552.
- [49] M. Gomez-Rodriguez, M. Grosse-Wentrup, J. Hill, A. Gharabaghi, B. Scholkopf, and J. Peters, “Towards brain-robot interfaces in stroke rehabilitation,” in *IEEE International Conference on Rehabilitation Robotics*, 2011, pp. 1 –6.
- [50] L. Jiang, C. Guan, H. Zhang, C. Wang, and B. Jiang, “Brain computer interface based 3D game for attention training and rehabilitation,” in *Industrial*

- Electronics and Applications (ICIEA), 2011 6th IEEE Conf. on*, 2011, pp. 124–127.
- [51] R. Khosrowabadi, H.-C. Q., A. Wahab, and K. K. Ang, “EEG-based emotion recognition using self-organizing map for boundary detection,” in *Pattern Recognition (ICPR), 2010 20th Int. Conf. on*, 2010, pp. 4242–4245.
- [52] R. Khosrowabadi, C. Q., K. K. Ang, S. W. Tung, and M. Heijnen, “A brain-computer interface for classifying eeg correlates of chronic mental stress,” in *Neural Networks (IJCNN), The 2011 Int. Joint Conf. on*, 2011, pp. 757–762.
- [53] D. Huang, H. Zhang, K. Ang, C. Guan, Y. Pan, C. Wang, and J. Yu, “Fast emotion detection from EEG using asymmetric spatial filtering,” in *Acoustics, Speech and Signal Processing (ICASSP), 2012 IEEE Int. Conf. on*, 2012, pp. 589–592.
- [54] T. Lalitharatne, A. Yoshino, Y. Hayashi, K. Teramoto, and K. Kiguchi, “Toward EEG control of upper limb power-assist exoskeletons: A preliminary study of decoding elbow joint velocities using eeg signals,” in *Micro-NanoMechatronics and Human Science (MHS), 2012 Int. Symposium on*, 2012, pp. 421–424.
- [55] J. Lv, Y. Li, and Z. Gu, “Decoding hand movement velocity from electroencephalogram signals during a drawing task,” p. 64, 2010.
- [56] H. Yuan, C. Perdoni, and B. He, “Relationship between speed and EEG activity during imagined and executed hand movements,” *J. Neural Eng.*, no. 2, pp. 124–127, 2010.
- [57] G. Pfurtscheller and A. Schlgl. (2003) Data set iii: motor imagery. [Online]. Available: <http://www.bbc.de/competition/ii/>
- [58] D. J. McFarland, L. A. Miner, T. M. Vaughan, and J. R. Wolpaw, “Mu and beta rhythm topographies during motor imagery and actual movements.” *Brain topography*, vol. 12, no. 3, pp. 177–186, 2000.

- [59] G. Pfurtscheller, C. Neuper, D. Flotzinger, and M. Pregenzer, “EEG-based discrimination between imagination of right and left hand movement,” *Electroencephalography and Clinical Neurophysiology*, vol. 103, no. 6, pp. 642 – 651, 1997.
- [60] A. Erdogan and V. Patoglu, “Slacking prevention during assistive contour following tasks with guaranteed coupled stability,” in *IEEE/RSJ International Conference on Intelligent Robots and Systems*, 2012, pp. 1587 –1594.
- [61] P. Li and R. Horowitz, “Passive Velocity Field Control (pvfc): Part I - Geometry and robustness,” *IEEE Transactions on Automatic Control*, vol. 46, no. 9, p. 2001, 2001.
- [62] P. Y. Li and R. Horowitz, “Passive Velocity Field Control (pvfc): Part II - Application to contour following,” *IEEE Transactions on Automatic Control*, vol. 46, no. 9, pp. 1360 –1371, 2001.
- [63] T.-C. Chiu, “Coordination control of multiple axes mechanical system: Theory and experiments,” Ph.D. dissertation, Univ. of California,, Dept. of Mechanical Engineering, Berkeley, CA, 1994.
- [64] E. D. Tung, “Identification and control of high-speed machine tools,” Ph.D. dissertation, Univ. of California,, Dept. of Mechanical Engineering, Berkeley, CA, 1993.
- [65] J.-J. Slotine and W. Li, *Applied Nonlinear Control*. Prentice Hall, 1990.
- [66] N. Sadegh and R. Horowitz, “Stability and robustness analysis of a class of adaptive controllers for robotic manipulators,” *International Journal of Robotics Research*, vol. 9, no. 3, pp. 74–92, 1990.
- [67] R. Ortega and M. Spong, “Adaptive motion control of rigid bodies,” *Automatica*, vol. 9, no. 3, pp. 877–888, 1989.
- [68] P. Li and R. Horowitz, “Control of smart exercise machines I : Problem formulation and nonadaptive control,” *IEEE/ASME Transactions on Mechatronics*, vol. 2, no. 4, pp. 237 –247, 1997.

- [69] P.Y.Li and R.Horowitz, “Passive Velocity Field Control of mechanical manipulators,” *IEEE Transactions on Robotics and Automation*, vol. 15, no. 4, pp. 751–763, 1999.
- [70] A. Erdogan and V. Patoglu, “Online generation of velocity fields for passive contour following,” in *IEEE World Haptics Conference*, 2011, pp. 245–250.
- [71] M. Bg, E. Erkocevic, M. Niemeier, J. Mathiesen, A. Smidstrup, and E. Karmavuko, “Investigation of the linear relationship between grasping force and features of intramuscular EMG,” in *15th Nordic-Baltic Conf. on Biomedical Engineering and Medical Physics*, ser. IFMBE Proceedings, vol. 34. Springer Berlin Heidelberg, 2011, pp. 121–124.
- [72] M. Fatourech, A. Bashashati, R. K. Ward, and G. E. Birch, “EMG and EOG artifacts in brain computer interface systems: A survey.” *Clinical neurophysiology*, vol. 118, no. 3, pp. 480–494, Mar. 2007.